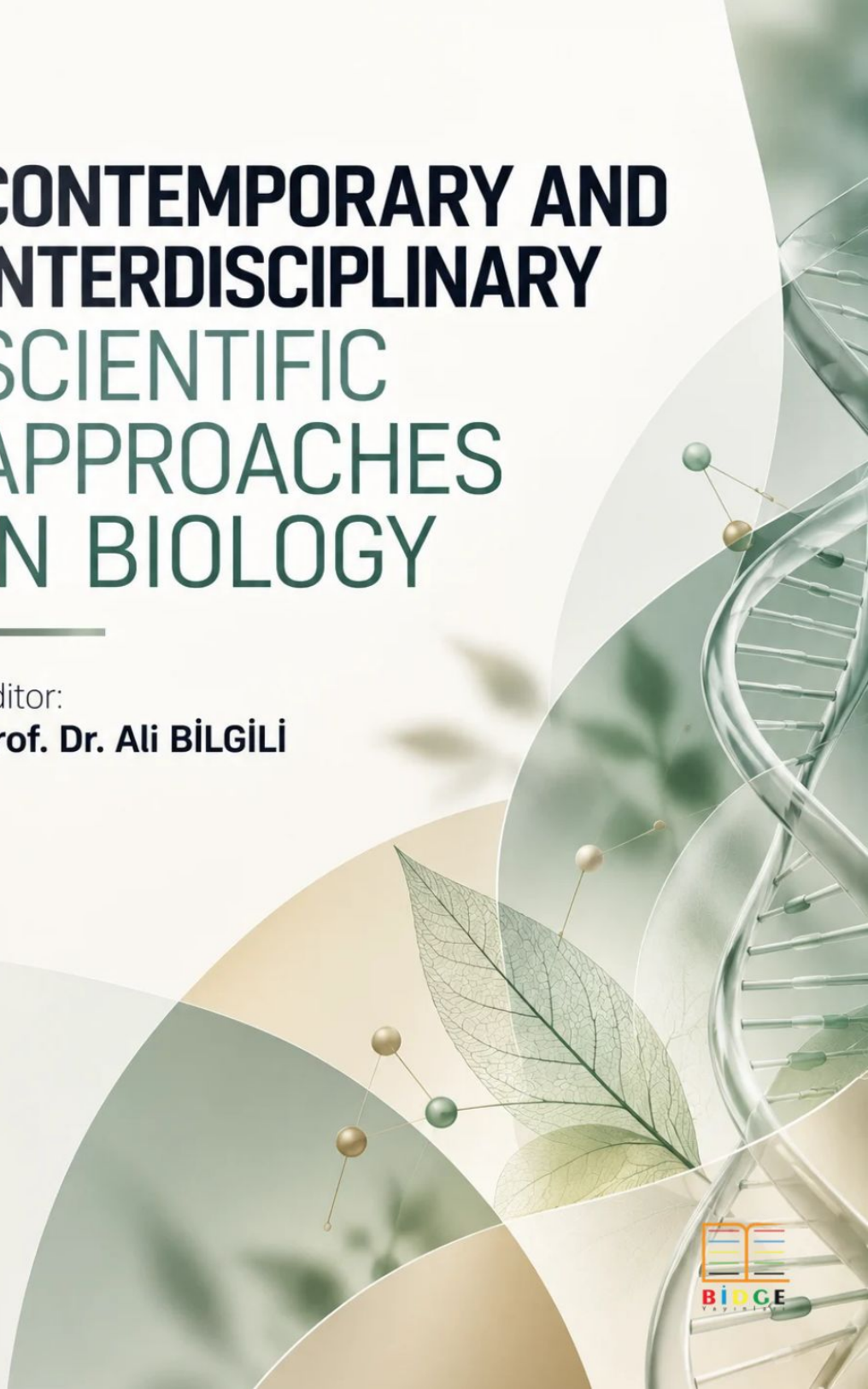
CONTEMPORARY AND INTERDISCIPLINARY SCIENTIFIC APPROACHES IN BIOLOGY

Editor:
Prof. Dr. Ali BİLGİLİ



BİDGE Yayınları

BİDGE Yayınları

Contemporary and Interdisciplinary Scientific Approaches in Biology

Editör: Prof. Dr. Ali BİLGİLİ

ISBN: 978-625-5057-57-0

1. Baskı
Sayfa Düzeni: Gözde YÜCEL
Yayınlama Tarihi: 2026-10-25
BİDGE Yayınları

Bu eserin bütün hakları saklıdır. Kaynak gösterilerek tanıtım için yapılacak kısa alıntılar dışında yayıncının ve editörün yazılı izni olmaksızın hiçbir yolla çoğaltılamaz.

Sertifika No: 71374
Yayın hakları © BİDGE Yayınları
www.bidgeyayinlari.com.tr - bidgeyayinlari@gmail.com
Krc Bilişim Ticaret ve Organizasyon Ltd. Şti.
Güzeltepe Mahallesi Abidin Daver Sokak Sefer Apartmanı No: 7/9 Çankaya / Ankara

PREFACE

Antimicrobial resistance, including antibiotic resistance, is a major global health challenge because it can make bacterial infections more difficult to treat and increase healthcare utilization, treatment costs, and mortality. The global burden of bacterial AMR was substantial in 2019, and inappropriate or unnecessary antibiotic use contributes to the selection pressure that favors resistant organisms. This chapter has discussed algae-derived bioactive compounds for combating antibiotic resistance in detail, focusing on their chemical diversity, antimicrobial mechanisms, and therapeutic potential, with supporting quotations from scientific sources.

The scientific value of converting medicinal and aromatic plants into carbon nanomaterials extends beyond obtaining a fluorescent product from an inexpensive feedstock. Botanical resources contain multiple classes of carbon-containing constituents, and processing can redistribute these constituents into new molecular and particulate forms. In this chapter, the antimicrobial and antioxidant potential of carbon dots derived from medicinal and aromatic plants have been examined from an original perspective in light of the scientific literature.

Azoxystrobin is a broad-spectrum systemic fungicide in the strobilurin group, used to control fungal diseases in crops. Its effects below ground therefore matter alongside its intended activity against plant pathogens. Soil enzymes provide measurable indicators of some of these biological processes and can respond to environmental disturbance and management. Dehydrogenase activity is commonly used as an indicator of overall microbial respiratory activity in soil. This review has explored in detail the effects of azoxystrobin on soil dehydrogenase activity, drawing on the scientific sources.

DNA barcoding is a molecular identification approach that aims to determine the identity of an organism from short, standardized DNA regions. In light of the scientific literature, this chapter has first briefly summarized DNA barcoding using markers

employed in major groups of organisms and then examined in detail why identifying a universal DNA barcode is more challenging in plants.

An active compound can produce a promising response in a biological assay without being delivered effectively by a pharmaceutical formulation. The relevant delivery question is whether the final preparation provides an appropriate exposure at the intended site for a useful duration. For botanical carbon dots, that question involves the associated drug, the carbon-containing carrier, and any soluble constituents that remain after preparation. Each can contribute to the observed response and each may follow a different biological path. This chapter has addressed drug loading, release, barrier transport, tissue distribution, and elimination as interrelated aspects of drug formulation through a synthesis of key scientific studies.

The nests of social insects represent some of the most structurally sophisticated animal constructions on Earth. Termite mounds of the genus *Macrotermes* can rise more than eight meters above the African savannah and house colonies of several million individuals, achieving internal atmospheric regulation through a system of tunnels and chimneys whose engineering is only now being understood in quantitative terms. This chapter has provided a comprehensive review of colonial piezoelectric seismic sensing in social insects, based on key scientific literature.

Prof. Dr. ALİ BİLGİLİ

ANKARA UNIVERSITY

İÇİNDEKİLER

Algae-derıved Bıoactıve Compounds ın Combatıng Antıbıotıc Resıstance: Chemıcal Dıversıty, Antımıcrobıal Mechanısms, and Therapeutıc Potentıal 1
OSMAN UÇ, TUĞBA DEMİRİZ YÜCER, KÖKSAL PABUÇCU

PLANT-DERIVED CARBON DOTS FOR DRUG DELIVERY AND BIOPHARMACEUTICAL APPLICATIONS 20
ASLIHAN CESUR TURGUT

ANTIMICROBIAL AND ANTIOXIDANT POTENTIAL OF CARBON DOTS DERIVED FROM MEDICINAL AND AROMATIC PLANTS 39
ASLIHAN CESUR TURGUT

AZOXYSTROBIN EFFECTS ON SOIL DEHYDROGENASE ACTIVITY: EVIDENCE AND ENVIRONMENTAL CONTEXT 67
BURAK KOÇAK

DNA BARCODING IN PLANT SYSTEMATICS: SPECIES IDENTIFICATION AND NEXT-GENERATION APPROACHES 89
HANDAN ŞAPCI SELAMOĞLU

COLONIAL PIEZOELECTRIC SEISMIC SENSING IN SOCIAL INSECTS ARCHITECTURE, MECHANISM, AND THE NEST AS EXTENDED SENSORY ORGAN 117
HAKAN BOZDOĞAN

BÖLÜM 1

ALGAE-DERIVED BIOACTIVE COMPOUNDS IN COMBATING ANTIBIOTIC RESISTANCE: CHEMICAL DIVERSITY, ANTIMICROBIAL MECHANISMS, AND THERAPEUTIC POTENTIAL

OSMAN UÇ[1]
TUĞBA DEMİRİZ YÜCER[2]
KÖKSAL PABUÇCU[3]

Introduction

Antimicrobial resistance (AMR), including resistance to antibiotics, is a major global health challenge because it can make bacterial infections more difficult to treat and increase healthcare

[1] Ph.D., Dicle University, Microbiology Laboratory, ORCID: 0000-0002-3738-9836

[2] Assistant Professor, Karabük University, Faculty of Health Sciences, Department of Nutrition and Dietetics, ORCID: 0000-0002-2494-4511

[3] Professor, Erzincan Binali Yıldırım University, Faculty of Pharmacy, Department of Professional Pharmaceutical Sciences, Division of Pharmacognosy, ORCID: 0000-0002-4473-8002

use, treatment costs, and mortality. The global burden of bacterial AMR was substantial in 2019, and inappropriate or unnecessary antibiotic use contributes to selection pressure that favours resistant organisms (Antimicrobial Resistance Collaborators, 2022, p. 629; Ventola, 2015, pp. 277–278). The World Health Organization's Bacterial Priority Pathogens List identifies resistant bacterial groups for which research and development of new interventions are particularly important (World Health Organization [WHO], 2024, p. x).

The problem is not limited to the emergence of resistance mechanisms in individual bacterial cells. Biofilm growth, altered metabolic states, persister cells, and restricted antibiotic penetration can contribute to reduced treatment susceptibility or tolerance. These phenomena are related but not interchangeable: antibiotic resistance generally denotes the ability to grow at antibiotic concentrations that inhibit susceptible organisms, whereas tolerance refers to survival during antibiotic exposure without necessarily increasing the minimum inhibitory concentration (MIC). Biofilm-associated tolerance may coexist with genetically encoded resistance, but biofilm formation alone does not establish that a strain is antibiotic-resistant (Hall & Mah, 2017, pp. 277–278; Liu et al., 2024, pp. 1, 4).

Natural products have contributed substantially to drug discovery, including the discovery of antimicrobial agents and compounds that serve as starting points for medicinal chemistry. Modern natural-product research combines biological screening with chemical characterization, isolation, structural elucidation, and optimization of promising molecules (Atanasov et al., 2021, pp. 200–202; Newman & Cragg, 2020, pp. 770–771). Algae are chemically diverse organisms and have attracted attention as sources of candidate antimicrobial compounds. Evidence includes direct antibacterial screening, antibiofilm investigations, and studies examining whether algal extracts can improve the activity of

selected antibiotics (Behzadnia et al., 2024, p. 1; EL-Sayed et al., 2023, pp. 3, 7; Silva et al., 2020, pp. 1–3; Zuorro et al., 2024, p. 1).

This chapter uses the term algae-derived compounds as an inclusive term because the literature discussed here includes marine macroalgae, freshwater filamentous algae, and a diatom. These groups differ taxonomically and ecologically: macroalgae or seaweeds are macroscopic marine algae, whereas *Spirogyra* and *Vaucheria* are freshwater-associated filamentous algae in many settings, and *Gomphonema olivaceum* is a microscopic diatom. They should not all be described as marine macroalgae. The chapter evaluates their chemical diversity and reported biological activities while distinguishing evidence of antimicrobial activity from evidence that a compound modifies antibiotic resistance.

The available findings should be interpreted as preclinical research evidence rather than proof of clinical efficacy. An extract that inhibits bacterial growth in vitro does not, by itself, demonstrate reversal of antibiotic resistance, safety in humans, or suitability for therapeutic use. Stronger conclusions require reproducible methods, well-characterized resistant isolates, mechanistic experiments, toxicity assessment, and ultimately appropriate in vivo and clinical evaluation.

Algae-Derived Bioactive Compounds

The chemical profile of an algal sample depends on its taxon, habitat, season, physiological state, cultivation conditions, harvesting and storage procedures, and extraction method. Major classes investigated for antimicrobial potential include phenolic compounds, fatty acids and other lipids, polysaccharides, pigments, terpenoids, and sterols. Chemical composition and biological activity should therefore be assessed together rather than inferred from taxonomic identity or total compound measurements alone

(Cotas et al., 2020, pp. 1, 2, 8, 9; Shannon & Abu-Ghannam, 2016, p. 2; Silva et al., 2020, pp. 9–12; Zuorro et al., 2024, pp. 12–13).

Phenolic compounds

Phenolic compounds are frequently investigated in algal extracts because their chemical structures can interact with proteins, membranes, and other cellular targets. Brown seaweeds are notable for phlorotannins, while phenolic acids and other phenolic-like compounds have also been reported in different algal materials. Some phenolics exhibit antimicrobial effects in experimental systems, but activity varies with molecular structure, concentration, bacterial species, and assay conditions (Cotas et al., 2020, pp. 2–3; Cushnie & Lamb, 2011, pp. 101–102; Daglia, 2012, pp. 176–178).

Total phenolic content is a useful screening parameter, not proof that phenolics are responsible for an observed antibacterial effect. Correlations between total phenolic content and activity can be confounded by other extract constituents and by differences in extraction yield. Where possible, profiling by chromatographic and spectrometric methods, testing isolated compounds, and conducting structure–activity analyses are needed to identify active constituents. Studies of *Vaucheria* species that combine phenolic measurements with antioxidant and antimicrobial testing are relevant examples of this integrated approach, but they do not by themselves demonstrate antibiotic-resistance reversal (Uç & Pabuçcu, 2024, pp. 16–17; Uç & Pabuçcu, 2026, pp. 1396–1397).

Fatty acids and other lipids

Certain free fatty acids can affect bacterial membranes, and their antimicrobial properties depend on chain length, degree of unsaturation, concentration, and the microorganism tested (Desbois & Smith, 2010, pp. 1632–1634). However, fatty-acid profiles are not equivalent to antimicrobial activity: detecting a fatty acid in an algal

sample does not establish that it is present at an active concentration or that it accounts for an extract's effect.

Chemical studies of the freshwater green alga *Cladophora fracta var. intricata* and the diatom *Gomphonema olivaceum* illustrate the value of characterizing algal lipids and related constituents (Demiriz Yücer & Pabuçcu, 2023, pp. 75–76; Demiriz Yücer & Pabuçcu, 2024, pp. 90–92). These studies support chemical-diversity research but should not be cited as direct demonstrations of activity against antibiotic-resistant bacteria unless such experiments were explicitly performed.

Polysaccharides

Algal polysaccharides are of interest in pharmaceutical, food, and biomaterials research. Their structures vary substantially across algal groups. Fucoidans are characteristic sulfated polysaccharides associated particularly with brown algae; agar and carrageenans are obtained from red algae; and alginates are characteristic polysaccharides of brown algae. The biological properties of these materials depend on features such as molecular mass, monosaccharide composition, sulfation pattern, purity, and formulation (Silva et al., 2020, pp. 10–11).

Some algal polysaccharides or polysaccharide-rich fractions have been investigated for antibiofilm or other biological effects, but effects cannot be generalized to all polysaccharides (Behzadnia et al., 2024, p. 10). A reduction in biofilm biomass may reflect impaired adhesion, altered matrix production, reduced bacterial growth, or a combination of processes. Appropriate controls and independent measures of bacterial viability are needed to distinguish these possibilities.

Pigments and other metabolites

Chlorophylls, carotenoids, terpenoids, sterols, and other low-molecular-weight metabolites contribute to algal chemical diversity and may be relevant to antimicrobial discovery. Nevertheless, antioxidant and antimicrobial activities are distinct endpoints. An extract's radical-scavenging activity does not establish that it kills bacteria or induces oxidative stress in them. Claims about a particular pigment or metabolite should therefore be supported by studies that directly test the proposed activity and, where possible, the purified compound (Gupta & Abu-Ghannam, 2011, pp. 317–319; Shannon & Abu-Ghannam, 2016, pp. 2, 5, 6; Zuorro et al., 2024, pp. 1, 9, 11).

Extraction and chemical characterization

Extraction procedures strongly influence the compounds recovered from algal biomass. Water, ethanol, methanol, acetone, and non-polar solvents differ in polarity and selectivity; consequently, extracts from the same species can have different chemical profiles and biological activities. Solvent residues, extraction yield, biomass processing, and the use of appropriate solvent controls must also be considered. Studies of *Spirogyra aequinoctialis* using different solvents illustrate why extraction conditions should be reported and compared carefully (Pabuçcu & Demiriz Yücer, 2022, pp. 928–930; Silva et al., 2020, pp. 3, 21, 22).

For reliable interpretation, studies should report taxonomic identification and voucher or culture information where available, collection or cultivation conditions, biomass processing, extraction yield, solvent controls, chemical characterization, test strains, inoculum preparation, and assay conditions. Activity-guided fractionation and metabolomic approaches can help connect biological effects with particular chemical constituents.

Mechanisms Relevant to Antibiotic Resistance and Treatment Tolerance

Algae-derived compounds are being explored not only for direct antimicrobial effects but also for potential effects on processes associated with bacterial survival, pathogenicity, and reduced treatment susceptibility. The principal areas of interest include membrane effects, biofilm formation, quorum sensing, efflux pumps, and interactions with existing antibiotics. The strength of evidence varies by compound and study; these mechanisms should be presented as demonstrated only when directly tested.

Effects on bacterial membranes and cell walls

The bacterial cell membrane maintains ion gradients and cellular homeostasis, while the cell wall provides structural support. Some antimicrobial compounds can disrupt membrane permeability or affect cell-wall-associated processes, ultimately impairing viability. Free fatty acids are one class of molecules for which membrane-associated antibacterial mechanisms have been investigated (Desbois & Smith, 2010, pp. 1633–1634).

However, a growth-inhibition zone or a low MIC does not identify the mechanism responsible. In crude algal extracts, membrane-permeability assays, measurements of intracellular leakage, microscopy, and testing of purified fractions may be required to establish whether membrane damage contributes to activity. It is also important not to assume that a membrane-active compound will automatically overcome resistance to antibiotics with unrelated targets.

Biofilm formation and biofilm-associated tolerance

Biofilms are microbial communities embedded in an extracellular matrix and attached to a surface or to one another. Their physiology can differ from that of planktonic cells. Matrix

properties, slow growth, altered gene expression, persister cells, and limited penetration or activity of some antibiotics can contribute to reduced treatment susceptibility (Flemming et al., 2016, pp. 563, 571, 572; Hall & Mah, 2017, pp. 277–278; Liu et al., 2024, pp. 1, 4).

Marine algae-derived compounds, including certain phenolics, lipids, pigments, and sulfated polysaccharides, have been discussed as candidate antibiofilm agents (Behzadnia et al., 2024, pp. 10–11). Nevertheless, preventing initial biofilm formation is different from disrupting an established biofilm. Biofilm biomass assays should ideally be paired with viable-cell measurements and, where relevant, microscopy or matrix analysis. A reduction in biomass alone does not establish bacterial killing or reversal of antibiotic resistance.

Quorum sensing and virulence-associated traits

Quorum sensing is a cell-density-dependent communication system through which bacteria regulate gene expression in response to signalling molecules. Depending on the organism, quorum-sensing pathways can influence biofilm development, motility, extracellular enzyme production, and other virulence-associated traits. Interfering with these pathways may reduce selected pathogenic traits without necessarily inhibiting bacterial growth (Behzadnia et al., 2024, pp. 3–4).

An antibiofilm effect does not by itself prove quorum-sensing inhibition. Reduced bacterial growth, altered adhesion, and changes in matrix production can produce similar observations. Evidence for quorum-sensing interference is stronger when reporter strains, signalling assays, gene-expression measurements, and purified compounds are used. Reviews of algal antibiofilm compounds and broader quorum-quenching strategies identify quorum sensing as a promising research area, but compound-specific

claims should remain proportional to the experimental evidence (Behzadnia et al., 2024, pp. 3, 4, 10; D'Aquila et al., 2024, pp. 1–3).

Efflux pumps

Efflux pumps are membrane-associated transport systems that can export antibiotics and other compounds from bacterial cells. Depending on the organism and pump, their activity can contribute to intrinsic or acquired resistance and may interact with other cellular processes (Blair et al., 2015, pp. 43–45; Ren et al., 2024, pp. 1–2).

Algae-derived compounds could be screened as potential efflux-pump modulators, but this possibility should not be described as an established property of algal extracts without direct evidence. Useful approaches include measuring intracellular accumulation of a suitable probe or antibiotic, assessing efflux activity, and using appropriate pump-deficient or pump-overexpressing strains where available. Cytotoxicity and non-specific membrane disruption must be considered because either can confound apparent efflux inhibition.

Interactions with existing antibiotics

Combination studies are among the most directly relevant approaches for assessing whether an algal extract may modify antibiotic activity. EL-Sayed et al. (2023, pp. 3, 7) investigated methanolic *Ulva lactuca* extract alone and in combination with selected antibiotics against *Klebsiella pneumoniae* RCMB 003 (1) ATCC 13883, described by the authors as multidrug-resistant. The authors reported enhanced inhibition for particular combinations, including a combination with gentamicin. This is a useful proof-of-concept study, but the finding should not be generalized to all *Ulva* extracts, antibiotics, or bacterial isolates.

Broth microdilution assays and fractional inhibitory concentration indices (FICI), together with time-kill experiments,

can help characterize combination effects (Balouiri et al., 2016, pp. 73, 77; Cushnie & Lamb, 2011, pp. 103–104). The assay method and interpretation thresholds should be stated explicitly. Agar diffusion alone can be difficult to interpret for synergy because diffusion rates differ between crude extracts and antibiotics. Further work should use chemically characterized fractions, multiple well-characterized resistant isolates, appropriate controls, and reproducible quantitative methods.

Even when a combination enhances inhibition in vitro, it does not automatically demonstrate that antibiotic doses can safely be reduced in patients. Such conclusions require pharmacological, toxicological, and clinical evidence.

Evidence from Algal Research

Published studies provide several types of evidence, which should be distinguished according to what they actually demonstrate. Antibacterial screening supports direct activity under the tested conditions; chemical-composition studies identify candidate constituents; antibiofilm studies examine a specific microbial phenotype; and combination studies may provide evidence of antibiotic-potentiating effects. These categories are complementary but not interchangeable.

The study of *Spirogyra aequinoctialis* by Pabuçcu and Demiriz Yücer (2022, pp. 928–930) examined antibacterial and antifungal activities of extracts prepared with different solvents. It supports the value of solvent-dependent screening of freshwater algal material, but it should not be presented as direct evidence of activity against antibiotic resistance unless resistant isolates and resistance-related endpoints were tested.

Studies of *Gomphonema olivaceum* and *Cladophora fracta var. intricata* characterized fatty acids and, in the latter case, vitamins and antioxidant properties (Demiriz Yücer & Pabuçcu, 2023, pp. 75–

76; Demiriz Yücer & Pabuçcu, 2024, pp. 91–92). These findings are relevant to algal chemical diversity and candidate discovery, but chemical detection and antioxidant assays do not establish antibacterial activity or resistance modification.

Uç and Pabuçcu (2024, pp. 16–18) investigated antioxidant and antibacterial properties of *Vaucheria frigida*, and Uç and Pabuçcu (2026, pp. 1396–1397) reported antioxidant and antimicrobial activities alongside phenolic composition for *Vaucheria aversa*. These studies are relevant examples of combining chemical and biological characterization in freshwater algae. Their results should be interpreted within the organisms, extracts, and test conditions investigated; they do not alone establish a mechanism for reversing antibiotic resistance.

The *Ulva lactuca* study by EL-Sayed et al. (2023, pp. 3, 7) is more directly related to antibiotic-combination research because it tested the extract in combination with selected antibiotics against *K. pneumoniae* RCMB 003 (1) ATCC 13883, described by the authors as multidrug-resistant. Its findings justify further investigation of algal extracts as potential antibiotic-potentiating candidates, while requiring replication, improved chemical attribution, and evaluation across additional isolates and methods.

The review of marine algal antibiofilm compounds synthesizes candidate compound classes and possible mechanisms, including adhesion, extracellular matrix production, and quorum sensing (Behzadnia et al., 2024, pp. 9–11). Broader reviews cover macroalgal antimicrobial compounds and extraction methods (Silva et al., 2020, pp. 9–12) and algal antimicrobial discovery (Zuorro et al., 2024, p. 1). Because reviews summarize heterogeneous studies, individual mechanistic claims should be traced to the primary experiments where possible. Research on antiproliferative effects of *Pseudopediastrum boryanum* extracts, for example, may inform the broader need for cellular safety and selectivity assessment, but it is

not direct evidence of anti-AMR activity (Demiriz Yücer, 2024, pp. 1027–1029).

Methodological Limitations and Future Directions

Several limitations currently constrain translation of algae-derived bioactive compounds into antimicrobial applications. First, differences in taxonomic identification, habitat, season, cultivation, biomass processing, extraction solvents, and test methods can make results difficult to compare. Standardized reporting and quality control are essential. Second, crude extracts contain mixtures of compounds, so activity cannot reliably be attributed to a particular molecule without fractionation, purification, and chemical analysis (Atanasov et al., 2021, pp. 201–202; Silva et al., 2020, pp. 3, 9, 27).

Third, studies should use clinically relevant and well-characterized bacterial strains. Where the research question concerns antibiotic resistance, investigators should specify the resistance phenotype or genotype and use appropriate susceptibility testing. Priority groups include methicillin-resistant *Staphylococcus aureus*, vancomycin-resistant *Enterococcus faecium*, third-generation-cephalosporin-resistant Enterobacterales, carbapenem-resistant *Acinetobacter baumannii*, and carbapenem-resistant *Pseudomonas aeruginosa*, consistent with the aims of the WHO priority-pathogen framework (WHO, 2024, pp. x–xi).

Fourth, mechanistic studies should match the claim being made. MIC and minimum bactericidal concentration measurements assess different endpoints (Balouiri et al., 2016, pp. 75–77); biofilm biomass, viable-cell counts, quorum-sensing reporters, efflux assays, and time-kill experiments answer different questions. Appropriate positive, negative, solvent, and growth controls are necessary. For combination studies, results should be reported for each tested pairing rather than generalized from a single successful combination.

Finally, safety and pharmacological feasibility require early attention. Cytotoxicity, haemolysis where relevant, selectivity indices, stability, solubility, bioavailability, metabolism, and pharmacokinetic properties may determine whether a promising in vitro hit can be developed further. In vivo studies and clinical investigations are needed before therapeutic claims can be made. Natural origin should not be equated with safety.

A practical research pathway is therefore to (1) authenticate and document the algal material; (2) prepare standardized extracts; (3) conduct reproducible antimicrobial screening; (4) characterize the chemistry of active extracts; (5) fractionate and identify active constituents; (6) validate proposed mechanisms; (7) test combinations against characterized resistant isolates; and (8) assess toxicity and preclinical feasibility. This workflow can help distinguish reproducible lead compounds from nonspecific or assay-dependent effects.

Conclusion

Algae-derived bioactive compounds represent a promising source of candidate molecules for antimicrobial research and the development of complementary strategies against antibiotic-resistant bacteria. Their potential applications extend beyond direct antimicrobial activity to include antibiofilm effects, interference with bacterial communication systems, and possible enhancement of antibiotic efficacy. However, these effects vary according to algal taxon, chemical composition, extraction procedures, target microorganisms, and experimental conditions. Antimicrobial activity alone should not be interpreted as evidence of resistance reversal or clinical efficacy. Future studies should prioritize chemical characterization, compound-level validation, standardized antimicrobial susceptibility testing, investigations using well-characterized resistant clinical isolates, antibiotic-combination

studies, and systematic toxicity and selectivity assessments. Through these approaches, algae-derived compounds may provide valuable starting points for the discovery of new antimicrobial agents and resistance-modifying adjuncts, although their clinical relevance must be established through rigorous preclinical and clinical evaluation.

References

Antimicrobial Resistance Collaborators. (2022). Global burden of bacterial antimicrobial resistance in 2019: A systematic analysis. *The Lancet, 399*(10325), 629–655. doi:10.1016/S0140-6736(21)02724-0

Atanasov, A., Zotchev, S., Dirsch, V., the International Natural Product Sciences Taskforce, & Supuran, C. (2021). Natural products in drug discovery: Advances and opportunities. *Nature Reviews Drug Discovery, 20*(3), 200–216. doi:10.1038/s41573-020-00114-z

Balouiri, M., Sadiki, M., & Ibnsouda, S. (2016). Methods for in vitro evaluating antimicrobial activity: A review. *Journal of Pharmaceutical Analysis, 6*(2), 71–79. doi:10.1016/j.jpha.2015.11.005

Behzadnia, A., & Moosavi-Nasab, M. (2024). Anti-biofilm activity of marine algae-derived bioactive compounds. *Frontiers in Microbiology, 15*, Article 1270174. doi:10.3389/fmicb.2024.1270174

Blair, J., Webber, M., Baylay, A., Ogbolu, D., & Piddock, L. (2015). Molecular mechanisms of antibiotic resistance. *Nature Reviews Microbiology, 13*(1), 42–51. doi:10.1038/nrmicro3380

Cotas, J., Leandro, A., Monteiro, P., Pacheco, D., Figueirinha, A., Gonçalves, A., & da Silva, G. (2020). Seaweed phenolics: From extraction to applications. *Marine Drugs, 18*(8), Article 384. doi:10.3390/md18080384

Cushnie, T., & Lamb, A. (2011). Recent advances in understanding the antibacterial properties of flavonoids. *International*

Journal of Antimicrobial Agents, 38(2), 99–107. doi:10.1016/j.ijantimicag.2011.02.014

D'Aquila, P., De Rose, E., Sena, G., Scorza, A., Cretella, B., & Passarino, G. (2024). Quorum quenching approaches against bacterial-biofilm-induced antibiotic resistance. *Antibiotics, 13*(7), Article 619. doi:10.3390/antibiotics13070619

Demiriz Yücer, T. (2023). Contents of fatty acid in Gomphonema olivaceum. *Gaziosmanpaşa Bilimsel Araştırma Dergisi, 12*(2), 73–79. Retrieved from https://dergipark.org.tr/tr/pub/gbad/article/1289262

Demiriz Yücer, T. (2024). Fatty acids, vitamins and antioxidant properties of Cladophora fracta var. intricata. *Journal of the Institute of Science and Technology, 14*(1), 87–95. doi:10.21597/jist.1362003

Desbois, A., & Smith, V. (2010). Antibacterial free fatty acids: Activities, mechanisms of action and biotechnological potential. *Applied Microbiology and Biotechnology, 85*(6), 1629–1642. doi:10.1007/s00253-009-2355-3

EL-Sayed, A., El-Sheekh, M., & Makhlof, M. (2023). Synergistic antibacterial effects of Ulva lactuca methanolic extract alone and in combination with different antibiotics on multidrug-resistant Klebsiella pneumoniae isolate. *BMC Microbiology, 23*, Article 106. doi:10.1186/s12866-023-02854-5

Flemming, H., Wingender, J., Szewzyk, U., Steinberg, P., & Rice, S. (2016). Biofilms: An emergent form of bacterial life. *Nature Reviews Microbiology, 14*(9), 563–575. doi:10.1038/nrmicro.2016.94

Gupta, S. (2011). Bioactive potential and possible health effects of edible brown seaweeds. *Trends in Food Science & Technology, 22*(6), 315–326. doi:10.1016/j.tifs.2011.03.011

Hall, C., & Mah, T. (2017). Molecular mechanisms of biofilm-based antibiotic resistance and tolerance in pathogenic bacteria. *FEMS Microbiology Reviews, 41*(3), 276–301. doi:10.1093/femsre/fux010

Investigation (in-vitro) of antiproliferative properties of Pseudopediastrum boryanum (Turpin) E. Hegewald extracts in various cancer cell lines. (2024). *Kahramanmaraş Sütçü İmam Üniversitesi Tarım ve Doğa Dergisi, 27*(5), 1026–1031. doi:10.18016/ksutarimdoga.vi.1420650

Liu, H., Prentice, E., & Webber, M. (2024). Mechanisms of antimicrobial resistance in biofilms. *npj Antimicrobials and Resistance, 2*, Article 27. doi:10.1038/s44259-024-00046-3

Newman, D., & Cragg, G. (2020). Natural products as sources of new drugs over the nearly four decades from 01/1981 to 09/2019. *Journal of Natural Products, 83*(3), 770–803. doi:10.1021/acs.jnatprod.9b01285

Pabuçcu, K. (2022). Spirogyra aequinoctialis'in farklı çözgenler ile hazırlanan ekstraktlarının antibakteriyal ve antifungal etkileri. *Kahramanmaraş Sütçü İmam Üniversitesi Tarım ve Doğa Dergisi, 25*(5), 927–932. doi:10.18016/ksutarimdoga.vi.979361

Polyphenols as antimicrobial agents. (2012). *Current Opinion in Biotechnology, 23*(2), 174–181. doi:10.1016/j.copbio.2011.08.007

Ren, J., Wang, M., & Zhou, W. (2024). Efflux pumps as potential targets for biofilm inhibition. *Frontiers in Microbiology, 15*, Article 1315238. doi:10.3389/fmicb.2024.1315238

Shannon, E. (2016). Antibacterial derivatives of marine algae: An overview of pharmacological mechanisms and applications. *Marine Drugs, 14*(4), Article 81. doi:10.3390/md14040081

Silva, A., Silva, S., Carpena, M., Garcia-Oliveira, P., Gullón, P., Barroso, M., & Prieto, M. (2020). Macroalgae as a source of valuable antimicrobial compounds: Extraction and applications. *Antibiotics, 9*(10), Article 642. doi:10.3390/antibiotics9100642

Uç, O. (2024). Vaucheria frigida (Roth) C. Agardh'ın antioksidan ve antibakteriyel özellikleri. *Gaziosmanpaşa Bilimsel Araştırma Dergisi, 13*(2), 12–20. Retrieved from https://dergipark.org.tr/en/pub/gbad/issue/88124/1495261

Uç, O. (2026). Antioxidant and antimicrobial activities and phenolic composition of Vaucheria aversa isolated from the Tigris River (Diyarbakır, Türkiye). *Kahramanmaraş Sütçü İmam Üniversitesi Tarım ve Doğa Dergisi, 29*(6), 1392–1401. doi:10.18016/ksutarimdoga.vi.1786253

Ventola, C. (2015). The antibiotic resistance crisis: Part 1: Causes and threats. *P&T, 40*(4), 277–283. Retrieved from https://pmc.ncbi.nlm.nih.gov/articles/PMC4378521/

World Health Organization. (2024). *WHO bacterial priority pathogens list, 2024: Bacterial pathogens of public health importance to guide research, development and strategies to prevent and control antimicrobial resistance.* Retrieved from https://iris.who.int/bitstream/handle/10665/376776/9789240093461-eng.pdf

Zuorro, A., Lavecchia, R., Contreras-Ropero, J., García Martínez, J., Barajas-Ferreira, C., & Barajas-Solano, A. (2024). Natural antimicrobial agents from algae: Current advances and future directions. *International Journal of Molecular Sciences, 25*(21), Article 11826. doi:10.3390/ijms252111826

BÖLÜM 2

PLANT-DERIVED CARBON DOTS FOR DRUG DELIVERY AND BIOPHARMACEUTICAL APPLICATIONS

ASLIHAN CESUR TURGUT[1]

Introduction

An active compound can produce a promising response in a biological assay without being delivered effectively by a pharmaceutical formulation. The relevant delivery question is whether the final preparation provides an appropriate exposure at the intended site for a useful duration. For botanical carbon dots, that question involves the associated drug, the carbon-containing carrier, and any soluble constituents that remain after preparation. Each can contribute to the observed response and each may follow a different biological path.

There are also two distinct pharmaceutical roles to consider. A dot may have intrinsic activity after a botanical precursor has been transformed, or it may carry a separately supplied therapeutic compound. The distinction is practical: the dose and molecular identity of a loaded drug can be measured independently, whereas

[1] Assoc. Prof. Dr., Burdur Mehmet Akif Ersoy University,Department of Plant and Animal Production, Orcid: 0000-0002-5824-971X

activity assigned to a carbonized botanical preparation requires evidence about the active fraction. A study of Plantago major-derived dots that examined purification alongside biological responses illustrates the importance of defining the preparation being tested, without establishing a general drug-carrier function for such materials (Altinkaya, 2025, p. 1).

This chapter examines drug loading, release, barrier transport, tissue distribution, and elimination as connected formulation questions. It is a critical narrative review of selected primary research rather than a systematic assessment of all reported carbon-dot carriers. Whole-plant-derived examples and isolated-phytochemical-derived systems are identified separately. Studies of synthetic or carbohydrate-derived dots are included where they provide mechanistic or analytical comparisons; their results are not treated as direct validation of medicinal-plant-derived formulations.

The available examples mainly address experimental formulations and preclinical models. The proposed evaluation steps are intended to help design interpretable studies, with the required evidence determined by the route and target. A local skin formulation may benefit from retention, whereas a systemic preparation must establish absorption or tissue exposure beyond the initial barrier. The same material characteristic can therefore have different implications for different delivery objectives.

Defining a Botanical Carbon-Dot Formulation

Precursor class and carrier identity

The carbon-dot designation includes structurally diverse products. Precursor-dependent classifications distinguish materials with different carbonized and polymer-like features, so fluorescence alone is insufficient to establish a specific subtype (Zeng et al., 2021, p. 1). This chapter uses carbon dot as the broad designation and retains more specific terminology only when describing a

publication that used it. Quantum confinement is not assumed for every botanical dispersion.

The botanical contribution should also be stated precisely. A carrier prepared from plant tissue or extract differs from one synthesized using an isolated phytochemical. A drug added after synthesis is a cargo rather than proof that the same molecule survived carbonization. For every delivery preparation, the proposed record should identify the plant species or molecular precursor, any co-precursor, the purified carrier, the added drug, and the procedure used to obtain the final formulation. A change in any of these elements may change the exposure being evaluated.

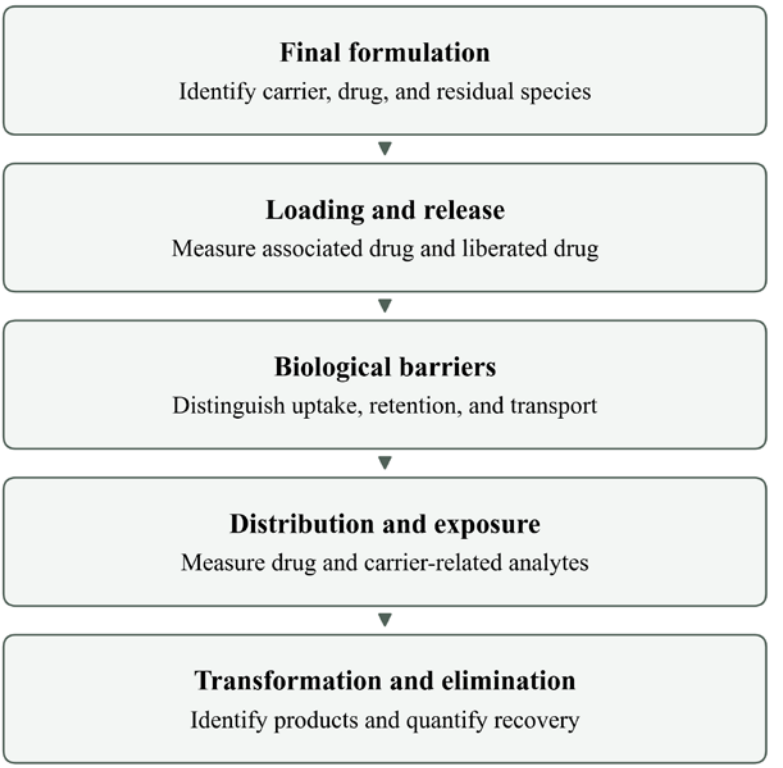
Purity and characterization of the administered material

Purification is part of formulation definition. A fluorescent reaction mixture may include molecular species as well as larger carbon-containing products, and these components can interact during separation. Research on purification and molecular fluorophores demonstrates why an optical signal must be interpreted with compositional evidence (Otten et al., 2022, p. 6148). This issue becomes particularly important when fluorescence is used to track an administered preparation.

The proposed characterization should therefore proceed beyond the unloaded stock. Dry-state morphology, hydrodynamic size, surface properties, drug integrity, and aggregation should be assessed for the final drug-loaded material under relevant medium conditions. Free drug and removable reaction products should be quantified or otherwise bounded by a validated separation method. Carrier concentration, drug concentration, and analytical recovery should remain identifiable throughout the study. These measurements provide the basis for interpreting the loading, transport, and fate experiments considered in the following sections.

Figure 1 summarizes the questions that connect formulation identity to biological fate. The arrows indicate a proposed assessment sequence rather than an experimentally established common pathway for all carbon dots. Drug and carrier-related measurements remain distinct at each stage.

Figure 1. Proposed assessment sequence for a drug-loaded botanical carbon-dot formulation.



Source: Conceptual assessment scheme developed by the author, informed by experimental studies of release, barrier transport, distribution, and clearance (Liao et al., 2021, p. 1; Licciardello et al., 2018, p. 9880; Modi & Anderson, 2013, p. 3076; Seven et al., 2021, p. 3942). Arrows represent assessment steps rather than a universal biological pathway.

Drug Loading and Controlled Release

Loading strategy and quantitative definitions

A biopharmaceutical assessment asks whether a formulation delivers an active substance to its intended site at an appropriate concentration and time. For botanical carbon dots, this requires separating the activity of the carrier from that of an externally loaded drug. Surface adsorption, covalent attachment, and incorporation into a larger composite should be described according to the preparation and analytical evidence. A carbonized phytochemical is not automatically equivalent to a carrier loaded with the intact parent compound. The proposed development strategy in this chapter therefore begins with identifying the drug, the purified carrier, and the final drug–carrier preparation as separate analytical samples.

Two quantities are particularly useful: loading efficiency, calculated as the mass of associated drug divided by the initially supplied drug mass, and loading content, calculated as the associated drug mass divided by the mass of the final drug–carrier material. Both can be expressed as percentages, but a drug-to-carrier mass ratio has a different denominator. These definitions must accompany reported values. In a curcumin–carbon-nanodot study, adsorption efficiencies of 91% and 82% coexisted with capacities of approximately 3.4–3.8% relative to carrier mass. This illustrates why efficient capture of the supplied drug does not necessarily mean that drug constitutes a large fraction of the administered formulation (Arvapalli et al., 2020, p. 8776).

For future botanical formulations, the author proposes validating drug quantification after removal of free drug, with recovery experiments and controls for carbon-dot interference. Chromatography can provide an independent measurement when fluorescence or ultraviolet absorbance overlaps with the carrier signal. A formulation record should include carrier mass, drug mass,

purification losses, and the stability of the associated drug during storage and incubation. Biological comparisons should use matched drug doses and report the accompanying carrier dose; otherwise, apparent improvements may reflect unequal exposure.

Botanical examples and acid-dependent release

Direct botanical examples support further investigation. Carbon dots prepared from bamboo leaves were used to carry curcumin, with enhanced release under a pH 5.5 test condition and greater cytotoxic responses in cultured cancer cells than those obtained with free curcumin. The reported experimental scope supports an in vitro delivery application, while a claim of improved systemic bioavailability would require additional pharmacokinetic measurements (Saini et al., 2025, p. 2282).

In another study, carbon dots derived from *Artemisia argyi* were loaded with doxorubicin. Reported loading efficiency and loading content were 66.4% and 57.1%, respectively. At 56 hours, cumulative release was 56.55% at pH 4.0 and 6.81% at pH 7.4, and the formulation was evaluated in a mouse hepatocellular carcinoma model. These findings establish acid-dependent release for the tested preparation; pH 4.0 should be interpreted as a strongly acidic experimental condition rather than assumed to represent the extracellular environment of every tumor. The animal results remain preclinical evidence (Jia et al., 2025, p. 37645).

Taken together, these examples motivate a formulation question: does drug association improve exposure under the intended route and biological conditions? The answer should be based on the final loaded preparation. Particle size, surface charge, aggregation, and drug integrity should be reassessed after loading rather than carried over from measurements of the unloaded dots.

Release testing and interpretation of kinetics

A slow concentration increase outside a dialysis membrane does not by itself demonstrate slow release from the carrier. Dynamic dialysis contains two sequential processes: liberation of drug from the formulation and transport of unbound drug through the membrane. Experimental and modeling work on nanoparticle release has shown that membrane transport and drug binding can distort the apparent release profile. Although that work examined other nanoparticle systems, its methodological lesson is relevant to carbon-dot formulations (Modi & Anderson, 2013, p. 3076).

The proposed assessment should therefore include a free-drug membrane control, recovery from the apparatus, suitable receiving-medium capacity, and correction for sampling and replacement volumes. Drug stability should be measured over the full experiment. Release profiles at different pH values should use comparable assay conditions, and a physiologically relevant protein-containing medium should be considered when feasible. Testing more than one carrier concentration can help identify concentration-dependent binding or aggregation.

Kinetic fitting should be used to summarize observations and compare plausible explanations. A high correlation coefficient for a selected equation is insufficient to establish diffusion, erosion, or a specific bond-cleavage mechanism. For a controlled-release claim, the useful endpoint is reproducible, formulation-dependent release with an identified practical benefit. For a targeting claim, additional evidence must link release to exposure and response at the intended site.

Transport Across Biological Barriers

Cellular uptake, protein adsorption, and epithelial transport

Cellular fluorescence can show that a signal associates with or enters cells, but it does not establish passage through an epithelial or endothelial barrier. A barrier assessment should distinguish surface adhesion, intracellular retention, movement to the opposite compartment, and delivery of an active payload. For the botanical systems considered here, the author proposes combining microscopy with drug quantification in donor and receiver compartments and a measurement of barrier integrity. Cell viability, electrical resistance where applicable, and an independent permeability tracer can help identify transport caused by barrier injury.

Biological exposure also changes the interface presented by a carbon dot. In a study of four amine-passivated carbon-dot preparations, serum protein adsorption depended on surface properties and was associated with differences in macrophage uptake and viability. This is mechanistic evidence from nonbotanical formulations; it supports testing protein interactions in botanical candidates rather than assuming that botanical origin predicts their behavior in serum (Arezki et al., 2022, p. 14695). The final drug-loaded formulation should be examined because its surface can differ from that of the unloaded carrier.

Mucus and skin as route-specific barriers

Mucosal delivery illustrates a trade-off between interaction and movement. A surface that binds strongly to biological material may favor retention but also restrict access to underlying cells. Engineered carbon dots prepared from citric acid and polyethyleneimine were investigated with polyethylene glycol, zwitterionic, and thiol-containing modifications. Their performance in mucus models and an airway epithelial model differed, and improved movement through mucus did not uniformly produce

stronger gene expression. The study shows why barrier transit and successful cargo delivery require separate endpoints; it is not direct evidence for whole-plant-derived dots (Arca et al., 2025, p. 1).

For a botanical formulation intended for a mucosal route, the proposed evaluation should use relevant mucus composition and an epithelial system that reflects that route. Carrier-associated signal, released drug, epithelial transport, and the intended pharmacological response should be measured separately. Residence time may be desirable for a local treatment, whereas a systemic formulation requires evidence of absorption beyond the epithelial surface. These are different development objectives.

Skin delivery likewise needs an explicit target. Carbon dots synthesized from epigallocatechin-3-gallate were incorporated into a hydrogel and investigated in a mouse model of atopic dermatitis, including epidermal penetration and anti-inflammatory responses. This example connects phytochemical-derived dots with local biological activity, rather than demonstrating delivery of an independently loaded drug. Penetration in diseased mouse skin should not be generalized to intact human skin or taken as proof of systemic transdermal absorption (Han et al., 2024, p. 24308).

For topical development, the author proposes measuring retention in the relevant skin layers and passage into the receiving compartment of a validated diffusion experiment. Comparisons with free active compound, unloaded carrier, and the vehicle can distinguish formulation effects. The preferred outcome should match the product objective: local skin retention, delivery to a deeper tissue, or systemic absorption.

The blood–brain barrier and limits of mechanistic inference

Glucose-derived carbon dots conjugated to fluorescein were investigated for cargo delivery across the blood–brain barrier in zebrafish and rats. The same study used glucose-transporter-positive

and transporter-deficient yeast to examine uptake. The yeast findings support a transporter-related uptake hypothesis in that experimental system, but they do not independently establish the transport mechanism at the rat blood–brain barrier. Moreover, fluorescein delivery is a probe-based demonstration rather than evidence of therapeutic efficacy in neurological disease (Seven et al., 2021, p. 3942).

For botanical carbon dots, a brain-delivery claim would require evidence specific to the tested formulation. A proposed sequence is to establish barrier integrity in a relevant model, quantify transport of both carrier and payload, and then distinguish vascular association from brain-tissue exposure in vivo. An observed brain signal should be interpreted alongside label stability and appropriate controls. Botanical origin and a small dry-state particle diameter are insufficient substitutes for these measurements.

Biodistribution and Pharmacokinetic Evaluation

Measuring drug and carrier exposure separately

The biological fate of a loaded preparation can differ from that of its free drug or unloaded carrier. This distinction is especially important when drug loading changes surface properties. In a sucrose- and serine-derived carbon-dot formulation for doxorubicin delivery, drug loading changed the reported zeta potential from approximately −14 to +58 mV. The study evaluated antitumor effects in a mouse renal carcinoma model, while biodistribution imaging used a dye-loaded preparation. Consequently, the imaging construct and therapeutic formulation should not be assumed to have identical behavior solely because they share the same carbon-dot precursor (Azmi et al., 2025, p. 2751).

The proposed pharmacokinetic strategy should measure drug concentration over time and, where analytically feasible, distinguish carrier-associated drug from released drug. Area under the

concentration–time curve, elimination half-life, clearance, and distribution volume should be calculated from an appropriate sampling design and explicitly identified analyte. Comparisons should match administration route and drug dose. Carrier exposure should be reported independently, with a validated method and its recovery limits. A separation procedure that changes drug binding during sample processing can itself bias the apparent free-drug fraction.

Organ localization and the limits of imaging

Whole-body fluorescence is useful for locating a detectable signal, but signal intensity is not automatically proportional to the amount of intact carrier. Tissue attenuation, local chemical conditions, degradation, and release of a fluorescent label can complicate interpretation. Complementary labeling approaches can strengthen an assessment: a primary study combined optical labeling and copper-64 radiolabeling to investigate ultrasmall carbon dots and silicon nanoparticles in animals. Their surface characteristics affected biological behavior, reinforcing the need for formulation-specific measurements rather than a universal fate assigned to all small dots (Licciardello et al., 2018, p. 9880).

For future botanical studies, the author proposes sampling plasma, the target tissue, and plausible clearance organs at defined intervals, with tissue blanks and calibration appropriate to each matrix. A stable label should be checked under the same exposure conditions as the formulation. Tissue drug concentration and tissue carrier-associated signal answer different questions and should be reported as such. Improved target exposure should also be linked to an independently measured biological response. Localization alone cannot establish active targeting, intracellular release, or a favorable therapeutic margin.

Metabolism and Excretion

Renal and hepatobiliary pathways

Carbon-dot clearance depends on the administered construct, including its hydrated dimensions, surface chemistry, protein interactions, and aggregation state. Transmission electron microscopy describes a dry-state core and cannot alone establish renal filterability of the loaded formulation. An instructive comparison involved approximately 100 nm polyethyleneimine-crosslinked assemblies containing multiple carbon dots. Imaging supported hepatobiliary transport and fecal elimination of these assemblies, whereas the individual polyethyleneimine-passivated dots showed a different clearance pattern. This synthetic system demonstrates that incorporating small dots into a larger construct can change biological fate; it does not provide a clearance rule for medicinal-plant-derived dots (Liao et al., 2021, p. 1).

The sucrose-derived doxorubicin study provides a further interpretive caution. Although its title describes renal-clearable carbon dots, the reported biodistribution imaging of dye-loaded material does not, by itself, quantify the fraction of intact drug-loaded dots eliminated in urine. Kidney-associated signal and urinary excretion are distinct endpoints (Azmi et al., 2025, p. 2751). A botanical candidate should therefore undergo direct collection and analysis of excreta if renal clearance is a central development claim.

Chemical transformation and an evidence-based mass balance

Loss of fluorescence should not be equated with carbon-dot degradation. A signal may decrease because of quenching, redistribution, chemical alteration of the fluorophore, or elimination of a label. Conversely, a persistent signal does not establish that the original carrier remains chemically intact. Claims of biodegradation require analytical evidence that identifies the material remaining and

its transformation products. The plant origin of a precursor does not demonstrate degradability of the carbonized product.

As an author-proposed framework, urine and feces should be collected at defined intervals and analyzed for carrier-related material, drug, and identifiable drug metabolites. Recovery should be expressed relative to administered dose, with the analytical method, label stability, and unrecovered fraction stated. Measurements in plasma and tissues should complement excreta data rather than substitute for them. If intact particles cannot be distinguished from soluble products, the result should be described as elimination of measured carrier-related species. Repeated exposure also warrants examination when the intended formulation is administered more than once.

Table 1 translates these considerations into practical questions for botanical carbon-dot development. It is a proposed evaluation framework, not a claim that every reviewed preparation has already satisfied these requirements. Its purpose is to connect material identity and formulation behavior with interpretable exposure and elimination data.

Table 1. Proposed biopharmaceutical evaluation framework for botanical carbon-dot formulations.

Development question	Measurements to consider	Interpretation supported
How much drug is associated?	Validated drug assay, free-drug removal, recovery, and stated mass denominators	Loading efficiency and content are distinguished
Is release formulation-dependent?	Free-drug control, membrane calibration, medium conditions, and drug stability	Carrier release is separated from assay limitations
Does the payload cross a barrier?	Receiver-side drug assay, carrier tracking, barrier integrity, and viability	Transport is distinguished from retention or injury

Development question	Measurements to consider	Interpretation supported
Where do drug and carrier distribute?	Plasma and tissue time courses, matrix calibration, and label stability	Analyte-specific exposure is established
Which species leave the body?	Interval urine and feces collection; drug, metabolite, and carrier-related assays	Elimination is distinguished from organ localization
Is the material chemically transformed?	Orthogonal identification of residual carrier and transformation products	Degradation is distinguished from signal loss

Source: Biopharmaceutical evaluation framework developed by the author, informed by studies of release methods, protein interactions, barrier transport, and biological fate (Arezki et al., 2022, p. 14695; Liao et al., 2021, p. 1; Licciardello et al., 2018, p. 9880; Modi & Anderson, 2013, p. 3076; Seven et al., 2021, p. 3942).

Biocompatibility and Therapeutic Interpretation

A delivery formulation should improve a defined exposure or response without introducing an unacceptable biological effect at the intended dose. This requires comparisons among free drug, unloaded carrier, and the loaded preparation, together with the formulation vehicle when relevant. Drug-equivalent comparisons are essential for evaluating therapeutic effects, while carrier-equivalent comparisons help identify carrier-associated effects. The author proposes stating both dose quantities and the exposure duration for every biological test.

Biocompatibility cannot be transferred from one carbon-dot family to another. In the study of polyethyleneimine-containing assemblies, the larger multiple-dot construct and the individual passivated dots differed in biological behavior and compatibility. That finding concerns the specific materials studied rather than a general safety advantage of carbon dots (Liao et al., 2021, p. 1). Protein adsorption and macrophage responses in a separate surface-charge study further support evaluating the biological interface of the actual formulation (Arezki et al., 2022, p. 14695).

The next experimental step should be chosen according to the intended use. For a local formulation, tissue compatibility and drug retention should be assessed together with the desired local response. For a systemic formulation, plasma and target-tissue exposure should accompany efficacy measurements, with clearance organs included where appropriate. Relevant empty-carrier controls and optical-interference controls remain necessary when the preparation itself is fluorescent or biologically active. An improved response in cultured cells does not establish improved systemic bioavailability, and a favorable animal result does not define suitability for human use.

Development Priorities and Future Perspectives

The most useful development pathway begins with the target and route, then identifies the measurements needed to test the formulation hypothesis. For example, a release design should specify where release is expected, what exposure duration is useful, and how the drug remains chemically active during that period. Barrier experiments should then establish whether the payload reaches the relevant compartment, followed by studies that connect drug and carrier exposure with the intended response. This sequence is proposed as a research strategy rather than evidence that current botanical formulations already meet each requirement.

Reproducibility should be examined at the level of the administered preparation. Independent botanical feedstock lots and synthesis batches should be carried through purification, drug loading, and biological testing. Release and exposure measurements should use a stable dose definition so that batch variation is distinguishable from analytical variation. A highly fluorescent batch is not necessarily the batch with the most useful loading, tissue exposure, or elimination behavior.

Future work would be strengthened by measurements that connect the different stages of delivery in the same formulation. Plasma drug analysis, carrier tracking, target-tissue assessment, and excreta collection can then be interpreted together rather than assembled from experiments using different labels or surface modifications. Where direct identification of the intact carrier is technically limited, the measured species and analytical uncertainty should be reported explicitly. A meaningful development decision depends on knowing which component reached a site and which component left the body.

Conclusion

Botanical carbon dots offer a basis for investigating pharmaceutical delivery, with selected studies demonstrating drug association, condition-dependent release, and biological responses in experimental systems. Their usefulness as carriers depends on the final drug-loaded preparation and on the route-specific delivery problem. Material characterization, loading definitions, and validated analytical methods are therefore part of the biopharmaceutical assessment rather than preliminary descriptive exercises.

The most defensible interpretation links release to barrier transport, drug and carrier exposure, and measured elimination. Cellular uptake, tissue fluorescence, and kidney localization each provide information, but they resolve different questions. Mechanistic studies of other carbon-dot systems help identify useful controls without establishing a universal behavior for botanical formulations. Progress requires studies that maintain the identity of the tested preparation across these stages and connect its biological fate with a reproducible therapeutic objective.

References

Altinkaya, E. (2025). Single-step hydrothermal synthesis of *Plantago major*-based carbon dots: Therapeutic and antimicrobial properties. *Diamond and Related Materials, 158*, Article 112624. https://doi.org/10.1016/j.diamond.2025.112624

Arca, S., Pons, F., & Lebeau, L. (2025). Engineered carbon dots for mucosal gene delivery. *European Journal of Pharmaceutical Sciences, 213*, Article 107222. https://doi.org/10.1016/j.ejps.2025.107222

Arezki, Y., Delalande, F., Schaeffer-Reiss, C., Cianférani, S., Rapp, M., Lebeau, L., Pons, F., & Ronzani, C. (2022). Surface charge influences protein corona, cell uptake and biological effects of carbon dots. *Nanoscale, 14*(39), 14695–14710. https://doi.org/10.1039/d2nr03611h

Arvapalli, D. M., Sheardy, A. T., Allado, K., Chevva, H., Yin, Z., & Wei, J. (2020). Design of curcumin loaded carbon nanodots delivery system: Enhanced bioavailability, release kinetics, and anticancer activity. *ACS Applied Bio Materials, 3*(12), 8776–8785. https://doi.org/10.1021/acsabm.0c01144

Azmi, F., Xu, X., Duong, H., Ye, P., Chen, T., Li, H., Chen, J., Ardekani, S. M., Dehghani, A., Zheng, G., Harris, D., Lu, H., Wang, Y., & Cao, Q. (2025). Renal clearable sucrose carbon dots for doxorubicin delivery to treat renal carcinoma. *Nanoscale Advances, 7*(9), 2751–2760. https://doi.org/10.1039/d4na01082e

Han, J., Choi, S., Hong, J., Gang, D., Lee, S., Shin, K., Ko, J., Kim, J.-U., Hwang, N. S., An, Y.-H., Gu, M., & Kim, S.-H. (2024). Superoxide dismutase-mimetic polyphenol-based carbon dots for multimodal bioimaging and treatment of atopic dermatitis. *ACS Applied Materials & Interfaces, 16*(19), 24308–24320. https://doi.org/10.1021/acsami.4c02634

Jia, R., Liu, P., Gong, Y., Gao, Y., Xiong, Y., Song, X., Peng, J., Lan, M., & Shi, X. (2025). pH-responsive doxorubicin-loaded *Artemisia argyi* carbon dots: Enhanced targeted therapy for hepatocellular carcinoma. *RSC Advances, 15*(45), 37645–37659. https://doi.org/10.1039/d5ra05688h

Liao, J., Yao, Y., Lee, C.-H., Wu, Y., & Li, P. (2021). In vivo biodistribution, clearance, and biocompatibility of multiple carbon dots containing nanoparticles for biomedical application. *Pharmaceutics, 13*(11), Article 1872. https://doi.org/10.3390/pharmaceutics13111872

Licciardello, N., Hunoldt, S., Bergmann, R., Singh, G., Mamat, C., Faramus, A., Ddungu, J. L. Z., Silvestrini, S., Maggini, M., De Cola, L., & Stephan, H. (2018). Biodistribution studies of ultrasmall silicon nanoparticles and carbon dots in experimental rats and tumor mice. *Nanoscale, 10*(21), 9880–9891. https://doi.org/10.1039/c8nr01063c

Modi, S., & Anderson, B. D. (2013). Determination of drug release kinetics from nanoparticles: Overcoming pitfalls of the dynamic dialysis method. *Molecular Pharmaceutics, 10*(8), 3076–3089. https://doi.org/10.1021/mp400154a

Otten, M., Hildebrandt, M., Kühnemuth, R., & Karg, M. (2022). Pyrolysis and solvothermal synthesis for carbon dots: Role of purification and molecular fluorophores. *Langmuir, 38*(19), 6148–6157. https://doi.org/10.1021/acs.langmuir.2c00508

Saini, A., Nandi, A., Gupta, G. D., Sharma, A., & Sharma, K. (2025). Green synthesis of curcumin loaded carbon dots as a sustained drug delivery for anticancer therapy. *Current Pharmaceutical Design, 31*(28), 2282–2289. https://doi.org/10.2174/0113816128353103250116112919

Seven, E. S., Seven, Y. B., Zhou, Y., Poudel-Sharma, S., Diaz-Rucco, J. J., Kirbas Cilingir, E., Mitchell, G. S., Van Dyken, J. D., & Leblanc, R. M. (2021). Crossing the blood–brain barrier with carbon dots: Uptake mechanism and in vivo cargo delivery. *Nanoscale Advances, 3*(13), 3942–3953. https://doi.org/10.1039/d1na00145k

Zeng, Q., Feng, T., Tao, S., Zhu, S., & Yang, B. (2021). Precursor-dependent structural diversity in luminescent carbonized polymer dots (CPDs): The nomenclature. *Light: Science & Applications, 10*(1), Article 142. https://doi.org/10.1038/s41377-021-00579-6

BÖLÜM 3

ANTIMICROBIAL AND ANTIOXIDANT POTENTIAL OF CARBON DOTS DERIVED FROM MEDICINAL AND AROMATIC PLANTS

ASLIHAN CESUR TURGUT[1]

Introduction

The scientific value of converting medicinal and aromatic plants into carbon nanomaterials extends beyond obtaining a fluorescent product from an inexpensive feedstock. Botanical resources contain multiple classes of carbon-containing constituents, and processing can redistribute these constituents into new molecular and particulate forms. Consequently, the relevant research question is whether the transformation produces a reproducible material with a biological function that can be distinguished from the activity of the original extract.

Early investigations established fluorescent carbon-containing species during carbon nanotube purification and subsequently demonstrated strongly luminescent carbon dots following surface passivation. These studies provide historical foundations, but they do not establish the identity or biological

[1] Assoc. Prof. Dr., Burdur Mehmet Akif Ersoy University,Department of Plant and Animal Production, Orcid: 0000-0002-5824-971X

behavior of every modern biomass-derived product (Sun et al., 2006, p. 7756; Xu et al., 2004, p. 12736). Plant-based preparations therefore require their own chemical and functional evidence.

The present chapter is a critical narrative review of selected experimental studies and foundational methodological papers, rather than an exhaustive systematic review. Its scope includes medicinal and aromatic plant biomass, selected plant-processing residues, isolated botanical compounds used as precursors, and related composite systems where the distinction is scientifically informative. Tea and apple residues are included as contextual examples of biomass valorization. They should not be treated as interchangeable with every medicinal or aromatic plant feedstock.

A central interpretive problem is the coexistence of antioxidant and antimicrobial claims. Radical scavenging may protect a material or biological system from oxidative damage, whereas some antimicrobial preparations act by increasing oxidative injury. These functions need not be mutually exclusive, but each must be demonstrated under defined conditions. This chapter develops a framework in which precursor chemistry, processing, purification, surface structure, biological environment, and formulation are examined together.

Terminology and Material Identity

Carbon dots and carbon quantum dots

Carbon dots (CDs) form a broader family than carbon quantum dots (CQDs). Structural discussions distinguish graphene quantum dots, CQDs, and carbonized polymer dots, with the latter retaining substantial polymer-like features. Nomenclature varies across publications; Zeng and colleagues explicitly emphasized precursor-dependent structural diversity in their proposed classification (Zeng et al., 2021, p. 1). A fluorescent plant-derived

dispersion should therefore not be assigned to a particular subtype solely because it emits visible light.

In this chapter, CD is used where the available evidence supports a carbon-dot designation but does not resolve the subtype. CQD is retained when discussing studies using that terminology, without implying that quantum confinement has been independently demonstrated. This distinction matters because a material dominated by molecular fluorophores or partially carbonized polymers may behave differently from a more extensively carbonized particle.

Botanical origin describes more than one material class

Three frequently conflated systems should be separated. Whole-plant or extract-derived dots arise from the transformation of a chemically mixed botanical feedstock. Phytochemical-derived dots are prepared from an isolated compound, often together with another reagent. Botanical-active composites contain a plant compound added to a dot or polymer system after, or alongside, material preparation. Tea-derived dots loaded with curcumin illustrate the composite category, while curcumin combined with ethylenediamine provides an example of a phytochemical-based mixed precursor system (Miao et al., 2025, p. 1; Wen et al., 2023, p. 1).

Table 1. Material classes used in the evaluation of botanical carbon-dot systems.

Material class	Origin of the carbon-dot fraction	Main attribution question	Representative study
Mixed botanical precursor	Plant tissue or extract transformed during synthesis	Does activity remain in the purified particulate fraction?	Turmeric leaves; (Saravanan et al., 2021, p. 1)

Material class	Origin of the carbon-dot fraction	Main attribution question	Representative study
Isolated phytochemical precursor	Purified plant compound, with or without a co-precursor	What contributions arise from the phytochemical and added reagent?	Curcumin/ethylene diamine; (Miao et al., 2025, p. 1)
Botanical-active composite	Dots combined with an externally supplied plant active	Is the response caused by the dots, cargo, or their combination?	Tea dots/curcumin; (Wen et al., 2023, p. 1)
Dot-containing formulation	Previously prepared dots incorporated into a film or carrier	Does the formulation preserve activity and alter exposure?	Rosemary-dot biopolymer films; (Rodríguez-Varillas et al., 2022, p. 1)

Source: Author's classification based on selected studies (Miao et al., 2025, p. 1; Rodríguez-Varillas et al., 2022, p. 1; Saravanan et al., 2021, p. 1; Wen et al., 2023, p. 1).

Table 1 is an interpretive classification developed for this chapter; it is not a replacement for structural CD nomenclature. Keeping these categories separate prevents an improvement obtained by loading curcumin from being attributed automatically to intrinsic activity of the unloaded dots.

Medicinal and Aromatic Plants as Precursors

Precursor composition and botanical authentication

The feedstock should be defined by species, plant part, collection or cultivation conditions, pretreatment, and extraction procedure. A label such as "plant-based CQDs" gives insufficient information for reproducibility. In the neem study of Gedda and colleagues, leaves were used to generate a fluorescent product evaluated for antioxidant and antimicrobial responses. Mardasi and colleagues compared *Salvia hydrangea* aerial material with plant cell cultures as alternative sources, demonstrating the value of

distinguishing precursor types within a single species (Gedda et al., 2023, p. 1; Mardasi et al., 2025, p. 1).

A useful precursor record would include a taxonomic identification, voucher information where available, moisture content, particle size after milling, and an analytical description of the starting extract. These are proposed reporting elements, not universal quality thresholds. Their purpose is to make it possible to identify whether changes in the final material originate from the biological feedstock or from processing.

Transformation is different from phytochemical preservation

Carbonization can reorganize the constituents of a botanical mixture. An FTIR band consistent with an oxygen-containing functional group does not identify a particular original phenolic compound. Claims that a plant active survives synthesis require direct molecular evidence or suitably designed comparison experiments. Chromatographic separation studies have shown that reaction mixtures can contain freely dissolved fluorophores, particle-associated fluorescent species, and less fluorescent carbon-rich fractions (Hinterberger et al., 2019, p. 8464; Otten et al., 2022, p. 6148).

The following questions provide a practical interpretation sequence: which constituents are present before processing; which soluble products remain after processing; what is associated with the isolated particulate fraction; and which fraction produces the measured activity? Answering them is more informative than describing all detected surface groups as preserved botanical bioactives.

Processing residues and sustainability

Plant residues can provide useful feedstocks, but waste utilization and environmental superiority are different claims. Murru

and colleagues studied dots prepared from tea and grape wastes, while Rodríguez-Varillas and colleagues evaluated rosemary- and apple-pomace-derived dots in biopolymer films (Murru et al., 2020, p. 1; Rodríguez-Varillas et al., 2022, p. 1). These examples establish possible routes for valorization; they do not by themselves quantify the environmental advantage of an entire production process.

For aromatic plants, post-distillation biomass is an attractive candidate for investigation. However, essential-oil extraction changes the feedstock, so results obtained with intact leaves should not be transferred directly to the spent biomass. A proposed sustainability assessment should account for drying energy, extraction inputs, reaction energy, purification water, material yield, and disposal of residual fractions. The preferred process would combine useful performance with a demonstrable reduction in resource burden.

Synthesis, Purification, and Reproducibility

Synthesis routes and their interpretation

Hydrothermal treatment is represented in several botanical studies, including turmeric leaves, rosemary leaves, and *Polygonatum kingianum* or *Gastrodia elata*. Neem-derived dots have also been reported using a sand-bath preparation. These methods differ in precursor handling and reaction environment and should not be described as chemically equivalent (Eskalen et al., 2021, p. 428; Gedda et al., 2023, p. 1; Saravanan et al., 2021, p. 1; Zhang et al., 2025, p. 23845).

For a comparative synthesis study, temperature, time, precursor loading, solvent composition, pH, and co-precursor ratio should be varied with a clearly stated objective. The highest fluorescence intensity need not identify the preparation with the strongest biological activity. Optical signal depends on emissive species and measurement conditions, while antimicrobial or

antioxidant responses depend on the composition and accessibility of reactive sites.

Microwave treatment and thermal routes may offer alternative processing strategies, but their suitability should be assessed using actual yield, energy input, product distribution, and biological performance. Short reaction time alone does not establish process efficiency. A convincing optimization compares purified materials at an equivalent, explicitly defined dose.

Purification as a scientific requirement

Purification determines what material is being tested. Centrifugation or a conventional syringe filter can remove large debris while leaving soluble metabolites and small reaction products in the dispersion. Dialysis, chromatography, or combinations of separation methods may be required, depending on the preparation. Hinterberger and colleagues resolved different fluorescent and particulate fractions chromatographically; Otten and colleagues examined interactions between molecular fluorophores and larger products during purification (Hinterberger et al., 2019, p. 8464; Otten et al., 2022, p. 6148).

The biological importance of purification is illustrated by a *Plantago major* study that examined filtration and dialysis in relation to therapeutic and antimicrobial properties (Altinkaya, 2025, p. 1). The general lesson is methodological: changing the separation procedure changes the tested mixture and may change the interpretation of its activity.

An informative experimental design would retain the crude product, purified retentate, and removed soluble fraction for parallel testing. If activity decreases after purification, this should prompt investigation of the active component rather than an assumption that purification damaged the dots. Conversely, persistent activity in a

purified fraction strengthens attribution, provided that residual contamination has been assessed.

Yield and batch consistency

A reproducible process needs a defined product yield and dose basis. The dry mass of a crude dispersion may contain salts, free metabolites, and other nonparticulate components. Reports should specify whether concentrations refer to crude solids, purified material, or another analytical measure. Independent synthesis batches should be characterized and tested separately; multiple measurements from one batch describe analytical repeatability, not manufacturing reproducibility.

Characterization Relevant to Biological Activity

A combined characterization strategy

Structural and chemical measurements should answer complementary questions. TEM provides information about particle morphology and dry-state dimensions. DLS describes hydrodynamic behavior in a dispersion; its result should not be treated as a second measurement of exactly the same quantity. FTIR supports functional-group analysis, while XPS adds surface-sensitive elemental and chemical-state information. Diffraction and Raman measurements can contribute evidence on carbon organization. Botanical studies using combinations of these methods show why multiple measurements are needed (Mardasi et al., 2025, p. 1; Saravanan et al., 2021, p. 1; Zhang et al., 2025, p. 23845).

The rosemary study reported a mean particle diameter of 16.13 nm, illustrating that materials described as CDs do not invariably fall within a strict sub-10-nm size convention (Eskalen et al., 2021, p. 428). A review should preserve such reported findings instead of forcing all preparations into one size definition.

Optical properties and purity

UV–visible absorption, excitation–emission measurements, fluorescence lifetime, and quantum yield describe optical behavior, but they do not independently establish a unique particle structure. Molecular fluorophores can remain associated with carbon-containing products or contribute to emission from the surrounding solution. Separation coupled with chemical analysis is therefore important when fluorescence is used to track material formation or biological uptake (Otten et al., 2022, p. 6148).

For bioimaging, a proposed control is to compare purified particles with the removed fluorescent fraction. Fluorescence within cells demonstrates uptake of an emissive species; establishing uptake of the intended nanomaterial requires additional evidence. Similarly, strong emission should not be presented as an indicator of high antioxidant or antimicrobial potency.

Characterization in the application medium

Measurements in water are a starting point. A formulation may expose the dots to electrolytes, proteins, surfactants, or polymer networks that alter their dispersion and available surface. The recommended characterization sequence therefore progresses from the purified stock to the biological test medium and finally to the intended formulation. Changes in size distribution, optical response, or surface charge should be considered alongside any change in biological performance.

Antioxidant Potential

Surface chemistry and proposed mechanisms

Antioxidant activity can involve reactions at surface sites and interactions with conjugated structures, but a single mechanism should not be assigned to every botanical dot. Ji and colleagues chemically modified carboxyl and amino groups to examine their

contributions to DPPH radical scavenging. Their results support involvement of these groups in direct or indirect hydrogen-transfer processes. Murru and colleagues considered several possible radical-scavenging pathways in biomass-derived preparations (Ji et al., 2019, p. 1; Murru et al., 2020, p. 1).

These studies support a structure–activity approach. For an uncharacterized botanical preparation, however, the presence of a hydroxyl or amino band is insufficient to quantify its contribution. Chemical modification, fractionation, and suitable reaction measurements provide stronger evidence than a correlation between an FTIR spectrum and an endpoint antioxidant percentage.

Chemical antioxidant assays

DPPH, ABTS, and FRAP evaluate different aspects of reactivity. The DPPH method monitors the response of a stable radical to an antioxidant. The improved ABTS assay uses a preformed radical cation, while FRAP measures ferric reduction under specified assay conditions. These foundational methods were developed independently and their numerical results are not interchangeable (Benzie & Strain, 1996, p. 70; Brand-Williams et al., 1995, p. 25; Re et al., 1999, p. 1231).

For carbon-dot samples, the proposed assay controls include a concentration-matched sample blank without the reporter reagent, a reagent control, and a reference antioxidant. Where appropriate, a second analytical readout should be used to test whether sample absorbance, fluorescence, scattering, or reporter interaction distorts the endpoint. A decrease in optical signal must be distinguished from a chemically verified decrease in the measured radical or oxidant.

Antioxidant percentages should always be linked to concentration, reaction time, solvent, and calculation method. IC50 and EC50 values require an explanation of the fitted response. Reporting a mass-based IC50 for a heterogeneous dot preparation

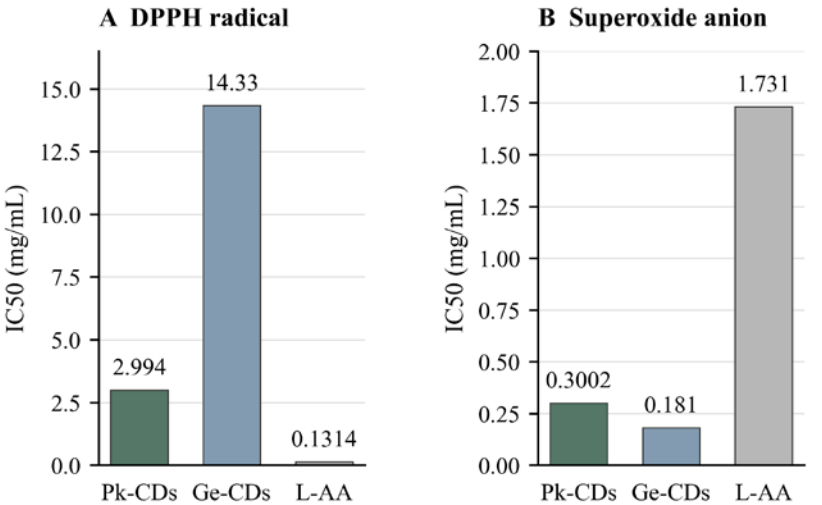
does not establish that it is intrinsically more effective than a molecular antioxidant measured on a molar basis.

Radical-dependent behavior and biological relevance

Different radicals can produce different rankings. In the experimental results of Zhang and colleagues, *P. kingianum*-derived dots showed a DPPH IC50 of 2.994 mg/mL, compared with 14.33 mg/mL for *G. elata*-derived dots. For superoxide scavenging, the respective reported IC50 values were 0.30 and 0.18 mg/mL. These outcomes favor different materials depending on the endpoint and argue against a single ranking of overall antioxidant superiority (Zhang et al., 2025, p. 23845).

Figure 1 makes the assay dependence of these comparisons visible and includes the molecular reference antioxidant used in the source study. The relative positions of the two dot preparations differ between the DPPH and superoxide assays, so the result should be interpreted within each assay rather than as a single ranking of biological antioxidant performance.

Figure 1. Assay-dependent antioxidant IC50 values for two botanical carbon-dot preparations and a reference antioxidant.



Source: Original plot prepared by the author using numerical values from the source study's Table 4 (Zhang et al., 2025, p. 23845). Pk-CDs: Polygonatum kingianum dots; Ge-CDs: Gastrodia elata dots; L-AA: L-ascorbic acid. Lower IC50 indicates greater activity within an assay. Panels use different y-axis scales; uncertainty estimates are not plotted.

Moving to a biological model requires evidence beyond a cell-free reaction. The same study examined oxidative-stress-associated markers in a D-galactose mouse model. Such findings extend the evidence within that particular model but do not establish clinical efficacy or safety for other exposure routes (Zhang et al., 2025, p. 23845).

For a proposed skin-related evaluation, chemically verified scavenging should be followed by a relevant cell model, a defined oxidative challenge, and measurements of both viability and oxidative damage. A lower ROS-probe signal is more persuasive when supported by an independent endpoint and when the material

has been tested for probe interference. Protection of cells, prevention of lipid oxidation, and stabilization of a cosmetic formulation are distinct outcomes and should be described separately.

Antimicrobial Potential

Membrane interactions and oxidative injury

Antimicrobial mechanisms may include surface association, membrane damage, and oxidative injury. Turmeric-leaf dots were reported to produce bactericidal responses involving ROS. Quaternized curcumin-derived dots were investigated for enhanced adherence to bacterial membranes, illustrating how an added surface functionality can influence the response (Saravanan et al., 2021, p. 1; Wu et al., 2022, p. 1).

These findings should not be generalized to every plant-derived dot. A proposed mechanistic evaluation combines viable counts with microscopy, membrane-permeability measurements, and tests of the suspected oxidative pathway. If ROS is proposed as the main cause of death, the timing and effect of pathway interventions should support causation. Observing a higher ROS-probe signal and fewer viable bacteria in parallel establishes an association but does not by itself identify the full killing mechanism.

Bacterial spectrum and resistant organisms

Different organisms and strains can respond differently to one preparation. Gram-positive and Gram-negative categories are useful descriptions, but they are insufficient predictors of susceptibility. Miao and colleagues studied curcumin/ethylenediamine-derived dots against *Escherichia coli*, *Pseudomonas aeruginosa*, and *Staphylococcus aureus*, including methicillin-resistant *S. aureus*. Their analysis included MIC determination, staining, morphological observations, and ROS-related measurements (Miao et al., 2025, p. 1).

Activity against a resistant strain establishes a relevant experimental result for that organism and test condition. It does not demonstrate that resistance cannot develop. A proposed resistance evaluation would examine multiple strains and repeated exposure, with appropriate comparators and clearly defined recovery conditions. Claims such as “resistance-free” should be limited to the experimental evidence actually obtained.

Antifungal activity and biofilms

Antifungal activity requires separate evaluation because fungal targets and growth conditions differ from bacterial ones. Neem-derived dots have been tested against bacterial and fungal strains using diffusion-based assays (Gedda et al., 2023, p. 1). Such results support further investigation, but a diffusion zone alone does not identify fungicidal activity or establish effectiveness against an established fungal biofilm.

For biofilm studies, prevention of attachment, reduction in total biomass, and killing within a mature biofilm should be treated as different endpoints. The proposed assessment combines a biomass measurement with viable recovery and, where useful, microscopy. A material may reduce matrix-associated staining without producing a corresponding decline in viable organisms; this possibility should be investigated rather than described automatically as eradication.

Light-dependent antimicrobial responses

Carbon-dot systems can also function as components of light-activated treatments. Yan and colleagues developed carbon-dot–curcumin nanocomposites with photodynamic and photothermal antibacterial properties. This study concerns an engineered composite and should not be used as evidence that every unloaded botanical dot produces the same light response (Yan et al., 2021, p. 6703).

A proposed factorial design includes untreated, light-only, material-only, and material-plus-light groups. Composite studies additionally require dots-only and active-only comparisons. Wavelength, irradiance, exposure time, delivered energy, and temperature should be reported. Separating light-driven chemistry from heating is particularly important when both photodynamic and photothermal effects are proposed.

Antimicrobial assay quality

MIC measurements require standardized growth conditions and a clear endpoint. EUCAST provides current recommendations for broth microdilution of aerobic and facultative anaerobic bacteria. These recommendations offer a methodological reference for controlling media, inoculum, and incubation, but clinical antibiotic breakpoints should not be transferred to an experimental carbon-dot preparation without validation (European Committee on Antimicrobial Susceptibility Testing, 2026, p. 1).

Carbon-dot assays also need controls for intrinsic color, turbidity, reporter interactions, and aggregation. MIC describes inhibition under the specified conditions; a bactericidal claim requires appropriate viable recovery evidence. Diffusion zones can be useful for screening, but the transport of the material through agar affects interpretation. Results from diffusion, broth inhibition, and time-kill experiments should therefore be reported with their own endpoint definitions.

Selected Experimental Studies and Comparative Interpretation

The studies in Table 2 illustrate distinct feedstocks and evidence types. They are selected examples, not a quantitative meta-analysis. Their concentrations, assays, organisms, and purification procedures differ, preventing a defensible pooled ranking.

Table 2. Selected botanical carbon-dot studies and the scope of their findings.

Precursor or system	Preparation and material evidence	Biological finding	Interpretive scope and reference
Curcuma longa leaves	Hydrothermal preparation; mean particle size 2.6 nm	At 0.25 mg/mL, complete killing of *E. coli* and *S. aureus* was reported after 8 h	A concentration- and exposure-specific bactericidal result; (Saravanan et al., 2021, p. 1)
Rosemary leaves	Hydrothermal preparation; mean diameter 16.13 nm	Microbial testing and a PVA-containing fruit-storage demonstration	Storage observations are qualitative and formulation-dependent; (Eskalen et al., 2021, p. 428)
Azadirachta indica leaves	Sand-bath preparation; TEM diameter approximately 3.5 nm	Radical-scavenging and diffusion-based antibacterial / antifungal responses	Read with dose, assay, and fraction-purity information; (Gedda et al., 2023, p. 1)
Tea and grape wastes	Biomass-derived dots characterized for chemical and optical properties	Antioxidant testing in aqueous media; selected preparations tested in oil	Matrix-dependent performance; (Murru et al., 2020, p. 1)
Rosemary and apple-pomace dots in biopolymer films	Dots incorporated at 0.25–1% by mass	Antioxidant-film evaluation, including edible and cosmetic oil samples	Proof of concept for a film system; (Rodríguez-Varillas et al., 2022, p. 1)
Green-tea dots loaded with curcumin	Hydrothermal dots combined with an external botanical active	Antioxidant and antibacterial nanocomposite evaluation	Composite response requires comparison with both components; (Wen et al., 2023, p. 1)
Salvia hydrangea aerial parts and cell cultures	Separate hydrothermal precursor routes	Antimicrobial, antioxidant, and cytotoxicity evaluations	Supports investigation of precursor-dependent properties; (Mardasi et al., 2025, p. 1)

Precursor or system	Preparation and material evidence	Biological finding	Interpretive scope and reference
Plantago major	Hydrothermal preparation with purification comparisons	Evaluation of antibacterial, antioxidant, and other biological responses	Purification is part of material definition; (Altinkaya, 2025, p. 1)
Polygonatum kingianum and *Gastrodia elata*	Separate hydrothermal products; mean sizes 6.2 and 6.8 nm	DPPH, superoxide, antibacterial, and an animal oxidative-stress model	Rankings depend on assay; (Zhang et al., 2025, p. 23845)

Source: Author's compilation of selected studies (Altinkaya, 2025, p. 1; Eskalen et al., 2021, p. 428; Gedda et al., 2023, p. 1; Mardasi et al., 2025, p. 1; Murru et al., 2020, p. 1; Rodríguez-Varillas et al., 2022, p. 1; Saravanan et al., 2021, p. 1; Wen et al., 2023, p. 1; Zhang et al., 2025, p. 23845).

A botanical label does not explain these differences. The relevant comparison begins with material class and fraction purity, then proceeds to dose basis, medium, and endpoint. Even studies sharing the same plant name may involve different extracts, tissue states, added reagents, or purification procedures.

Three attribution questions emerge from this comparison. First, can activity be assigned to the purified carbon-dot fraction? Second, is a measured improvement retained when components are compared at equivalent doses? Third, does the response persist in the intended application environment? These questions provide a more useful foundation for research planning than a table of the largest reported inhibition zones or scavenging percentages.

Linking Antioxidant and Antimicrobial Functions

A multifunctional material must be evaluated as a system. A preparation that consumes radicals in a chemical assay may still alter microbial survival through membrane effects or through oxidative processes under another exposure condition. Likewise, attaching an antioxidant cargo to a photoactive carrier may change both

functions. This chapter proposes evaluating redox behavior and antimicrobial activity in the same relevant medium, dose range, and illumination conditions whenever a dual function is claimed.

The main translational question is selectivity. For an infection-related application, microbial injury should be assessed together with compatibility toward relevant host cells. For packaging, the goal may instead be to reduce microbial contamination while slowing product oxidation. For cosmetics, preventing lipid oxidation and preserving a formulation are separate from any claimed effect on skin biology.

Table 3. Proposed controls for attributing biological activity in botanical carbon-dot systems.

Evaluation question	Comparison or control	Interpretation enabled
Do soluble reaction products contribute?	Crude dispersion, purified dots, and removed fraction	Distinguishes particulate activity from mixture activity
Does the original extract explain the response?	Starting extract at a clearly justified equivalent basis	Tests changes introduced by synthesis
Is a loaded active responsible?	Dots, active, physical mixture, and engineered composite	Separates carrier, cargo, and combination effects
Does light change the mechanism?	Light-only, material-only, and combined exposure	Resolves dark and photoactivated behavior
Does the material distort the assay?	Sample blanks and an independent biological or chemical endpoint	Tests optical or reporter interference
Is the effect selective?	Microbial viability and relevant host-cell responses	Relates efficacy to compatibility

Evaluation question	Comparison or control	Interpretation enabled
Is the product reproducible?	Independently synthesized and tested batches	Separates batch variation from measurement repeatability

Source: Evaluation framework developed by the author, informed by purification, antimicrobial-method, and composite studies (European Committee on Antimicrobial Susceptibility Testing, 2026, p. 1; Hinterberger et al., 2019, p. 8464; Otten et al., 2022, p. 6148; Wen et al., 2023, p. 1).

Table 3 is a proposed evaluation framework, not a claim that all cited studies performed every comparison. Its value lies in assigning a specific alternative explanation to each control. A control becomes scientifically useful when it resolves an attribution problem rather than merely increasing the number of experimental groups.

Application Potential

Antimicrobial materials and wound applications

Potential applications include antimicrobial carriers, wound-associated materials, and combined imaging/treatment systems. Quaternized curcumin-derived dots were investigated for infected wound healing, providing an example of an engineered material designed around a specific biological problem (Wu et al., 2022, p. 1). Translation requires attention to the material used in that study; similar behavior cannot be presumed for a different botanical precursor or surface treatment.

For a proposed wound formulation, testing should distinguish release of the active material from immobilized contact effects and should consider fluid composition and exposure duration. Host-cell compatibility, microbial killing, and tissue-related outcomes need separate measurements. Fluorescent tracking may support distribution studies but does not substitute for establishing clearance or biological safety.

Packaging and product protection

Dot-containing films offer an application in which the final matrix is central to performance. Rodríguez-Varillas and colleagues investigated antioxidant biopolymer films containing rosemary or apple-pomace dots, including proof-of-concept tests with edible and cosmetic oils. This evidence supports further material development; it does not establish suitability for every packaging configuration or contact condition (Rodríguez-Varillas et al., 2022, p. 1).

A proposed packaging study should assess oxidative stability, microbial response where relevant, migration, barrier properties, and mechanical behavior over the intended storage period. Protection observed during a short experiment should not be presented as a validated commercial shelf-life extension.

Cosmetic and dermocosmetic development

For cosmetic applications, the immediate research opportunities are protection of formulation ingredients against oxidation and investigation of skin-related effects in suitable models. The oil-protection example above concerns a material–product interaction, not proof of an anti-aging effect on human skin. This distinction should remain explicit when discussing botanical dots as candidate cosmetic ingredients.

Emulsions and gels introduce additional questions: where the dots reside, whether they aggregate, how they interact with other ingredients, and whether activity changes during storage. A proposed development pathway includes physicochemical stability, photostability, compatibility with the formulation, and biological evaluation relevant to the intended exposure. Antimicrobial activity in a laboratory culture does not establish preservative performance in a finished product. Claims concerning preservation, skin benefits, and antimicrobial treatment require different evidence.

Biocompatibility, Safety, and Environmental Evaluation

Botanical origin does not determine safety. The exposure includes the final particle structure, surface chemistry, residual soluble components, and formulation. Gedda and colleagues reported concentration-dependent compatibility in L929 fibroblasts, while Mardasi and colleagues included cytotoxicity evaluation in their comparison of *Salvia hydrangea*-derived preparations. Such findings are tied to the tested model and conditions (Gedda et al., 2023, p. 1; Mardasi et al., 2025, p. 1).

A proposed safety strategy begins with a well-defined purified material and application-relevant exposure. Cell viability should be interpreted alongside membrane integrity and other appropriate biological endpoints, with interference controls for the chosen readouts. Repeated exposure, light-dependent responses, and the effect of formulation components may require additional assessment. Lack of an adverse response in one assay should not be converted into a universal claim of nontoxicity.

Environmental evaluation should address the final material and the production process separately. An environmentally preferable feedstock can still produce a dispersion that requires assessment of persistence, transformation, or effects on non-target organisms. Conversely, immobilization in a matrix may change exposure but requires evidence on release. Regulatory and product-development decisions should be based on the defined material, intended use, and applicable requirements rather than a general “natural” designation.

Research Priorities and Future Perspectives

The proposed priorities are directed toward resolving uncertainty that limits meaningful comparison. The first is attribution: determine whether the active component is a particulate material, an associated molecule, a soluble reaction product, or a

composite. The second is reproducibility: identify the precursor and manufacturing variables responsible for variation among batches. The third is validation in the intended medium: show that activity survives incorporation into the target formulation or matrix.

Research on aromatic-plant residues would benefit from direct comparisons of intact biomass and processing residues, using a consistent synthesis and purification scheme. Phytochemical fingerprinting before synthesis could then be connected to surface chemistry and biological response after synthesis. This approach would test whether precursor differences have functional consequences without assuming preservation of specific molecules.

Mechanistic work should also examine the boundaries of multifunctionality. Rather than measuring antioxidant activity and bacterial inhibition in unrelated conditions, future studies could map both responses across the same dose, pH, and illumination ranges. Such experiments would identify conditions in which the material protects the target product or host while inhibiting microorganisms.

Finally, scale-up should be judged by yield, reproducibility, purification demand, energy use, and final performance. A successful laboratory synthesis is a starting point. An application-ready process needs acceptance criteria linked to the intended function, with clear limits for variability and impurities. These recommendations constitute a research framework; they are not evidence that current botanical carbon-dot products have already satisfied those requirements.

Conclusion

Medicinal and aromatic plants provide diverse precursors for carbon-dot systems whose antioxidant and antimicrobial responses depend on material composition and exposure conditions. Selected studies demonstrate activity in chemical assays, microbial cultures, films, and defined biological models. These findings support further

development while requiring careful distinction among purified dots, soluble reaction products, and composites containing additional active compounds.

The central requirement is attribution: the measured effect should be connected to a characterized fraction and then confirmed in the intended medium or formulation. Redox behavior and microbial responses should be evaluated together when multifunctionality is claimed, with controls that address optical interference, illumination, component contributions, and host-cell compatibility. Such evidence is more informative than botanical origin or fluorescence alone. Progress toward wound materials, protective films, and cosmetic formulations will depend on reproducible preparation and application-specific validation of the biological function.

References

Altinkaya, E. (2025). Single-step hydrothermal synthesis of *Plantago major*-based carbon dots: Therapeutic and antimicrobial properties. *Diamond and Related Materials, 158*, Article 112624. https://doi.org/10.1016/j.diamond.2025.112624

Benzie, I. F. F., & Strain, J. J. (1996). The ferric reducing ability of plasma (FRAP) as a measure of “antioxidant power”: The FRAP assay. *Analytical Biochemistry, 239*(1), 70–76. https://doi.org/10.1006/abio.1996.0292

Brand-Williams, W., Cuvelier, M. E., & Berset, C. (1995). Use of a free radical method to evaluate antioxidant activity. *LWT - Food Science and Technology, 28*(1), 25–30. https://doi.org/10.1016/s0023-6438(95)80008-5

Eskalen, H., Çeşme, M., Kerli, S., & Özğan, Ş. (2021). Green synthesis of water-soluble fluorescent carbon dots from rosemary leaves: Applications in food storage capacity, fingerprint detection, and antibacterial activity. *Journal of Chemical Research, 45*(5–6), 428–435. https://doi.org/10.1177/1747519820953823

European Committee on Antimicrobial Susceptibility Testing. (2026). *EUCAST recommendations for MIC determination of aerobic and facultative anaerobic bacterial species with broth microdilution* (Version 1.0, September 2026). https://www.eucast.org/fileadmin/eucast/pdf/Document_Archive/bacteria/disk_diffusion_methodology/EUCAST_recommendations_for_broth_microdilution_MIC_determination_September_2026.pdf

Gedda, G., Sankaranarayanan, S. A., Putta, C. L., Gudimella, K. K., Rengan, A. K., & Girma, W. M. (2023). Green synthesis of multi-functional carbon dots from medicinal plant leaves for antimicrobial, antioxidant, and bioimaging applications. *Scientific Reports, 13*(1), Article 6371. https://doi.org/10.1038/s41598-023-33652-8

Hinterberger, V., Damm, C., Haines, P., Guldi, D. M., & Peukert, W. (2019). Purification and structural elucidation of carbon dots by column chromatography. *Nanoscale, 11*(17), 8464–8474. https://doi.org/10.1039/c9nr01029g

Ji, Z., Sheardy, A., Zeng, Z., Zhang, W., Chevva, H., Allado, K., Yin, Z., & Wei, J. (2019). Tuning the functional groups on carbon nanodots and antioxidant studies. *Molecules, 24*(1), Article 152. https://doi.org/10.3390/molecules24010152

Mardasi, M., Mirjalili, M. H., Rahmandoust, M., Ghassempour, A., & Shahsavarani, H. (2025). *Salvia hydrangea*-derived carbon quantum dots via sustainable synthesis: Unraveling physicochemical properties, biocompatibility, and biological efficacy. *Journal of Science: Advanced Materials and Devices, 10*(4), Article 101028. https://doi.org/10.1016/j.jsamd.2025.101028

Miao, H., Wang, P., Wu, J., Li, X., Du, Y., Yan, H., You, Q., Dong, W., & Li, L. (2025). Highly efficient and broad-spectrum antibacterial carbon dots combat antibiotic resistance. *Talanta, 281*, Article 126926. https://doi.org/10.1016/j.talanta.2024.126926

Murru, C., Badía-Laíño, R., & Díaz-García, M. E. (2020). Synthesis and characterization of green carbon dots for scavenging radical oxygen species in aqueous and oil samples. *Antioxidants, 9*(11), Article 1147. https://doi.org/10.3390/antiox9111147

Otten, M., Hildebrandt, M., Kühnemuth, R., & Karg, M. (2022). Pyrolysis and solvothermal synthesis for carbon dots: Role of purification and molecular fluorophores. *Langmuir, 38*(19), 6148–6157. https://doi.org/10.1021/acs.langmuir.2c00508

Re, R., Pellegrini, N., Proteggente, A., Pannala, A., Yang, M., & Rice-Evans, C. (1999). Antioxidant activity applying an improved ABTS radical cation decolorization assay. *Free Radical Biology and Medicine, 26*(9–10), 1231–1237. https://doi.org/10.1016/s0891-5849(98)00315-3

Rodríguez-Varillas, S., Murru, C., Díaz-García, M. E., & Badía-Laíño, R. (2022). Green carbon dots as additives of biopolymer films for preserving from oxidation of oil-based products. *Antioxidants, 11*(11), Article 2193. https://doi.org/10.3390/antiox11112193

Saravanan, A., Maruthapandi, M., Das, P., Luong, J. H. T., & Gedanken, A. (2021). Green synthesis of multifunctional carbon dots with antibacterial activities. *Nanomaterials, 11*(2), Article 369. https://doi.org/10.3390/nano11020369

Sun, Y.-P., Zhou, B., Lin, Y., Wang, W., Fernando, K. A. S., Pathak, P., Meziani, M. J., Harruff, B. A., Wang, X., Wang, H., Luo, P. G., Yang, H., Kose, M. E., Chen, B., Veca, L. M., & Xie, S.-Y. (2006). Quantum-sized carbon dots for bright and colorful photoluminescence. *Journal of the American Chemical Society, 128*(24), 7756–7757. https://doi.org/10.1021/ja062677d

Wen, F., Li, P., Zhang, Y., Zhong, H., Yan, H., & Su, W. (2023). Preparation, characterization of green tea carbon quantum dots/curcumin antioxidant and antibacterial nanocomposites. *Journal of Molecular Structure, 1273*, Article 134247. https://doi.org/10.1016/j.molstruc.2022.134247

Wu, L., Gao, Y., Zhao, C., Huang, D., Chen, W., Lin, X., Liu, A., & Lin, L. (2022). Synthesis of curcumin-quaternized carbon quantum dots with enhanced broad-spectrum antibacterial activity for promoting infected wound healing. *Biomaterials Advances, 133*, Article 112608. https://doi.org/10.1016/j.msec.2021.112608

Xu, X., Ray, R., Gu, Y., Ploehn, H. J., Gearheart, L., Raker, K., & Scrivens, W. A. (2004). Electrophoretic analysis and purification of fluorescent single-walled carbon nanotube fragments. *Journal of the American Chemical Society, 126*(40), 12736–12737. https://doi.org/10.1021/ja040082h

Yan, H., Zhang, B., Zhang, Y., Su, R., Li, P., & Su, W. (2021). Fluorescent carbon dot–curcumin nanocomposites for remarkable antibacterial activity with synergistic photodynamic and photothermal abilities. *ACS Applied Bio Materials, 4*(9), 6703–6718. https://doi.org/10.1021/acsabm.1c00377

Zeng, Q., Feng, T., Tao, S., Zhu, S., & Yang, B. (2021). Precursor-dependent structural diversity in luminescent carbonized polymer dots (CPDs): The nomenclature. *Light: Science & Applications, 10*(1), Article 142. https://doi.org/10.1038/s41377-021-00579-6

Zhang, S., Tao, H., Zheng, X., Zhao, S., & Wei, Y. (2025). Multifunctional carbon dots from *Polygonatum kingianum* and *Gastrodia elata*: Synthesis, characterization, and biomedical applications. *RSC Advances, 15*(29), 23845–23861. https://doi.org/10.1039/d5ra03140k

BÖLÜM 4

AZOXYSTROBIN EFFECTS ON SOIL DEHYDROGENASE ACTIVITY: EVIDENCE AND ENVIRONMENTAL CONTEXT

BURAK KOÇAK[1]

Introduction

Azoxystrobin is a broad-spectrum systemic fungicide in the strobilurin group, used to control fungal diseases in crops (Bartlett et al., 2002:649-662). Although it is commonly applied to foliage, seed, or crop furrows, some of the applied compound can reach soil. Its effects below ground therefore matter alongside its intended activity against plant pathogens (Adetutu et al., 2008: 1777–1790). The extent and duration of soil exposure can vary with conditions: experiments in two rice-growing soils found that azoxystrobin persistence differed between soil types and moisture regimes, and that compost amendment had different effects in the two soils (Singh & Singh, 2010: 676–681). These findings make soil conditions relevant when interpreting reported biological responses.

Soil microorganisms contribute to processes that sustain soil fertility, including organic matter decomposition and nutrient

[1] Assoc. Prof., Cukurova University, Faculty of Arts and Sciences, Department of Biology, Orcid: 0000-0003-4144-6079

cycling (Aka Sağlıker & Cenkseven, 2016:649-655; Boga et al., 2017:1052-1060; Cenkseven, 2026:178-188). Soil enzymes provide measurable indicators of some of these biological processes and can respond to environmental disturbance and management (Utobo & Tewari, 2015:148-149). This broader context is relevant to pesticide exposure because changes in microbial activity or enzyme responses may signal effects on soil functions (Koçak & Cenkseven, 2021:1-2), although individual enzyme results should not be treated as direct evidence of changes in overall soil health (Yasir et al., 2025:11-13).

Dehydrogenase activity is commonly used as an indicator of overall microbial respiratory activity in soil. Because dehydrogenase is associated with cellular metabolism, its measured activity can help characterize microbial responses to disturbance (Neemisha & Sharma, 2022:173-188). However, enzyme assays can differ in their reaction conditions and measurement procedures, which limits direct comparison among studies unless methods and units are considered (Utobo & Tewari, 2015:148-149). Dehydrogenase is therefore useful as a response indicator, but its results need to be interpreted alongside experimental design, soil properties, exposure conditions, and other microbial or biochemical measurements.

Studies of azoxystrobin show why this context matters. Adetutu et al. (2008: 1777–1790) reported changes in fungal community responses under some incubation conditions, while bacterial diversity was unaffected in their experiment. In a separate Spodosol study, azoxystrobin exposure was associated with changes in several enzyme activities, carbon-source utilization, and bacterial community structure; the measured enzymes did not include dehydrogenase (Wang et al., 2020:3-7). These studies point to biological responses that may be relevant to soil functioning, but they do not establish a uniform dehydrogenase response across soils or experimental settings. The broader pesticide literature also links changes in microbial communities and enzyme activity with nutrient

cycling and soil fertility, while recognizing that outcomes depend on the pesticide and soil context (Yasir et al., 2025:11-13).

This review examines the effects of azoxystrobin on soil dehydrogenase activity and considers how those findings relate to the fungicide's environmental fate, soil properties, microbial communities, and other enzyme responses. It distinguishes studies that directly measured dehydrogenase from those that provide supporting evidence on azoxystrobin persistence or other soil biological endpoints. By considering dose, exposure duration, soil conditions, and measurement methods, the review aims to clarify what the available studies show and where the evidence remains limited.

Literature Identification and Evaluation

Sources and search terms

The literature considered in this chapter was identified using the Web of Science Core Collection and supplemented with relevant full-text articles and review papers examining azoxystrobin fate, soil microbial responses, and soil enzyme interpretation

The concepts used to organize the literature included *azoxystrobin*, *soil*, *dehydrogenase*, *soil enzyme activity*, *soil microbial activity*, *soil microbial community*, *pesticide degradation*, and *soil fertility*. These terms describe the subject areas covered by the supplied records and articles; they should not be interpreted as a fully documented database search string. The search date, exact Boolean operators, and any filters applied to the Web of Science search were not available in the records provided.

Study selection and relevance

Studies were considered directly relevant when they investigated azoxystrobin exposure in soil and reported dehydrogenase activity. Studies addressing azoxystrobin

degradation or persistence, other soil enzyme activities, microbial activity, or microbial community structure were retained as supporting evidence when they helped explain soil exposure or provide context for biological responses.

Reviews and meta-analyses on soil enzymes were used to inform the interpretation of dehydrogenase activity and methodological differences. They were not treated as primary experiments testing azoxystrobin. Studies conducted in specialized systems, such as biobed substrates, or involving amendments and microbial inoculation were considered separately because their conditions do not directly represent an ordinary agricultural-soil exposure experiment.

Evaluation and limitations

Findings were compared with attention to soil type and properties, azoxystrobin dose, formulation, exposure and sampling duration, amendments, experimental setting, and dehydrogenase assay method. Numerical results were interpreted in light of the units and comparison groups reported by each study. Where an article reported a result only in a figure, that value should be identified as figure-derived and distinguished from values reported in tables or the main text.

Direct comparison among studies is limited by differences in experimental design, measurement protocols, reporting units, and the availability of treatment and control means, measures of variability, and sample sizes. Repeated sampling times from the same experiment and multiple dose groups sharing a control are statistically dependent; they should not be treated as independent observations in a pooled analysis without an appropriate method to account for that dependence. For these reasons, the present chapter uses a narrative synthesis and does not calculate a single pooled effect estimate.

Soil Dehydrogenase Activity

Biochemical basis and significance

Dehydrogenases are oxidoreductase enzymes involved in the transfer of hydrogen and electrons from organic substrates to acceptors during oxidation shown in Figure 1. In soil, dehydrogenase activity (DHA) is commonly used as an indicator of microbial oxidative activity and of transformations associated with organic matter. The principal reason for its use is that soil DHA is generally associated with intact, viable microbial cells. Unlike many extracellular enzymes that can persist after release into the soil matrix, dehydrogenase activity is rapidly lost following cell death. This makes DHA a useful measure of a biologically active component of soil processes (Nannipieri et al., 2018:12-13; Utobo & Tewari, 2015:148-149).

DHA is therefore often described as a sensitive biological indicator of soil condition. It can respond to changes caused by environmental disturbance or management, and has been applied in studies of natural, agricultural, reclaimed, and mine-affected soils (Kumar et al., 2013:899-902; Utobo & Tewari, 2015: 148-149). Its value lies in the fact that it provides information about microbial oxidative processes that may not be apparent from soil chemical measurements alone. However, DHA should be interpreted as one indicator of soil biological functioning, rather than as a complete measure of soil health or microbial abundance.

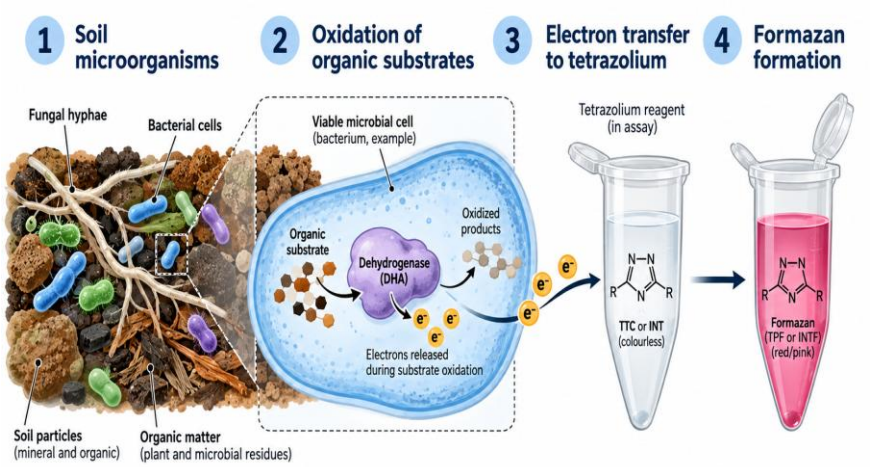
A distinction is needed between *microbial activity*, *microbial biomass*, and *dehydrogenase activity*. Although DHA is often used as a proxy for microbial activity, the measured enzyme response does not necessarily track every aspect of microbial functioning. Nannipieri et al. (2018:12-13) note that DHA does not always correlate closely with other measures such as oxygen consumption. Consequently, DHA should not be treated as interchangeable with

respiration, total microbial biomass, or the activity of the entire soil microbial community. It reflects a particular, assay-defined aspect of microbial oxidative activity.

Principles of measurement

Soil DHA is commonly assessed by adding a tetrazolium compound that can act as an artificial electron acceptor (Figure 1). Microbial reduction of the compound produces a coloured formazan product, which is extracted and quantified, typically by spectrophotometry. The two substrates are triphenyltetrazolium chloride (TTC) and iodonitrotetrazolium chloride (INT). The resulting products are commonly reported as triphenyl formazan (TPF) or iodonitrotetrazolium formazan (INTF), respectively (Kumar et al., 2013:899–902; Utobo & Tewari, 2015:148-149).

Figure 1. Soil dehydrogenase activity



The assay is practical and has been widely adopted, but it does not directly measure an undisturbed, in situ rate of soil metabolism. Instead, it measures the formation of formazan under the specific conditions established by the assay. Substrate identity and concentration, soil mass and moisture, incubation duration and

temperature, pre-incubation, aeration, extraction, and the analytical procedure can all influence the result (Kumar et al., 2013: 899–902; Nannipieri et al., 2018:12-13). Values obtained using different protocols are therefore not automatically comparable, even when both studies describe their endpoint as "dehydrogenase activity."

The reporting unit also matters. Studies may express activity per unit of dry soil and time, but use different mass units or formazan products. A value reported as TPF cannot be assumed to be directly equivalent to a value reported as INTF, and results reported per gram, kilogram, or another soil basis require appropriate conversion before comparison. Such conversions do not correct for differences in assay chemistry or incubation conditions. For quantitative synthesis, the assay method, substrate, incubation conditions, soil basis, time unit, and reported variability should be recorded alongside the numerical result.

Factors influencing measured activity

The observed DHA response is shaped by both soil conditions and laboratory protocol. Moisture and aeration affect the environment in which microbial oxidation occurs; temperature, incubation duration, and pre-incubation can also change formazan production. Kumar et al. (2013:899–902) emphasize these conditions as important sources of variation and discuss the use of both TTC and INT assays. Utobo and Tewari (2015: 148-149) likewise describe DHA as a responsive indicator whose interpretation depends on the biological and environmental context of the soil.

The soil itself is not a uniform assay medium. Differences in soil type and condition can influence microbial communities and the processes being measured. The review by Kumar et al. (2013: 899–902), for example, compares DHA observations across natural, managed, reclaimed, and mine-affected settings. Those comparisons

illustrate why an activity value should be read in the context of the sampled soil and its history, rather than interpreted against a single universal reference range.

Evidence from a meta-analysis of heavy-metal effects further illustrates the sensitivity of soil enzyme responses to the contaminant and soil context. Aponte et al. (2020:3-9) found that enzyme responses differed among enzyme types and were associated with factors including contaminant characteristics and soil properties; DHA was among the enzyme activities considered. This evidence concerns heavy-metal contamination, not azoxystrobin. It is relevant here as an example of why results for one stressor cannot simply be generalized to another, and why soil and study characteristics should be considered when interpreting or synthesizing enzyme data.

Interpretation and limitations

DHA is useful because it is linked to viable-cell oxidative processes and can respond to soil disturbance. Its interpretation nevertheless requires several qualifications. First, a change in DHA indicates a change in the assay-measured activity; by itself, it does not identify the ecological mechanism responsible. Second, a higher value should not automatically be interpreted as an improvement in overall soil quality, nor should a lower value alone be taken as proof of broad microbial damage. The direction and meaning of a response depend on the soil, the experimental conditions, the timing of measurement, and the other endpoints considered (Nannipieri et al., 2018:12-13; Utobo & Tewari, 2015:148-149).

Third, comparisons across studies require protocol transparency. Nannipieri et al. (2018:12-13) caution that methodological differences and incomplete descriptions can undermine the interpretation of soil enzyme data and their use in meta-analysis. For DHA, comparisons are especially difficult when studies differ in tetrazolium substrate, incubation conditions, units,

sampling time, or the way results are normalized. These differences should be evaluated before effect estimates are combined.

For a review of azoxystrobin and soil dehydrogenase, DHA is best treated as a biologically informative but method-dependent endpoint. A study's result should be interpreted together with its soil characteristics, exposure conditions, sampling time, assay protocol, and other microbial or enzymatic measurements. This framing allows DHA to contribute evidence about microbial oxidative activity without overstating what a single assay can establish about the wider soil ecosystem.

Properties and Environmental Fate of Azoxystrobin

Mode of action and uses

Azoxystrobin is a synthetic fungicide belonging to the strobilurin group. Strobilurins were developed from naturally occurring fungicidal compounds and became an important class of agricultural fungicides. In their review, Bartlett et al. (2002: 649–662) describe azoxystrobin among the commercially developed strobilurin fungicides and discuss its use across a range of crops and fungal disease-management systems.

Azoxystrobin acts by inhibiting mitochondrial respiration in susceptible fungi. It binds at the quinol oxidation (Qo) site of the cytochrome bc_1 complex in the mitochondrial electron-transport chain. This interferes with electron transfer from cytochrome *b* to cytochrome c_1 and disrupts energy production, including ATP generation (Bartlett et al., 2002: 649–662). This biochemical mode of action underlies its fungicidal activity against plant-pathogenic fungi.

Azoxystrobin has been marketed for preventative and curative disease-control purposes (Edwards et al., 2016:450-457). Its application in agricultural production can involve different delivery

methods, depending on the crop and product use. For example, the Midwestern United States field study by Edwards et al. (2016:450-457) examined a formulation containing azoxystrobin and propiconazole applied to corn by air and to soybean by ground equipment. Because the study evaluated a mixture of active ingredients, its field observations describe the behavior of that formulation and application system; they should not be interpreted as evidence that every observed effect was caused by azoxystrobin alone.

Routes of entry into soil

Azoxystrobin can reach soil during crop spraying when part of the applied spray passes through the crop canopy and deposits at the soil surface. In the field study by Edwards et al. (2016:450-457), canopy penetration to soil level was observed following both aerial and ground applications. The extent of deposition will depend on application conditions and crop canopy characteristics; the study therefore supports canopy penetration as a direct route of soil exposure under the conditions examined.

A second potential route is spray drift beyond the treated crop area. Edwards et al. (2016:450-457) detected drift associated with aerial application, whereas drift was not associated with the ground application in their study. Drift can move fungicide away from the intended application zone, although the study's drift measurements should not be taken as a direct measure of azoxystrobin deposition in every neighboring soil.

Effects of Azoxystrobin on Soil Dehydrogenase Activity

Direction and magnitude of the response

The 13 studies reviewed here do not show one consistent direction or magnitude of change in soil dehydrogenase activity (DHA) following azoxystrobin exposure. Several report inhibition,

often most clearly at early sampling times or higher concentrations. Others report no statistically significant effect, or increases under particular field, soil-amendment, or microbial-inoculation conditions. Differences in soil properties, exposure design, formulation, dose, sampling time, and assay procedure need to be considered before comparing the results.

One clear early response was reported by Bending et al. (2007:84-87). They applied azoxystrobin at 5 mg kg^{-1} to two soils with contrasting management histories. In Long Close soil, DHA was 89.4% of the unamended control at 0.25 months and 86.3% at one month; both reductions were reported as significant ($p < 0.05$). At two months, activity had returned to 97.7% of the control, and at three months it was 113.7%. In the higher-organic-matter Hunts Mill soil, no significant DHA effect was reported. The authors' comparison is particularly useful because the soils had similar pH (6.5) but differed in total organic carbon (1.18% versus 1.62%) and microbial biomass (139.4 versus 622.6 mg C kg^{-1} dry soil). The study therefore documents a soil-dependent response, rather than a uniform effect of the 5 mg kg^{-1} treatment.

Sopeña and Bending (2013:1527-1529) also found lower DHA following azoxystrobin application. Their laboratory experiment used 25 mg kg^{-1} and compared unamended soil with soils containing 0.1%, 1%, or 2% biochar. In unamended soil, DHA was approximately 51%, 58%, and 30% lower in treated than untreated samples at one, three, and five months, respectively. In biochar-amended soils, the reported one-month decreases relative to the matching biochar-only treatments were 28% at 0.1% biochar, 34% at 1%, and 40% at 2%. Thus, biochar increased the underlying DHA but did not remove the azoxystrobin-associated reduction. These comparisons are based on the authors' reported results and Figure 2; the biochar-treated groups must be compared with their corresponding biochar-only controls, not with unamended soil.

Howell et al. (2014:197-198) reported a concentration-dependent decrease and subsequent recovery in DHA in a four-month laboratory experiment. After one month, activity ranged from 75% of the control at 1 mg kg^{-1} to 45% at 25 mg kg^{-1}. These levels persisted to the two-month sampling. By month three, activity was 102.9% and 103.6% of control in the 1 and 5 mg kg^{-1} treatments, and 88.4% and 98.8% in the 10 and 25 mg kg^{-1} treatments, respectively. At month four, DHA in the 10 and 25 mg kg^{-1} treatments had risen to 137.4% and 133.2% of control, whereas values in the 1 and 5 mg kg^{-1} treatments were 87.1% and 97.8%. The authors interpreted the time course as evidence of recovery in DHA, even though azoxystrobin residues were still present in the soil. The late values above the control should not be interpreted as proof that azoxystrobin generally stimulates DHA: the response followed a pronounced early decline and could reflect biological recovery or other changes during incubation.

Several studies with short laboratory incubation periods also found inhibition. Wang et al. (2015:3336–3343) tested 0.1, 1, and 10 mg kg^{-1} in brown soil and measured microbial and enzyme outcomes on days 7, 14, 21, and 28. The article reports reductions in DHA, soil respiration, and viable microbial numbers, and describes DHA as the most sensitive of the four enzyme activities assessed. Dehydrogenase activity was significantly reduced ($p < 0.05$) across all sampling dates and concentrations, although differences between the 1.0 and 10.0 mg kg^{-1} treatments were not significant on days 14 and 21. By day 28, DHA had decreased by 55%, 72%, and 85% relative to the control at 0.1, 1.0, and 10.0 mg kg^{-1}, respectively. In Cambisol, Wang et al. (2018:2777–2780) tested 0.1, 1, and 10 mg kg^{-1} and measured activity on days 7, 14, 21, and 28. DHA was significantly lower in azoxystrobin-treated soils than in the control except on day 7. By day 28, activity was 19.1%, 49.8%, and 69.4% lower than control at 0.1, 1, and 10 mg kg^{-1}, respectively. Negative

correlations between concentration and DHA were reported on days 14, 21, and 28 ($r = -0.87$, -0.77, and -0.80, respectively).

The results of Baćmaga et al. (2015:1-15) were more modest. In a sandy-loam soil, the authors tested 0.075, 2.25, 11.25, and 22.50 mg kg^{-1} and assessed enzymes after 30, 60, and 90 days. At the highest dose, mean dehydrogenase activity was reported to be 7.04% lower. Dehydrogenases were the most resistant of the enzymes assessed in that experiment, and the lowest DHA was observed on day 30. These findings differ in magnitude from the larger response reported by Wang et al. (2018:2777–2780); they should not be treated as interchangeable estimates because the soils, experimental procedures, and dose series differed.

Dose, formulation, and sampling time

The data suggest that higher concentrations can produce larger decreases in DHA, but the pattern is not identical across studies. Howell et al. (2014:197-198) found a stronger initial reduction at higher concentrations, while Wang et al. (2018:2777–2780) reported progressively greater day-28 reductions across 0.1, 1, and 10 mg kg^{-1}. Baćmaga et al. (2015:1-15), by contrast, reported only a 7.04% decrease in mean dehydrogenase activity at 22.50 mg kg^{-1}. These differences caution against treating nominal concentration as the sole determinant of response. Soil type, fungicide preparation, moisture, incubation conditions, and assay method also differ.

The 2022 Quadris® experiment should be distinguished from studies applying azoxystrobin as a technical active ingredient. Boteva et al. (2022:382-392) used Quadris® in loamy-sand soil at azoxystrobin concentrations of 2.90, 14.65, and 35.00 mg kg^{-1} dry soil. Enzyme activity was measured on days 1, 30, 60, 90, and 120. The reported overall DHA means across the sampling period were 20.11 ± 9.2 µg g^{-1} dry soil h^{-1} in the untreated control, 13.51 ± 4.2 at

2.90 mg kg^{-1}, 12.25 ± 4.3 at 14.65 mg kg^{-1}, and 11.36 ± 4.4 at 35.00 mg kg^{-1}. The authors reported an overall reduction of 33–44%, with DHA among the enzymes most sensitive to Quadris®. In the table, the control and all three Quadris® treatments were assigned different significance groups from the control for DHA ($p < .05$). Because this study used a commercial formulation, its estimates refer to the tested Quadris® treatment, not necessarily to the active ingredient alone.

A complementary pattern was reported by Baćmaga et al. (2024:9-14), who studied Amistar 250 SC in sandy-clay soil at a field dose of 0.110 mg kg^{-1} and a polluting dose of 32.92 mg kg^{-1}. The experiment used three sampling dates: 30, 60, and 90 days. At the field dose, DHA was 28.359, 28.139, and 19.719 µmol TPF kg^{-1} dry soil h^{-1}, compared with control values of 28.050, 27.454, and 19.159 on those dates. At the polluting dose, DHA was 27.034, 26.424, and 19.073, corresponding to reported decreases of approximately 3.62%, 3.75%, and 0.45% relative to the controls. The authors found that the field dose increased DHA at all three sampling times, while the polluting dose decreased it. They also reported that incubation time accounted for most of the variation in enzyme activity (η^2 = 87.86–99.76% across the enzymes), whereas dose and the dose-by-time interaction had comparatively little influence. This is a much smaller DHA response than the one reported in some other studies, and it should be described as such rather than generalized to all concentrations or soils.

Time after application changes the interpretation of these findings. Bending et al. (2007) and Howell et al. (2014:197-198) observed early decreases followed by movement toward, or above, control levels. Wang et al. (2018) found that the high-concentration response remained evident at day 28. Boteva et al. (2022:382-392) reported that DHA was most sensitive early in the time profile, with the temporal pattern continuing across their 120-day experiment. Baćmaga et al. (2024:9-14), in contrast, found substantial differences

between sampling dates but comparatively small treatment-related DHA changes. A result at one date therefore cannot characterize the full response. Nor does a later return of DHA to the control establish that microbial community composition or other soil functions have also recovered.

Soil amendments, field conditions, and biological interventions

Soil amendments and field conditions can alter measured DHA independently of the fungicide effect. In the biochar study, biochar increased DHA, and azoxystrobin still reduced activity relative to matched biochar-only controls (Sopeña & Bending, 2013:1527-1529). The field-versus-laboratory vineyard study by Herrero-Hernández et al. (2015:85) likewise found higher DHA in spent-mushroom-substrate (SMS)-amended than unamended soil. The authors attributed this difference to the organic matter, available carbon, and microbial populations associated with the amendment. Under field conditions, mean DHA was higher in azoxystrobin-treated soils than in untreated soils across the two tested doses (LSD = 27.73, $p = .0001$); the increase was smaller in SMS-amended than in unamended soil. The authors also reported significant effects of sampling time, soil, and their interactions on DHA ($p < 0.0001$). These results are specific to the vineyard soil and SMS amendment, and do not establish that azoxystrobin stimulates DHA generally.

Manna et al. (2013: 2956–2957) found no significant effect of azoxystrobin on DHA in rice soil under outdoor ambient CO_2, ambient CO_2 in open-top chambers, or elevated CO_2 in open-top chambers. The study measured DHA from day 0 to day 50 and reported no effect of elevated CO_2 on DHA; azoxystrobin likewise had no effect on DHA, fluorescein diacetate hydrolase, or acid phosphatase activities, although it slightly inhibited alkaline phosphatase activity up to day 40. Its table gives DHA in µg TPF released g^{-1} soil day^{-1}, but the authors' reported overall interpretation is that there was no significant DHA response. Accordingly,

individual differences in table entries should not be recast as significant treatment effects.

Adak et al. (2020:1357–1358) studied fungicides in rice rhizosphere soil under field conditions across two years. Azoxystrobin was applied at 125 g active ingredient ha^{-1}. Although fungicide-treated soils had lower DHA than controls at some sampling points, the authors state that azoxystrobin's effect on DHA was not significant. They describe the azoxystrobin treatment as hindering DHA, while the broader microbial response was short-term and had recovered by day 30. This field study is relevant to agricultural conditions but is not directly equivalent to a laboratory soil-spiking experiment: it involved a crop rhizosphere, field variability, and several fungicide treatments.

Baćmaga et al. (2017:6-7) examined bioaugmentation of soil contaminated with azoxystrobin at 22.50 mg kg^{-1}. The laboratory experiment utilized two soil types (loamy sand and sandy loam) and assessed enzyme activity after 90 days of incubation, with and without inoculation using specific bacterial and fungal consortia. In uninoculated soils treated solely with azoxystrobin at 22.50 mg kg^{-1}, dehydrogenase activity was reduced relative to uncontaminated controls. Following the application of a bacterial consortium (comprising *Bacillus* strains) to contaminated loamy sand, dehydrogenase activity was 44% higher than in the soil contaminated with azoxystrobin but left uninoculated; in sandy loam, the corresponding increase achieved by the bacterial consortium was 15%. These contrasts reflect bioaugmentation outcomes rather than standalone fungicide effects and demonstrate that microbial inoculation can modify dehydrogenase activity in contaminated soils.

The biobed study by Kumari et al. (2019:845-848) is also not a conventional agricultural-soil experiment. It used rice-straw/corn-cob and peat/compost biomixtures to study degradation of

azoxystrobin and imidacloprid. Conditioning the biomixtures for 10 days increased microbial biomass and DHA; pesticide application to the conditioned mixtures did not show a negative impact on microbial parameters. These results are useful for understanding pesticide treatment systems, but biobed substrates should not be combined with field-soil DHA outcomes.

Conclusion

Soil dehydrogenase activity is a useful indicator of microbial oxidative processes because it is associated primarily with viable microbial cells and responds to changes in soil conditions. Its value lies in providing evidence about one important aspect of soil biological functioning; it should not be interpreted on its own as a direct measure of total microbial biomass, respiration, or overall soil health.

The meaning of a DHA result depends on both the soil context and the assay protocol. Substrate type, incubation conditions, moisture, aeration, units, and sampling time can affect the measured activity and limit direct comparisons among studies. Reliable interpretation therefore requires clear reporting of methods and consideration of the soil's properties and experimental conditions. These requirements are particularly important when synthesizing results across studies.

For research on azoxystrobin, DHA can help assess changes in soil microbial oxidative activity, but it should be considered alongside other biological and soil measurements. Consistent methods and transparent reporting will make it easier to distinguish treatment-related responses from variation due to soil conditions or measurement procedures. Taken together, these principles support a cautious interpretation of DHA and its use as one component of a broader assessment of soil responses to fungicide exposure.

References

Adak, T., Mukherjee, A. K., Berliner, J., Pokhare, S. S., Yadav, M. K., Bag, M. K., Lenka, S., Munda, S., & Jena, M. (2020). Target and non-target effect of commonly used fungicides on microbial properties in rhizospheric soil of rice. *International Journal of Environmental Analytical Chemistry*, *100*(12), 1350–1361. https://doi.org/10.1080/03067319.2019.1653457

Adetutu, E. M., Ball, A. S., & Osborn, A. M. (2008). Azoxystrobin and soil interactions: Degradation and impact on soil bacterial and fungal communities. *Journal of Applied Microbiology*, *105*(6), 1777–1790. https://doi.org/10.1111/j.1365-2672.2008.03948.x

Aka Sağlıker, H., & Cenkseven, S. (2016). How lime dust does affect carbon mineralization of *Eucalyptus camaldulensis* soil? *Scholars Academic Journal of Biosciences*, *4*(8), 649–655. https://doi.org/10.36347/sajb.2016.v04i08.009

Aponte, H., Meli, P., Butler, B., Paolini, J., Matus, F., Merino, C., Cornejo, P., & Kuzyakov, Y. (2020). Meta-analysis of heavy metal effects on soil enzyme activities. *Science of the Total Environment*, *737*, 139744. https://doi.org/10.1016/j.scitotenv.2020.139744

Baćmaga, M., Kucharski, J., & Wyszkowska, J. (2015). Microbial and enzymatic activity of soil contaminated with azoxystrobin. *Environmental Monitoring and Assessment*, *187*(10), Article 615. https://doi.org/10.1007/s10661-015-4827-5

Baćmaga, M., Wyszkowska, J., & Kucharski, J. (2017). Bioaugmentation of soil contaminated with azoxystrobin. *Water, Air, & Soil Pollution*, *228*(1), Article 19. https://doi.org/10.1007/s11270-016-3200-9

Baćmaga, M., Wyszkowska, J., & Kucharski, J. (2024). Response of soil microbiota, enzymes, and plants to the fungicide azoxystrobin. *International Journal of Molecular Sciences*, *25*(15), Article 8104. https://doi.org/10.3390/ijms25158104

Bartlett, D. W., Clough, J. M., Godwin, J. R., Hall, A. A., Hamer, M., & Parr-Dobrzanski, B. (2002). The strobilurin fungicides. *Pest Management. Science*, *58*, 649–662. https://doi.org/10.1002/ps.520

Bending, G. D., Rodríguez-Cruz, M. S., & Lincoln, S. D. (2007). Fungicide impacts on microbial communities in soils with contrasting management histories. *Chemosphere*, *69*(1), 82–88. https://doi.org/10.1016/j.chemosphere.2007.04.042

Boga, T., Aka Sagliker, H., & Cenkseven, S. (2017). The first effect of *Eucalyptus camaldulensis* leaves and eucalyptol additions on soil carbon mineralization. *Fresenius Environmental Bulletin*, *26*, 1052–1060.

Boteva, S. B., Kenarova, A. E., Petkova, M. R., Georgieva, S. S., Chanev, C. D., & Radeva, G. S. (2022). Soil enzyme activities after application of fungicide Quadris® at increasing concentration rates. *Plant, Soil and Environment*, *68*(8), 382–392. https://doi.org/10.17221/127/2022-PSE

Cenkseven, S. (2026). Interaction effects of eucalyptus biochar and chlorantraniliprole on soil carbon mineralization under different soil moistures. *Chilean Journal of Agricultural Research*, *86*(2), 178–188. https://doi.org/10.4067/s0718-58392026000200178

Edwards, P. G., Murphy, T. M., & Lydy, M. J. (2016). Fate and transport of agriculturally applied fungicidal compounds, azoxystrobin and propiconazole. *Chemosphere*, *146*, 450-457. https://doi.org/10.1016/j.chemosphere.2015.11.116

Herrero-Hernández, E., Marín-Benito, J. M., Andrades, M. S., Sánchez-Martín, M. J., & Rodríguez-Cruz, M. S. (2015). Field versus laboratory experiments to evaluate the fate of azoxystrobin in an amended vineyard soil. *Journal of Environmental Management*, *163*, 78–86. https://doi.org/10.1016/j.jenvman.2015.08.010

Howell, C. C., Hilton, S., Semple, K. T., & Bending, G. D. (2014). Resistance and resilience responses of a range of soil eukaryote and bacterial taxa to fungicide application. *Chemosphere*, *112*, 194–202. https://doi.org/10.1016/j.chemosphere.2014.03.031

Koçak, B., & Cenkseven, S. (2021). Effects of three commonly used herbicides in maize on short-term soil organic carbon mineralization. *Water Air & Soil Pollution, 232*(9), 386 https://doi.org/10.1007/s11270-021-05337-3

Kumar, S., Chaudhuri, S., & Maiti, S. K. (2013). Soil dehydrogenase enzyme activity in natural and mine soil—A review. *Middle-East Journal of Scientific Research*, *13*(7), 898–906. https://doi.org/10.5829/idosi.mejsr.2013.13.7.2801

Kumari, A., Singh, N., & Ramakrishnan, B. (2019). Parameters affecting azoxystrobin and imidacloprid degradation in biobed substrates in the North Indian tropical environment. *Journal of Environmental Science and Health, Part B*, *54*(10), 843–857. https://doi.org/10.1080/03601234.2019.1633857

Manna, S., Singh, N. & Singh, V.P. (2013). Effect of elevated CO_2 on degradation of azoxystrobin and soil microbial activity in rice soil. *Environmental Monitoring Assessment 185*, 2951–2960 https://doi.org/10.1007/s10661-012-2763-1

Nannipieri, P., Trasar-Cepeda, C., & Dick, R. P. (2018). Soil enzyme activity: A brief history and biochemistry as a basis for appropriate interpretations and meta-analysis. *Biology and Fertility of Soils*, *54*, 11–19. https://doi.org/10.1007/s00374-017-1245-6

Neemisha, & Sharma, S. (2022). Soil enzymes and their role in nutrient cycling. In B. Giri, R. Kapoor, Q. S. Wu, & A. Varma (Eds.), *Structure and functions of pedosphere* (pp. 173-188). Springer. https://doi.org/10.1007/978-981-16-8770-9_8

Singh, N., & Singh, S. B. (2010). Effect of moisture and compost on fate of azoxystrobin in soils. *Journal of Environmental Science and Health, Part B*, *45*(7), 676–681. https://doi.org/10.1080/03601234.2010.502445

Sopeña, F., & Bending, G. D. (2013). Impacts of biochar on bioavailability of the fungicide azoxystrobin: A comparison of the effect on biodegradation rate and toxicity to the fungal community. *Chemosphere*, *91*(11), 1525–1533. https://doi.org/10.1016/j.chemosphere.2012.12.031

Utobo, E. B., & Tewari, L. (2015). Soil enzymes as bioindicators of soil ecosystem status. *Applied Ecology and Environmental Research*, *13*(1), 147–169. https://doi.org/10.15666/aeer/1301_147169

Wang, F. H., Zhu, L. S., Lv, D. D., Guo, P. P., Wang, J., & Wang, J. H. (2015). Effects of azoxystrobin on soil micro-organisms and enzymatic activities. *Fresenius Environmental Bulletin*, *24*(10A), 3336–3343.

Wang, F., Li, X., Zhu, L., Du, Z., Zhang, C., Wang, J., Wang, J. & Lv, D. (2018). Responses of soil microorganisms and enzymatic activities to azoxystrobin in cambisol. *Polish Journal of Environmental Studies,* *27*(6), 2775–2783. https://doi.org/10.15244/pjoes/81086

Wang, X., Lu, Z., Miller, H., Liu, J., Hou, Z., Liang, S., Zhao, X., Zhang, H., & Borch, T. (2020). Fungicide azoxystrobin induced changes on the soil microbiome. *Applied Soil Ecology*, *145*, 103343. https://doi.org/10.1016/j.apsoil.2019.08.005

Yasir, M., Hossain, A., & Pratap-Singh, A. (2025). Pesticide degradation: Impacts on soil fertility and nutrient cycling. *Environments*, *12*(8), 272. https://doi.org/10.3390/environments12080272

BÖLÜM 5

DNA BARCODING IN PLANT SYSTEMATICS: SPECIES IDENTIFICATION AND NEXT-GENERATION APPROACHES

HANDAN ŞAPCI SELAMOĞLU[1]

INTRODUCTION

DNA barcoding is a molecular identification approach that aims to determine the identity of an organism from short, standardised DNA regions. Its modern framework took shape when Hebert et al. (2003) demonstrated that the mitochondrial cytochrome c oxidase subunit I (COI) region could be used for species identification in animals. Rather than replacing morphological identification, the approach has made it easier to test taxonomic identity, particularly in specimens that are incomplete, sterile, juvenile, processed or lack diagnostic morphological characters. The underlying principle of DNA barcoding is simple: a short sequence obtained from an unknown (query) specimen is compared with reliable, taxonomically verified reference sequences, and the result is interpreted together with morphology and other biological evidence (Hebert et al., 2003; Ratnasingham & Hebert, 2007).

[1] Assoc. Prof. Dr., Kayseri University, Develi Hüseyin Şahin Vocational School, Department of Plant and Animal Production, ORCID: 0000-0001-8150-0450

Early studies expected an ideal barcode to show sufficient variation among species, to be relatively conserved among individuals of the same species, to be amplifiable with the same primers across broad taxonomic groups, to yield short, high-quality sequences, and to be recoverable from partially degraded material such as museum and herbarium specimens. These criteria remain valid today; however, next-generation sequencing, mini-barcodes, metabarcoding and whole-plastome approaches have led to the notions of an "ideal length" or a "single universal locus" being reconsidered according to the application. In other words, current barcoding is shifting from the search for a single gene fragment towards building a scalable molecular identification system with a resolution appropriate to the research question (Hollingsworth et al., 2011; Rani et al., 2026).

This chapter first briefly summarises DNA barcoding through the markers used in the major groups of organisms, and then examines in detail why finding a standard barcode is more difficult in plants. The historical development of plant barcodes; the strengths and weaknesses of *rbcL*, *matK*, ITS/ITS2 and supplementary loci; the barcode gap; the distinction between species identification and species delimitation; reference infrastructures such as BOLD and GenBank; herbarium material; the authentication of medicinal and economic plants; metabarcoding; environmental DNA; and plastome-based "super-barcoding" approaches are discussed in the light of the current literature. This work is not a systematic review but a narrative and critical synthesis that considers landmark publications together with recent reviews from 2024–2026.

CONCEPTUAL BASIS AND HISTORICAL DEVELOPMENT OF DNA BARCODING

Barcode Regions in Different Groups of Organisms

Although the underlying logic of DNA barcoding is similar across all groups of organisms, the genomic region used is not the same. In animals, COI became the classical standard barcode because of its high copy number, sufficient interspecific variation in most groups and relatively easy alignment. In fungi, owing to the amplification and discrimination problems of COI, the nuclear ribosomal internal transcribed spacer (ITS) region was adopted as the primary barcode (Schoch et al., 2012). In bacteria and archaea, 16S rRNA sequences are a widely used identification tool, although resolution may be limited among closely related species and genomic approaches may be required. Because protists are an extremely heterogeneous group, there is no single universal species-level barcode; the variable regions of 18S rDNA are used as a pre-barcode, while COI, *rbcL* and other group-specific markers are used complementarily in different lineages (Antil et al., 2023; Pawlowski et al., 2012; Rani et al., 2026).

Table 1. Common DNA Barcode Markers in Major Groups of Organisms

Group	**Common marker**	**Genome/region**	**Key note**
Animals	COI	Mitochondrion	High species discrimination in many animal groups; complementary loci are needed in some groups.
Fungi	ITS	Nuclear ribosomal	Primary barcode for broad fungal diversity; additional genes may be needed for some closely related species.
Bacteria and archaea	16S rRNA	Ribosomal	Wide range of use; genomic resolution may be needed for closely related species and species boundaries.
Land plants	*rbcL* + *matK*; ITS/ITS2 supplementary	Plastid + nuclear	A single locus is usually insufficient; hybridisation and recent speciation reduce resolution.

Group	Common marker	Genome/region	Key note
Algae / protists	18S, COI, *rbcL*, tufA, etc.	Varies by group	Evolutionary diversity requires group-specific barcodes and a multi-step approach.

Source: Compiled by the author from Schoch et al. (2012), Antil et al. (2023) and Rani et al. (2026).

Properties Expected of an Ideal Barcode Region

The usefulness of a DNA region as a barcode does not depend on high variability alone. A successful barcode should show high PCR and sequencing success across broad taxonomic samples; its sequences should be easy to orient and align; it should not be excessively variable within a species; and it should provide sufficient discrimination among closely related species. Standardisation, identification from minimal data and scalability to large numbers of samples have been listed among the core design principles of plant barcoding (Hollingsworth et al., 2009; Hollingsworth et al., 2011). For herbarium, processed-product and environmental samples, the production of short amplicons becomes particularly important; therefore, alongside classical barcodes of approximately 500–900 base pairs, mini-barcodes of 100–300 base pairs have emerged as a practical solution (Nazar et al., 2025; Taberlet et al., 2007).

When interspecific variation is clearly greater than intraspecific variation, an identification window known as the "barcode gap" may arise. However, it cannot be assumed that this gap will be present in all taxa or at all loci. In plants in particular, hybridisation, polyploidy, chloroplast capture and incomplete lineage sorting may cause interspecific and intraspecific genetic distances to overlap. The performance of a barcode locus should therefore be assessed not only by mean distance values but also in relation to sampling density, the accuracy of reference sequences,

monophyly, identification success and biological context (Fazekas et al., 2009; Ho et al., 2026).

THE DNA BARCODING WORKFLOW

Sampling, Vouchers and Taxonomic Verification

DNA barcoding begins not with DNA extraction in the laboratory but with correct sampling and correct taxonomic identification. A reference sequence is only as reliable as the identity of the specimen to which it is linked. Wherever possible, each barcode sequence should therefore be associated with a collection number, locality, date, collector information, photographs and a herbarium voucher. In plant reference libraries in particular, herbarium specimens verified by experts are critical because they provide physical evidence that can be re-examined later. In national-scale barcode libraries, systematic sampling of herbarium collections improves both taxonomic quality and geographic coverage (Kartzinel et al., 2025; Whitley et al., 2024).

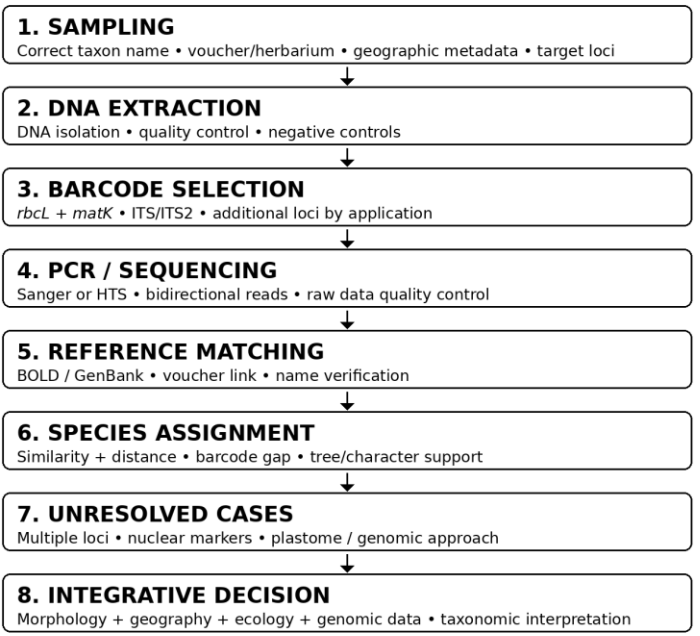
DNA Extraction, PCR and Sequencing

Although fresh leaf tissue is suitable for obtaining high-molecular-weight DNA in most plant species, secondary metabolites, polysaccharides and phenolic compounds can inhibit DNA extraction and PCR. Tissue rapidly dried in silica gel is a common option in fieldwork. Because DNA in herbarium specimens and commercial products is more fragmented, extraction conditions, amplicon length and contamination control are especially important. In classical barcoding projects, the PCR product is usually read by Sanger sequencing, whereas high-throughput sequencing platforms are preferred for mixed samples, studies involving hundreds of taxa, or environmental DNA (Kress, 2017; Whitley et al., 2024).

Raw Sequence Quality and Reference Matching

After sequencing, chromatogram quality should be checked, low-quality ends trimmed, bidirectional reads assembled and possible contamination screened. In protein-coding loci, unexpected stop codons or frameshifts may indicate off-target amplification or a pseudogene. In reference matching, it is not sufficient to look only at the highest BLAST percentage; the sampling level of the closest species, the discriminatory power of the region used, the overlap length between query and reference sequences, the voucher link and the current taxon name should all be considered together. BOLD is a barcode data system developed to bring molecular data together with specimen, morphological and distribution information, whereas GenBank is a broader-purpose nucleotide archive (Ratnasingham & Hebert, 2007).

Figure 1. Workflow of DNA Barcoding From Sampling to Integrative Taxonomic Decision



Source: Prepared by the author.

WHY IS DNA BARCODING MORE DIFFICULT IN PLANTS?

Low Substitution Rate in the Plant Mitochondrial Genome

The high success of COI in animals raised the expectation that the same locus could be used universally in plants; however, the lower nucleotide substitution rate of mitochondrial genes in land plants compared with many animal groups prevented COI from discriminating most plant species. Plant barcode research therefore turned to the plastid genome and nuclear ribosomal regions (Chase et al., 2005; Kress et al., 2005). In plants there is a strong trade-off between a genomic region being easily amplified with universal primers and evolving rapidly enough to separate closely related species.

Hybridisation and Chloroplast Capture

Interspecific hybridisation is more common in plants than in many animal groups, and because the plastid genome is inherited from a single parent in most angiosperms, interspecific gene flow can carry plastid lineages independently of species boundaries. This process can produce patterns known as “chloroplast capture”. As a result, two morphologically well-separated species may share the same plastid barcode, or geographically very different plastid lineages may occur within a single species. Fazekas et al. (2009) reported lower species monophyly and a smaller barcode gap in plant barcodes than in animals and suggested that hybridisation may be one of the main causes of this difference. In such cases, nuclear loci and morphological/ecological data are essential complements to plastid barcodes (Ho et al., 2026; Hollingsworth et al., 2016).

Polyploidy, Apomixis and Rapid Speciation

Polyploidy, allopolyploidy, apomixis and shifts in breeding system allow new taxa to arise in plants over relatively short evolutionary timescales. The fact that newly formed species are morphologically and ecologically differentiated does not mean that sufficient nucleotide divergence has accumulated in slowly evolving plastid loci such as *rbcL* or *matK*. In allopolyploids, the coexistence of nuclear copies derived from different progenitors can also complicate the interpretation of multicopy regions such as ITS. In closely related plant species, “barcode failure” may therefore be not merely a technical shortcoming but a genuine biological reflection of speciation history (Fazekas et al., 2009; Hollingsworth et al., 2011; Kumar et al., 2026).

Incomplete Lineage Sorting and Gene Tree–Species Tree Discordance

In recently diverged lineages, ancestral polymorphisms may persist in the new species for some time. Incomplete lineage sorting

causes the gene tree of a single locus to appear different from the true species tree. The sharing of a barcode region between two species therefore does not always indicate misidentification or ongoing hybridisation. Because standard barcodes provide a limited number of linked characters, resolution is reduced especially in rapid radiations. Although current genomic approaches aim to generate more characters from whole plastomes or many independent nuclear loci, a large number of characters derived from a single line of inheritance does not automatically resolve biological conflict; independent genomic compartments may need to be evaluated together (Hollingsworth et al., 2016; Shah et al., 2026).

CORE AND SUPPLEMENTARY BARCODE REGIONS IN LAND PLANTS

rbcL

rbcL is a plastid gene encoding the large subunit of ribulose-1,5-bisphosphate carboxylase/oxygenase and has long been used in plant phylogenetics. Its high primer universality and sequence quality make it advantageous for large-scale reference libraries. By contrast, its variability among closely related species is often low. *rbcL* has therefore been regarded as an important component of the core barcode because of its reliable recovery and higher-level taxonomic placement rather than high species resolution on its own (CBOL Plant Working Group, 2009; Hollingsworth et al., 2011).

matK

matK is a rapidly evolving region located within the plastid *trnK* intron that encodes a maturase. It can provide higher species discrimination than *rbcL* in most groups; however, the unequal performance of universal primers across land plants was long a significant technical problem. Taking into account the balance between recoverability, sequence quality and discriminatory power,

the CBOL Plant Working Group (2009) proposed the *rbcL* + *matK* pair as the core barcode for land plants. Lahaye et al. (2008) reported that *matK* alone could achieve high identification success in the floras of biodiversity hotspots. This decision does not imply that every species will be unambiguously separated; rather, it provides a common starting framework for international standardisation.

ITS and ITS2

The ITS region of nuclear ribosomal DNA is a powerful complement, particularly for discriminating closely related species, because it can evolve faster than plastid genes and carries a biparentally inherited nuclear signal. Using a large dataset, the China Plant BOL Group (2011) supported the incorporation of ITS into the core barcode for seed plants. A large-scale study of medicinal plants reported that ITS2 can achieve high identification success (Chen et al., 2010). Nevertheless, ITS is multicopy; paralogues, incomplete concerted evolution, fungal contamination and double peaks during sequencing can cause problems of interpretation. Reviewing 197 angiosperm barcoding studies in 2025, Aygören Uluer emphasised that ITS2 performs well in amplification and genus-level identification, but that species-level success is not universal and that none of the regions examined can be considered a universal barcode for all angiosperms on its own (Aygören Uluer, 2025).

***trnH-psbA*, *trnL* and Other Supplementary Regions**

Because of its high variability, the plastid *trnH-psbA* intergenic spacer was, together with *rbcL*, among the early proposals for a plant barcode (Kress & Erickson, 2007). However, length variation, inversions, homopolymer regions and alignment difficulties can cause problems in broad phylogenetic samples. The short P6 loop of the *trnL* intron, despite its lower species discrimination, has become an important mini-barcode for metabarcoding of faeces, soil, ancient material and processed

samples because it yields very short amplicons (Deiner et al., 2017; Taberlet et al., 2007). In certain taxonomic groups, *ycf1*, plastid spacers other than *trnH-psbA*, or group-specific nuclear loci may also complement the standard core barcodes (Dong et al., 2015).

Table 2. Comparison of Common Barcoding Approaches in Plants

Marker	**Recovery**	**Species resolution**	**Main advantage**	**Main limitation**
rbcL	High	Low–moderate	Universality and high sequence quality	Insufficient variation among close relatives
matK	High in angiosperms; variable in other groups	Moderate–high	More variable than *rbcL*; core barcode	Low primer universality in some groups
ITS/ITS2	Moderate–high (high for ITS2)	Moderate–high	Nuclear, rapidly evolving signal	Paralogues, intragenomic variation, contamination
trnH-psbA	High	Moderate–high	Variable spacer; easy amplification	Indels, inversions and alignment problems
trnL P6	Very high	Low–moderate	Very short; suitable for degraded DNA and eDNA	Limited species-level discrimination
Plastome / super-barcode	Depends on genomic data	High	Many characters; design of group-specific mini-barcodes	Cost, data analysis; biological limits of a single plastid lineage

Source: Compiled by the author from CBOL Plant Working Group (2009), Hollingsworth et al. (2011) and Li et al. (2015).

BARCODE GAP, SPECIES IDENTIFICATION AND SPECIES DELIMITATION

Interpreting the Barcode Gap

One of the most widely used concepts in DNA barcoding is the barcode gap, which rests on the expectation that intraspecific genetic distances are lower than interspecific distances. A clear gap facilitates identification; however, the threshold value is not

expected to be constant across all taxa. Insufficient sampling, geographic structure, introgression and misidentified reference specimens can artificially widen or narrow the gap. A percentage similarity or a single genetic distance threshold should therefore not be used as an automatic species decision, especially in plants (Fazekas et al., 2009; Hollingsworth et al., 2011; Meyer & Paulay, 2005).

Species Identification and Species Delimitation Are Not the Same Process

Species identification aims to assign an unknown specimen to a previously described taxon, whereas species delimitation seeks to determine the boundaries of evolutionarily independent lineages. High similarity between a query sequence and a reference species may provide evidence that the specimen is consistent with that species; however, it does not by itself demonstrate the existence of a new species or that two closely related taxa are independent species. Early debates over whether DNA barcoding should replace classical taxonomy have largely been superseded by the integrative taxonomy approach, which combines morphology, geography, ecology and multiple sources of genetic data (Dayrat, 2005; DeSalle et al., 2005; Will et al., 2005).

Neighbour-joining trees or barcode clusters are useful visualisations for identification and for revealing potential cryptic diversity; however, they are not synonymous with detailed phylogenetic analysis. In particular, high similarity in a single-locus barcode tree does not fully resolve the shared evolutionary history of species. When species delimitation is required, hypotheses should be tested with independent nuclear loci, genomic SNP data, coalescent-based methods and phenotypic/ecological evidence (DeSalle et al., 2005; Will et al., 2005).

REFERENCE LIBRARIES: BOLD, GENBANK AND THE VOUCHER PROBLEM

The success of a barcoding system depends not only on a good choice of marker but also on the accuracy of the reference library against which the query is compared. BOLD is a dedicated system that aims to link barcode sequences with vouchers, images, geographic coordinates and collection data (Ratnasingham & Hebert, 2007). GenBank, in contrast, is a much broader sequence archive that also contains genomic data beyond barcodes. Both systems are indispensable; however, users should check whether taxonomic names are up to date, which physical specimen a sequence is based on, and whether the identification has been verified by an expert.

Evaluating more than 373,584 plant barcodes in global public databases in 2025, Kartzinel et al. reported that these records cover only about a quarter of the approximately 435,000 extant land plant species and that at least 17% of plant families have no reference barcode at all. This result clearly shows that even a technically flawless metabarcoding protocol cannot produce species-level results when suitable reference sequences are lacking. Moreover, the fact that most specimens originate from the Global North leads to geographic and taxonomic gaps in tropical biodiversity hotspots (Kartzinel et al., 2025).

The Role of Herbaria in Reference Barcode Libraries

Herbaria are unique for reference barcode libraries because they hold millions of specimens whose names have been determined by experts and which can be re-examined. They make it possible to generate barcodes without new field collections, especially for rare, endemic or currently inaccessible species. However, age, drying method, chemical treatment and storage conditions can increase DNA fragmentation. Short amplicons, multiple short regions, target

enrichment and high-throughput sequencing are therefore becoming increasingly important in herbarium barcoding (Whitley et al., 2024).

APPLICATIONS OF DNA BARCODING

Biodiversity Inventories, Conservation and Ecological Monitoring

DNA barcoding provides rapid preliminary identification in large biodiversity inventories where morphological identification is time-consuming or expertise is scarce. Species can be assigned to material lacking diagnostic morphological characters, such as seedlings, seeds, roots, wood fragments, pollen or leaf fragments. Important applications include the identification of endangered and trade-regulated species in products or parts, the early detection of invasive species and the resolution of ecological interaction networks (Kress, 2017; Rani et al., 2026). Nevertheless, in studies that inform conservation decisions, the accuracy of the reference library is especially critical, because false-positive or false-negative species assignments may have legal and management consequences.

Agricultural, Food and Forensic Applications

Accurate identification of agricultural pests and pathogens, import–export controls and the authentication of plant-derived food products are applied areas of barcoding. In materials whose morphological characters have been lost, such as ground spices, herbal teas or processed foods, DNA-based methods are powerful for label verification and the detection of adulteration. A comprehensive 2024 review emphasised that DNA barcoding is widely used to authenticate plant-derived food, feed and medicinal products, and that ddPCR, isothermal amplification and metabarcoding have expanded the toolkit in this field (Lanubile et al., 2024).

Authentication of Medicinal Plants

In medicinal plants, the use of the wrong species, synonyms, local names that refer to more than one taxon, morphologically similar adulterants and the loss of diagnostic characters in processed material are major quality problems. The success of ITS2 in identifying medicinal plants was demonstrated early on a large sample, and mini-barcode, metabarcoding and plastome-based approaches have since advanced the field (Chen et al., 2010; Chen et al., 2023). However, DNA does not measure the amount of active chemical constituents or pharmacological quality. In modern quality assurance, an orthogonal approach in which DNA barcoding and morphological, microscopic and chemical profiling methods corroborate one another is therefore considered more robust (Nazar et al., 2025).

MINI-BARCODING, METABARCODING AND ENVIRONMENTAL DNA

Mini-Barcodes

Amplification of full-length standard barcodes may fail in old herbarium specimens, boiled crude drugs, capsule/tablet contents and highly processed products. Mini-barcodes increase the likelihood of obtaining results from fragmented DNA by using short, informative subregions that discriminate the target species. The *trnL* P6 loop is a classic example in plant eDNA and diet studies because of its very short inter-primer length; however, a short sequence also reduces the number of characters that discriminate at species level (Taberlet et al., 2007). In mini-barcode design, a balance must therefore be struck between amplification success and discriminatory power.

DNA Metabarcoding

Metabarcoding aims to identify many organisms present in a single sample by simultaneously amplifying their barcode regions with universal or broad-range primers and sequencing them by high-throughput sequencing. Soil, water, pollen, honey, faeces, stomach contents, plant mixtures and commercial preparations are typical examples of this approach. Unlike classical barcoding, metabarcoding usually works on a mixed DNA pool rather than a single clean DNA template. Primer bias, copy number in different species, amplicon length, sequencing depth and bioinformatic filters can therefore affect the interpretation of the relative abundances of species (Deiner et al., 2017).

Environmental DNA (eDNA)

Environmental DNA makes it possible to investigate the presence of an organism from the DNA it releases into water, soil, air or other environmental media, without the need to capture the organism directly. In plants, eDNA offers opportunities for community-level monitoring through pollen, root material, shed cells and particles. Although eDNA and metabarcoding scale up biodiversity monitoring, contamination, transported DNA, the persistence of DNA in the environment and gaps in reference libraries can complicate the ecological interpretation of a “presence” signal. Laboratory and field negative controls, replicates and explicit bioinformatic thresholds are therefore essential (Deiner et al., 2017; Rani et al., 2026).

FROM CLASSICAL BARCODES TO PLASTOME AND GENOMIC BARCODING

Super-Barcoding and Plastome Sequencing

The limited performance of the standard *rbcL* + *matK* system among closely related species has brought the use of the whole chloroplast genome as a “super-barcode” onto the agenda. Because

plastomes contain far more variable characters than standard barcodes, they can markedly improve the discrimination of closely related species when appropriate reference specimens are available. Li et al. (2015) proposed that single-locus and plastome approaches be used not as alternatives but as complementary tools depending on the taxon and the scale of application. In recent years, falling sequencing costs have made the routine production of plastomes through genome skimming easier, and it has also become possible to select shorter, lineage-specific, highly variable mini-barcodes from plastomes (Hollingsworth et al., 2016; Shah et al., 2026).

The availability of more characters at the plastome scale does not mean that all species-boundary problems will be solved. If chloroplast capture or ongoing hybridisation is present, the whole plastome represents the same line of inheritance and may reproduce an incorrect species relationship with high support. In closely related, reticulately evolving or polyploid groups, nuclear single- or low-copy genes, target enrichment or genome-wide SNPs should therefore be evaluated together with plastome data (Ho et al., 2026; Hollingsworth et al., 2016).

Long-Read Sequencing and Machine Learning

Long-read platforms such as Nanopore and PacBio facilitate the rapid recovery of longer amplicons, complete ribosomal regions and, in some cases, organelle genomes. These technologies have considerable potential for field-based sequencing and real-time identification (Srivathsan et al., 2021); however, raw-read error profiles, reference library quality and analytical standardisation must be managed carefully according to the application. Machine learning approaches can learn classification patterns from high-dimensional sequence data; however, model performance depends on the taxonomic accuracy and representativeness of the training dataset (Shah et al., 2026). Recent reviews from 2026 regard the future of

plant barcoding not as a single locus but as a “genomic toolkit” in which classical markers are used together with plastomes, multiple loci, metabarcoding and computational classification (Ho et al., 2026; Kumar et al., 2026; Shah et al., 2026).

Table 3. Major Problems in Plant DNA Barcoding and Suitable Solutions

Problem	**Possible consequence**	**Recommended approach**
Recent speciation / incomplete lineage sorting	The same barcode haplotype shared by more than one species	Denser sampling, independent nuclear loci, genomic species delimitation
Hybridisation / chloroplast capture	Plastid tree inconsistent with species boundaries	Nuclear markers + morphology + geographic/ecological evidence
Polyploidy and paralogues	Multicopy signal in ITS and nuclear sequences	Copy awareness, target enrichment, genomic data
Degraded DNA	PCR failure of long barcodes	Mini-barcodes, short amplicons, HTS
Incomplete reference library	Species-level assignment not possible	Voucher-based national/regional reference libraries
Mixed sample	Overlapping signal in the Sanger sequence	Metabarcoding with appropriate negative/positive controls
Incorrect reference name	Wrong species assignment with high similarity	Voucher re-examination, taxon name updating, multiple databases

Source: Prepared by the author.

WHAT DNA BARCODING IS NOT

DNA barcoding is not an “automated taxonomy” that replaces the existing body of taxonomic knowledge. Without correctly named reference specimens, the barcode system itself cannot provide reliable identification. Moreover, a single barcode tree is not synonymous with a phylogeny; resolving historical

relationships among species requires model selection, multiple gene regions or genomic data, and appropriate outgroup sampling. Likewise, high sequence similarity is not by itself sufficient evidence for describing a new species or for a species delimitation decision (DeSalle et al., 2005; Will et al., 2005).

The most powerful use of DNA barcoding is the rapid identification of unknown specimens against references verified by expert morphological identification, the detection of discordant specimens, and the flagging of lineages that require more detailed taxonomic study. Deep genetic divergence in a barcode dataset may raise a new species hypothesis; however, any nomenclatural decision should be supported by type material, morphology, distribution, ecology and, where possible, independent genetic evidence. This approach makes DNA data not a rival to classical systematics but a powerful component of integrative taxonomy (Dayrat, 2005; Kress, 2017).

CURRENT STATUS AND FUTURE PERSPECTIVES

Since 2003, DNA barcoding has evolved from the idea of COI-based standard identification into a molecular identification ecosystem operating at very different scales as of 2026. The standardisation provided by a single powerful mitochondrial locus in animals has never been achieved to the same extent in plants; this limitation reflects the reticulate and multi-genomic nature of plant evolution rather than a weakness of plant barcoding. The current approach is not to abandon standard core loci such as *rbcL* and *matK* but to complement them stepwise, according to the application, with ITS/ITS2, short mini-barcodes, whole plastomes and independent nuclear markers (Ho et al., 2026; Kumar et al., 2026).

The most important need in the coming years is not simply to produce more sequences but to produce the right sequences from the right specimens. The large geographic and taxonomic reference gaps

demonstrated by Kartzinel et al. (2025) increase the importance of expert-verified libraries based on herbarium and living collections if new sequencing technologies are to be used efficiently. Recording barcodes in national flora projects according to an “extended specimen” concept, together with the current taxon name, voucher, photographs, distribution and, where possible, genomic data, will provide a shared infrastructure for basic systematic research, eDNA monitoring and forensic/economic applications.

For plant systematics, the future lies in a decision-tree approach rather than the search for a single “best barcode”. Standard barcodes may be economical and sufficient for routine authentication; ITS and additional plastid/nuclear loci may come into play for closely related species; many independent nuclear regions are needed when hybridisation or polyploidy is suspected; mini-barcodes and metabarcoding come to the fore for processed or mixed material; and plastome and genomic data can be used for groups that standard barcodes cannot resolve. This stepwise strategy balances cost and resolution while also preventing biological over-interpretation of the results.

CONCLUSIONS AND RECOMMENDATIONS

DNA barcoding is a powerful molecular tool, complementary to classical taxonomy, that evaluates organismal identity from short, standardised DNA sequences. The differences in the loci used across groups of organisms stem from differences in genomic evolutionary rates and modes of inheritance. While COI is common in animals, ITS in fungi, 16S rRNA in bacteria and archaea, and group-specific combinations in protists, in land plants the *rbcL* + *matK* core system is supported by ITS/ITS2 and other supplementary markers. In plants, low mitochondrial substitution rates, hybridisation, chloroplast capture, polyploidy and incomplete lineage sorting have hindered the development of a single universal species barcode.

The most reliable approach in plant barcoding is therefore a stepwise workflow that begins with a correctly identified voucher specimen, proceeds through appropriate locus selection and sequence quality control, uses more than one reference source, and integrates the results with morphological/ecological evidence. While standard loci retain their importance in routine identification, mini-barcodes for herbarium and processed material, metabarcoding for mixed samples, and plastome and independent nuclear genomic approaches for closely related species are increasing resolution. However advanced the technology becomes, the value of a barcode sequence is limited by the correctly named specimen it represents and by a reliable reference library. The future of DNA barcoding in plant systematics is therefore taking shape within an integrative framework in which molecular speed and classical taxonomic accuracy advance together.

References

Antil, S., Abraham, J. S., Sripoorna, S., Maurya, S., Dagar, J., Makhija, S., Bhagat, P., Gupta, R., Sood, U., Lal, R., & Toteja, R. (2023). DNA barcoding, an effective tool for species identification: A review. *Molecular Biology Reports, 50*(1), 761–775. https://doi.org/10.1007/s11033-022-08015-7

Aygören Uluer, D. (2025). Is ITS2 more successful in angiosperm DNA barcoding than the entire ITS, ITS1, matK and trnH-psbA regions? A review. *Anales del Jardín Botánico de Madrid, 82*(1), e155. https://doi.org/10.3989/ajbm.624

CBOL Plant Working Group. (2009). A DNA barcode for land plants. *Proceedings of the National Academy of Sciences of the United States of America, 106*(31), 12794–12797. https://doi.org/10.1073/pnas.0905845106

Chase, M. W., Salamin, N., Wilkinson, M., Dunwell, J. M., Kesanakurthi, R. P., Haidar, N., & Savolainen, V. (2005). Land plants and DNA barcodes: Short-term and long-term goals. *Philosophical Transactions of the Royal Society B: Biological Sciences, 360*(1462), 1889–1895. https://doi.org/10.1098/rstb.2005.1720

Chen, S., Yao, H., Han, J., Liu, C., Song, J., Shi, L., Zhu, Y., Ma, X., Gao, T., Pang, X., Luo, K., Li, Y., Li, X., Jia, X., Lin, Y., & Leon, C. (2010). Validation of the ITS2 region as a novel DNA barcode for identifying medicinal plant species. *PLOS ONE, 5*(1), e8613. https://doi.org/10.1371/journal.pone.0008613

Chen, S., Yin, X., Han, J., Sun, W., Yao, H., Song, J., & Li, X. (2023). DNA barcoding in herbal medicine: Retrospective

and prospective. *Journal of Pharmaceutical Analysis, 13*(5), 431–441. https://doi.org/10.1016/j.jpha.2023.03.008

China Plant BOL Group. (2011). Comparative analysis of a large dataset indicates that internal transcribed spacer (ITS) should be incorporated into the core barcode for seed plants. *Proceedings of the National Academy of Sciences of the United States of America, 108*(49), 19641–19646. https://doi.org/10.1073/pnas.1104551108

Dayrat, B. (2005). Towards integrative taxonomy. *Biological Journal of the Linnean Society, 85*(3), 407–415. https://doi.org/10.1111/j.1095-8312.2005.00503.x

Deiner, K., Bik, H. M., Mächler, E., Seymour, M., Lacoursière-Roussel, A., Altermatt, F., Creer, S., Bista, I., Lodge, D. M., de Vere, N., Pfrender, M. E., & Bernatchez, L. (2017). Environmental DNA metabarcoding: Transforming how we survey animal and plant communities. *Molecular Ecology, 26*(21), 5872–5895. https://doi.org/10.1111/mec.14350

DeSalle, R., Egan, M. G., & Siddall, M. (2005). The unholy trinity: Taxonomy, species delimitation and DNA barcoding. *Philosophical Transactions of the Royal Society B: Biological Sciences, 360*(1462), 1905–1916. https://doi.org/10.1098/rstb.2005.1722

Dong, W., Xu, C., Li, C., Sun, J., Zuo, Y., Shi, S., Cheng, T., Guo, J., & Zhou, S. (2015). ycf1, the most promising plastid DNA barcode of land plants. *Scientific Reports, 5*, 8348. https://doi.org/10.1038/srep08348

Fazekas, A. J., Kesanakurti, P. R., Burgess, K. S., Percy, D. M., Graham, S. W., Barrett, S. C. H., Newmaster, S. G., Hajibabaei, M., & Husband, B. C. (2009). Are plant species inherently harder to discriminate than animal species using

DNA barcoding markers?. *Molecular Ecology Resources, 9*(Suppl. 1), 130–139. https://doi.org/10.1111/j.1755-0998.2009.02652.x

Hebert, P. D. N., Cywinska, A., Ball, S. L., & deWaard, J. R. (2003). Biological identifications through DNA barcodes. *Proceedings of the Royal Society B: Biological Sciences, 270*(1512), 313–321. https://doi.org/10.1098/rspb.2002.2218

Ho, S.-W., Chao, C.-T., & Liao, P.-C. (2026). Beyond a single locus: Evolutionary constraints and genomic alternatives to plant DNA barcoding. *Taiwania, 71*(1), 185–197. https://doi.org/10.6165/tai.2026.71.185

Hollingsworth, M. L., Clark, A. A., Forrest, L. L., Richardson, J., Pennington, R. T., Long, D. G., Cowan, R., Chase, M. W., Gaudeul, M., & Hollingsworth, P. M. (2009). Selecting barcoding loci for plants: Evaluation of seven candidate loci with species-level sampling in three divergent groups of land plants. *Molecular Ecology Resources, 9*(2), 439–457. https://doi.org/10.1111/j.1755-0998.2008.02439.x

Hollingsworth, P. M., Graham, S. W., & Little, D. P. (2011). Choosing and using a plant DNA barcode. *PLOS ONE, 6*(5), e19254. https://doi.org/10.1371/journal.pone.0019254

Hollingsworth, P. M., Li, D.-Z., van der Bank, M., & Twyford, A. D. (2016). Telling plant species apart with DNA: From barcodes to genomes. *Philosophical Transactions of the Royal Society B: Biological Sciences, 371*(1702), 20150338. https://doi.org/10.1098/rstb.2015.0338

Kartzinel, T. R., Hoff, H. K., Divoll, T. J., Littleford-Colquhoun, B. L., Anderson, H., Burak, M. K., Kuzmina, M. L., Musili, P. M., Rogers, H. S., Troncoso, A. J., & Kartzinel, R. Y.

(2025). Global availability of plant DNA barcodes as genomic resources to support basic and policy-relevant biodiversity research. *Molecular Ecology, 34*(7), e17712. https://doi.org/10.1111/mec.17712

Kress, W. J. (2017). Plant DNA barcodes: Applications today and in the future. *Journal of Systematics and Evolution, 55*(4), 291–307. https://doi.org/10.1111/jse.12254

Kress, W. J., & Erickson, D. L. (2007). A two-locus global DNA barcode for land plants: The coding rbcL gene complements the non-coding trnH-psbA spacer region. *PLOS ONE, 2*(6), e508. https://doi.org/10.1371/journal.pone.0000508

Kress, W. J., Wurdack, K. J., Zimmer, E. A., Weigt, L. A., & Janzen, D. H. (2005). Use of DNA barcodes to identify flowering plants. *Proceedings of the National Academy of Sciences of the United States of America, 102*(23), 8369–8374. https://doi.org/10.1073/pnas.0503123102

Kumar, S., Gupta, U., Kushwaha, N., Srivastava, M., Gupta, V. K., Huh, Y. S., & Srivastava, S. (2026). DNA barcoding in plants for species identification: Insights from single locus markers to chloroplast genome sequencing. *Gene Reports, 44*, 102541. https://doi.org/10.1016/j.genrep.2026.102541

Lahaye, R., van der Bank, M., Bogarin, D., Warner, J., Pupulin, F., Gigot, G., Maurin, O., Duthoit, S., Barraclough, T. G., & Savolainen, V. (2008). DNA barcoding the floras of biodiversity hotspots. *Proceedings of the National Academy of Sciences of the United States of America, 105*(8), 2923–2928. https://doi.org/10.1073/pnas.0709936105

Lanubile, A., Stagnati, L., Marocco, A., & Busconi, M. (2024). DNA-based techniques to check quality and authenticity of food, feed and medicinal products of plant origin: A review.

Trends in Food Science & Technology, 149, 104568. https://doi.org/10.1016/j.tifs.2024.104568

Li, X., Yang, Y., Henry, R. J., Rossetto, M., Wang, Y., & Chen, S. (2015). Plant DNA barcoding: From gene to genome. *Biological Reviews, 90*(1), 157–166. https://doi.org/10.1111/brv.12104

Meyer, C. P., & Paulay, G. (2005). DNA barcoding: Error rates based on comprehensive sampling. *PLOS Biology, 3*(12), e422. https://doi.org/10.1371/journal.pbio.0030422

Nazar, N., Saxena, A., Sebastian, A., Slater, A., Sundaresan, V., & Sgamma, T. (2025). Integrating DNA barcoding within an orthogonal approach for herbal product authentication: A narrative review. *Phytochemical Analysis, 36*(1), 7–29. https://doi.org/10.1002/pca.3466

Pawlowski, J., Audic, S., Adl, S., Bass, D., Belbahri, L., Berney, C., Bowser, S. S., Cepicka, I., Decelle, J., Dunthorn, M., Fiore-Donno, A. M., Gile, G. H., Holzmann, M., Jahn, R., Jirků, M., Keeling, P. J., Kostka, M., Kudryavtsev, A., Lara, E., . . . de Vargas, C. (2012). CBOL Protist Working Group: Barcoding eukaryotic richness beyond the animal, plant, and fungal kingdoms. *PLOS Biology, 10*(11), e1001419. https://doi.org/10.1371/journal.pbio.1001419

Rani, V., Chauhan, C., & Sengar, R. S. (2026). DNA barcoding markers: A comprehensive review and taxonomic classification across species. *Computational Biology and Chemistry, 122*, 108872. https://doi.org/10.1016/j.compbiolchem.2025.108872

Ratnasingham, S., & Hebert, P. D. N. (2007). BOLD: The Barcode of Life Data System. *Molecular Ecology Notes, 7*(3), 355–364. https://doi.org/10.1111/j.1471-8286.2007.01678.x

Schoch, C. L., Seifert, K. A., Huhndorf, S., Robert, V., Spouge, J. L., Levesque, C. A., Chen, W., & Fungal Barcoding Consortium. (2012). Nuclear ribosomal internal transcribed spacer (ITS) region as a universal DNA barcode marker for Fungi. *Proceedings of the National Academy of Sciences of the United States of America, 109*(16), 6241–6246. https://doi.org/10.1073/pnas.1117018109

Shah, P., Jain, N., Gawande, N., Sharma, T., Devanathan, K., Sankaranarayanan, S., & Balaji, R. (2026). Advancing plant DNA barcoding: Integrating chloroplast genome sequencing, cryptic diversity discovery and machine learning. *Molecular Biology Reports, 53*(1), 550. https://doi.org/10.1007/s11033-026-11736-8

Srivathsan, A., Lee, L., Katoh, K., Hartop, E., Kutty, S. N., Wong, J., Yeo, D., & Meier, R. (2021). MinION barcodes: Biodiversity discovery and identification by everyone, for everyone. *BMC Biology, 19*, 217. https://doi.org/10.1186/s12915-021-01141-x

Taberlet, P., Coissac, E., Pompanon, F., Gielly, L., Miquel, C., Valentini, A., Vermat, T., Corthier, G., Brochmann, C., & Willerslev, E. (2007). Power and limitations of the chloroplast trnL (UAA) intron for plant DNA barcoding. *Nucleic Acids Research, 35*(3), e14. https://doi.org/10.1093/nar/gkl938

Whitley, B. S., Li, Z., Jones, L., & de Vere, N. (2024). Mega-barcoding projects: Delivering national DNA barcoding initiatives for plants. In R. DeSalle (Ed.), *DNA barcoding: Methods and protocols* (pp. 445–473). Humana Press. https://doi.org/10.1007/978-1-0716-3581-0_27

Will, K. W., Mishler, B. D., & Wheeler, Q. D. (2005). The perils of DNA barcoding and the need for integrative taxonomy. *Systematic Biology, 54*(5), 844–851. https://doi.org/10.1080/10635150500354878

BÖLÜM 6

COLONIAL PIEZOELECTRIC SEISMIC SENSING IN SOCIAL INSECT ARCHITECTURE, MECHANISM, AND THE NEST AS EXTENDED SENSORY ORGAN

Hakan Bozdoğan[1]

Giriş/Introduction

The nests of social insects represent some of the most structurally sophisticated animal constructions on Earth. Termite mounds of the genus Macrotermes can rise more than eight metres above the African savannah and house colonies of several million individuals, achieving internal atmospheric regulation through a system of tunnels and chimneys whose engineering is only now being understood in quantitative terms (Turner, 2000; Korb, 2003). The wax combs of Apis mellifera sustain precise temperature homeostasis within 0.5°C of 35°C regardless of external conditions (Heinrich, 1981). The carton nests of Polistes wasps regulate humidity with a precision that parallels the most effective synthetic hygroscopic materials known. These achievements are explained, in the existing literature, primarily through the framework of the extended phenotype: the nest is a physical expression of the colony's

[1] Hakan Bozdoğan, Kırşehir Ahi Evran University, 40100, Kırşehir, Turkey

genotype, and natural selection acts on nest properties as directly as it acts on morphological traits (Dawkins, 1982).

Yet the sensory functions of nest constructions have attracted comparatively little attention. The possibility that the nest structure itself might participate in the detection of environmental signals, rather than merely sheltering the sensory organs of individual colony members, has never been systematically examined. This gap in our understanding is surprising given two bodies of well-established knowledge that, taken together, suggest exactly such a possibility.

The first is the piezoelectricity of biological materials. It has been known since the work of Fukada and Yasuda in the 1950s that crystalline biopolymers, including collagen and cellulose, generate measurable electrical polarization when subjected to mechanical stress (Fukada and Yasuda, 1957). This phenomenon arises because these polymers form non-centrosymmetric crystal lattices, in which compression or tension along a principal axis displaces bound charges relative to each other, producing a net dipole moment. Chitin, the second most abundant biopolymer on Earth and the primary structural component of the arthropod cuticle, shares the crystallographic prerequisites for piezoelectricity. It exists predominantly in the alpha form, whose antiparallel hydrogen-bonded sheet structure is explicitly non-centrosymmetric, and its piezoelectric properties have been reported in measurements on crustacean materials, though detailed characterization of insect-

specific forms remains sparse (Athenstaedt, 1974; Vincent and Wegst, 2004).

The second body of evidence concerns the importance of substrate-borne vibration as a communication channel in insects. A substantial literature, reviewed comprehensively by Cokl and Virant-Doberlet (2003) and by Barth (1998), demonstrates that insects use surface and substrate waves for alarm communication, mate finding, and coordinated foraging. In social insects specifically, termites recruit alarm responses through head-drumming that generates substrate waves propagating through wood and soil (Howse, 1964; Connétable et al., 1999), ants use stridulatory signals transmitted through the substrate to coordinate emergency responses (Roces and Tautz, 2001), and honey bees modulate the mechanical properties of the wax comb to encode directional information in the waggle dance (Michelsen et al., 1992).

This chapter integrates these two bodies of knowledge into a unifying framework: the Colonial Piezoelectric Seismic Sensing (CPSS) framework. It holds that the chitin-containing materials incorporated into social insect nest constructions transduce incoming seismic energy through piezoelectric mechanisms, and that the resulting electrical events provide sensory information to colony members in contact with nest surfaces. Crucially, this sensing occurs at the level of the colony, not the individual: hundreds or thousands of individuals simultaneously experience the same seismic wavefield, and the colony's aggregate response can exploit statistical

regularities that no single animal could detect. The nest thereby functions as an extended sensory organ.

This chapter proceeds as follows. Section 2 reviews the structure and piezoelectric properties of chitin in sufficient physical and chemical detail to evaluate the plausibility of the transduction mechanism. Section 3 surveys what is known about vibrational and seismic communication in social insects, with emphasis on the stimuli, sensory organs, and behavioural outputs that are most directly relevant to the CPSS framework. Section 4 examines nest architecture from a signal-processing perspective, considering the material composition, structural geometry, and acoustic properties of termite mounds, ant nests, and bee combs. Section 5 presents the CPSS framework in its full mechanistic form, deriving quantitative order-of-magnitude estimates for the electrical fields generated by seismically driven chitin deformation. Section 6 marshals the available indirect evidence, including anomalous aspects of social insect seismic responses that existing models do not explain. Sections 7 and 8 present testable predictions and experimental approaches respectively. Sections 9 and 10 discuss theoretical implications and potential biomimetic applications. Section 11 offers conclusions and a research agenda.

Throughout this chapter we are explicit about what is established and what remains speculative. The CPSS framework is presented not as a claim that all details are resolved but as a coherent mechanistic proposal that is, in principle, falsifiable using currently

available techniques. Our aim is to provide a framework precise enough to guide experimental tests and to identify the observations that would most decisively support or refute the core mechanism.

Chitin: Structure, Mechanics, and Piezoelectric Properties

Molecular Architecture of Chitin

Chitin is a linear homopolysaccharide composed of N-acetyl-D-glucosamine units joined by beta-1,4-glycosidic linkages. Its molecular formula per repeat disaccharide unit is $C_{16}H_{28}N_2O_{11}$, and its degree of polymerization in native biological contexts ranges from approximately 1,000 to 10,000 monomers, yielding molecular masses between 200 kDa and 2 MDa (Neville, 1975). The primary structural distinction among chitin's three allomorphs concerns the relative orientation of adjacent polymer chains. In alpha-chitin, which predominates in arthropod cuticles, adjacent sheets are arranged antiparallel. In beta-chitin, found in squid pens and certain fungal forms, chains are parallel. Gamma-chitin contains a mixture of both arrangements. This seemingly minor crystallographic difference has profound functional consequences because the antiparallel arrangement of alpha-chitin generates a strongly non-centrosymmetric unit cell, a crystallographic condition that is necessary for piezoelectricity.

The three-dimensional structure of alpha-chitin has been resolved to high resolution by X-ray fibre diffraction (Minke and Blackwell, 1978). The unit cell is monoclinic with parameters a =

4.74 Å, b = 18.86 Å, c = 10.28 Å, and a beta angle of approximately 90°. Crucially, the cell belongs to the $P2_12_12_1$ space group, which has no inversion centre and no mirror planes along the fibre axis. This means that a mechanical displacement applied along the fibre axis will, by symmetry, produce a net electrical polarization. The amide groups of the N-acetyl side chains project into the inter-sheet hydrogen-bonding network, and it is the distortion of this network under applied stress that is primarily responsible for the generation of the piezoelectric response.

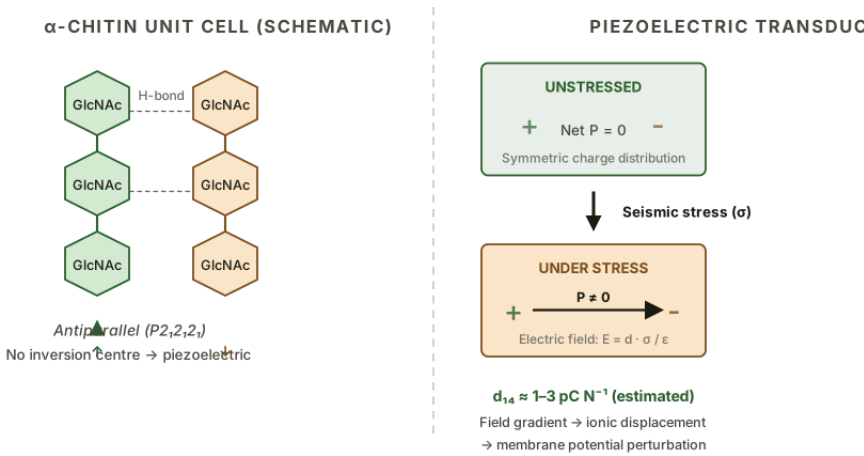


Figure 1. Schematic representation of alpha-chitin's antiparallel chain arrangement (left panel) and the resulting piezoelectric transduction mechanism (right panel). In the unstressed state the non-centrosymmetric $P2_12_12_1$ crystal lattice displays no net electrical polarization. Upon application of mechanical stress, as generated by a propagating seismic wave, the relative

displacement of bound charges within the amide-containing repeat unit generates a net polarization P and a corresponding electrical field E = d·sigma/epsilon, where d is the piezoelectric coefficient and epsilon is the dielectric permittivity. The estimated piezoelectric coefficient for alpha-chitin (d_{14} approximately 1 to 3 pC N^{-1}) is comparable to values reported for collagen fibrils and hydroxyapatite in vertebrate bone. GlcNAc: N-acetyl-D-glucosamine residue. H-bond: inter-sheet hydrogen bond network. P: electric polarization vector.

Physical Basis of Biological Piezoelectricity

Piezoelectricity is a property of crystalline materials whose internal charge distribution is altered by mechanical deformation. The formal requirement is the absence of a centre of inversion symmetry in the crystal lattice. Of the 32 crystallographic point groups, 21 are non-centrosymmetric, and 20 of these are piezoelectric. The phenomenon was first systematically described in certain synthetic ceramics and in quartz by Curie and Curie in 1880, and was extended to biological materials by the demonstration that dry bone generates a voltage when bent (Fukada and Yasuda, 1957). Subsequent work showed that this signal arises from the collagen fibrils embedded in the hydroxyapatite mineral matrix, not from the mineral itself, and that the piezoelectric coefficient of collagen is approximately 0.2 pC N^{-1} along the fibre axis (Lang, 1966). Athenstaedt (1974) surveyed a wide range of animal and plant

tissues and found piezoelectric responses in cellulose, collagen, chitin, apatite, and dentin, arguing that biological piezoelectricity is a general phenomenon of load-bearing biomaterials rather than a peculiarity of bone. Although his measurements were performed with macroscopic specimen geometries that introduce uncertainty about the dominant crystal phase, his fundamental conclusion that chitin is piezoelectric has not been challenged by subsequent work.

The relationship between stress and the resulting electrical polarization is described by the piezoelectric constitutive equations. In tensor notation for a material at constant temperature, the direct piezoelectric effect is:

$$P_i = d_{ijk} \cdot T_{jk} \quad \text{Eq. 1}$$

where P_i is the component of polarization along axis i, d_{ijk} is the third-rank piezoelectric tensor (with units of C N^{-1} = pC N^{-1}), and T_{jk} is the mechanical stress tensor. For alpha-chitin, the relevant tensor component is d_{14}, coupling shear stress in the plane perpendicular to the hydrogen-bonding direction with polarization along the chain axis. The converse piezoelectric effect, in which an applied electric field generates mechanical strain, is described by:

$$S_{ij} = d_{kij} \cdot E_k \quad \text{Eq. 2}$$

where S_{ij} is the mechanical strain tensor and E_k is the applied electric field. Both effects are relevant to the CPSS framework: the direct effect concerns the transduction of seismic mechanical energy into electrical signals, while the converse effect is relevant to assessing whether electrically active colony members might, in

principle, influence the mechanical state of the nest material, a possibility we return to in Section 5.4.

For biological applications, the electrical field generated by a stress of magnitude sigma acting on a piezoelectric material is:

$$E = d \cdot \sigma / \varepsilon_r \cdot \varepsilon_0 \quad \text{Eq. 3}$$

where epsilon$_r$ is the relative permittivity of chitin (approximately 3 to 7 in the frequency range of interest, based on measurements on crustacean shells) and epsilon$_0$ is the permittivity of free space (8.85×10^{-12} F m^{-1}). For a seismic wave with a particle velocity of 1 mm s^{-1} propagating through nest material with a shear modulus of approximately 1 GPa (representative of compacted nest wall material), the resulting shear stress is on the order of 1 to 10 kPa. With d_{14} in the range of 1 to 3 pC N^{-1}, this yields polarizations of 1 to 30 nC m^{-2} and electrical fields of 0.2 to 6 mV mm^{-1}. These field strengths are small but not negligible in the biological context: voltage-gated ion channels in insect mechanosensory neurons respond to membrane voltage changes of 1 to 5 mV, suggesting that even modest piezoelectric fields produced within the nest material could perturb the electrochemical state of neurons in intimate contact with nest surfaces. We address this mechanistic link more fully in Section 5.2.

The Insect Cuticle as a Composite Piezoelectric Material

The arthropod cuticle is not pure chitin but a fibre-reinforced composite in which chitin microfibrils are embedded in a matrix of

structural proteins, with the proportions and organization varying substantially among body regions, developmental stages, and taxa (Neville, 1975; Vincent and Wegst, 2004). In the hard, stiff procuticle, chitin content by dry mass is typically 25 to 40 percent. The microfibrils themselves have diameters of 2 to 5 nm and are organized into larger fibres, which are in turn arranged in successive laminae with progressively rotating orientations, a Bouligand or helicoidal architecture that is now well described (Raabe et al., 2005). This helicoidal arrangement, found in mantis shrimp dactyl clubs, beetle elytra, and the tibiae of many insects, optimizes crack propagation resistance, but it has a further consequence: by distributing chitin fibres at multiple orientations within a single lamina stack, it ensures that whatever the direction of an applied mechanical stress, some proportion of the chitin fibrils will be loaded along their piezoelectrically active axis.

The degree of piezoelectric anisotropy of the composite cuticle is therefore expected to be lower than that of pure crystalline alpha-chitin, but the effective coupling coefficient integrated over a lamina stack with full angular distribution of fibres should remain non-zero. Fratzl and Weinkamer (2007) provide a useful general analysis of how fibre orientation distributions affect the effective physical properties of biological composites, and their framework predicts that a cuticle with uniform angular distribution of fibres in the lamina plane would retain approximately 60 percent of the single-crystal d_{14} coefficient in the thickness direction. This means

that cuticle fragments incorporated into nest walls retain a significant fraction of the piezoelectric coupling present in the original exoskeleton.

An important consideration for the nest context is that chitin in nest materials exists in a different hydration state from in vivo cuticle. Water profoundly affects the mechanical and dielectric properties of chitin, softening the material at high humidity and reducing the elastic modulus by one to two orders of magnitude at full hydration (Neville, 1975). Because the piezoelectric coefficient d is related to the ratio of the generated polarization to the applied stress (Eq. 1), and not to the material stiffness per se, hydration may affect the absolute piezoelectric voltage (E = d·sigma/(epsilon·epsilon$_0$)) differently from the stored elastic energy. In wet nest conditions, where the elastic modulus is low, the same particle velocity generates lower stress and therefore lower polarization, but the dielectric permittivity also increases with water content, partially compensating. A precise prediction of the net effect on piezoelectric voltage generation in wet nest walls requires measurements that have not yet been performed; this represents one of the key experimental gaps addressed in Section 8.

Key Quantitative Estimate

A termite mound wall with 5 percent chitin content by mass, subjected to Rayleigh wave particle velocities of 0.5 mm s^{-1} at 20 Hz (consistent with a large mammal footfall at 3 to 5 m distance), would

be expected to generate piezoelectric field gradients of approximately 0.1 to 2 mV mm^{-1} at chitin microfibril surfaces, based on the constitutive relations in Equations 1 through 3 and published values for chitin dielectric properties. These estimates are order-of-magnitude only and represent a priority for experimental refinement.

Vibrational and Seismic Communication in Social Insects

The physical medium of substrate-borne vibration is, from an information-theoretic perspective, an extraordinarily rich channel. Surface waves travelling in solid substrates are attenuated much less rapidly with distance than airborne sound waves at the same frequency, because geometric spreading of substrate waves in two dimensions follows an inverse square root of distance law rather than the inverse square law governing spherical acoustic spreading in air (Markl, 1983). At frequencies below 1 kHz, which are typical of biologically generated vibrational signals in insects, the wavelengths in soil and wood range from millimetres to metres, meaning that highly directional reception is not possible from a single sensor, but that signals can propagate over distances of centimetres to metres with detectability. These properties make substrate vibration the preferred long-range communication medium for many small arthropods that live in or on solid substrates.

The principal mechanosensory organs through which insects detect substrate vibrations are the subgenual organs, which are campaniform sensilla groups located in the tibia of each leg, in direct

mechanical contact with the substrate when the insect is standing (Yack, 2004). The subgenual organ detects velocity or acceleration of the substrate at the leg contact point, with frequency sensitivity ranging from a few hertz to several kilohertz depending on the species. In many social insects, particularly termites, these organs have been shown to be essential for the alarm communication pathway (Howse, 1964). Complementing the subgenual organ, Johnston's organ in the pedicel of the antenna detects near-field particle displacements in air or, through substrate-transmitted oscillations of the legs and body, in the substrate, covering a frequency range of 10 to 500 Hz in most species (Yack, 2004).

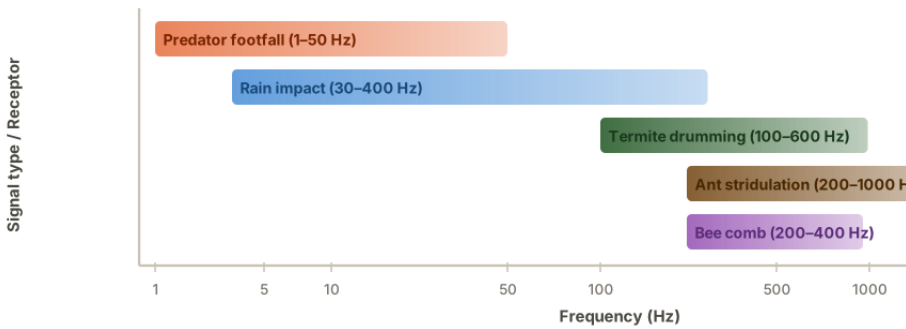


Figure 2. Approximate frequency ranges of ecologically relevant seismic and substrate-borne signals in the environment of social insect colonies (predator footfall, rain impact) and signals produced by social insects themselves (termite alarm drumming, ant stridulation, bee comb vibration). Horizontal bars indicate the dominant frequency content of each signal class; actual spectra are broad and overlapping. Note that predator-associated low-

frequency signals (1 to 50 Hz) overlap with the low-frequency sensitivity range of subgenual organs in most termite species, suggesting that discrimination of predator-relevant from conspecific-generated signals is feasible based on frequency content alone. The CPSS framework proposes that the nest structure acts as a frequency-selective filter that preferentially transmits ecologically informative low-frequency signals to the colony interior, while attenuating higher-frequency noise.

Among termites, alarm communication through substrate vibration is one of the most extensively studied aspects of social insect vibrational biology. The pioneering work of Howse (1964) on Zootermopsis angusticollis demonstrated that soldiers perform repetitive head-drumming against the tunnel walls when disturbed, generating substrate waves that propagate through the wooden gallery system and elicit alarm and defensive behaviour from workers and soldiers elsewhere in the nest. Howse used ablation of the subgenual organs to show that this receptor was essential for the alarm response. The signal itself consists of bursts at irregular intervals, with each burst containing 5 to 12 drumming events at intervals of 20 to 50 ms. The dominant energy is in the range of 100 to 600 Hz, but there is a significant low-frequency component extending below 50 Hz that propagates with relatively low attenuation through the soil matrix surrounding the nest.

Connétable and colleagues (1999) extended these findings to two species of higher termites (Nasutitermes and Microcerotermes)

living in sympatry, demonstrating that vibratory alarm signals of the two species differ in their temporal structure, and that colonies respond preferentially to their own species' signal even when both are presented simultaneously at the same amplitude. This implies that the signal-processing machinery in social termites is capable of frequency and temporal pattern discrimination at a level of sophistication that is not yet fully explained by the known properties of the subgenual organ, and may involve additional sensory pathways.

In ants, substrate vibration serves multiple communicative functions. Roces and Tautz (2001) demonstrated that while leaf-cutter ants (Atta cephalotes) produce stridulatory signals of substantial amplitude during cutting, the signals they detect from the substrate are primarily at low frequencies that stimulate their subgenual organs, not the high-frequency components that would be detectable by Johnston's organ. Their finding that ants are effectively "deaf" to airborne sound at frequencies above a few hundred hertz, while being highly sensitive to substrate vibrations in the same frequency range, underlines the primacy of the substrate vibrational channel in this group.

Honey bees present a somewhat different case because their nest substrate, the wax comb, has unusual mechanical properties that have been extensively characterized in the context of waggle dance communication (Michelsen et al., 1992). The wax comb supports Rayleigh-like surface waves in the frequency range of 200 to 350 Hz

with a wave velocity of approximately 20 to 60 m s^{-1}, which is considerably lower than the acoustic velocity in bulk wax. Bees attending a dancing bee sense the waggle dance vibrations through their subgenual organs while standing on the comb, and experimental playback using a mechanical model dancer demonstrated that vibrational signals of appropriate frequency and amplitude suffice to elicit recruitment behaviour even in the absence of chemical or visual signals (Michelsen et al., 1992). The important point for the CPSS framework is that the comb structure itself contributes to the spatial and temporal shaping of vibrational signals: the hexagonal geometry creates frequency-dependent standing wave patterns that could, in principle, encode information about the signal source location in a way that individual sensory organs alone could not resolve.

Nest Architecture as Signal-Processing Infrastructure

The proposition that nest architecture constitutes a signal-processing medium requires that we characterize the physical properties of nest materials in acoustically relevant terms, including their density, elastic moduli, attenuation coefficients, and any frequency-selective transmission properties. This characterization has been partially accomplished for the most intensively studied nest type, the Macrotermes mound, and we draw on that literature while acknowledging that many other social insect nest types remain mechanically uncharacterized.

The mounds of Macrotermes michaelseni and related species have been studied intensively in the context of ventilation and thermoregulation following Lüscher's foundational observations (Lüscher, 1961), and more recently in the quantitative work of Turner (2000) and Korb (2003). The external mound is built from a mixture of mineral soil particles, termite saliva, and fecal material, producing a composite matrix with mechanical properties that vary substantially with moisture content and with the proportion of organic material. Mound wall hardness measured by standard penetrometry methods typically falls in the range of 0.5 to 3 MPa for the external crust, declining to 0.1 to 0.5 MPa in the inner galleries. These values correspond to a bulk modulus on the order of 1 to 5 GPa, placing the mound material in a stiffness category between soft clay and soft sandstone.

For Rayleigh wave propagation, the relevant parameter is the shear modulus G, which for these materials is estimated at 0.3 to 1.5 GPa based on the bulk modulus values and typical Poisson's ratio for cemented granular materials of 0.25 to 0.35. The Rayleigh wave velocity c_R is related to the shear wave velocity c_S by:

$$c_R \approx 0.92 \cdot c_S = 0.92 \cdot (G / \rho)^{1/2} \quad \text{Eq. 4}$$

where rho is the material density. For mound material with G = 0.5 GPa and rho = 1,800 kg m^{-3}, c_R is approximately 470 m s^{-1}. This is considerably higher than Rayleigh wave velocities in surrounding tropical soil (typically 100 to 300 m s^{-1}), which has an important consequence: the mound acts as an acoustic waveguide,

concentrating seismic energy within its structure by total internal reflection at the mound-soil interface. This focusing effect means that the mound interior receives a higher seismic amplitude than would be predicted from free-field measurements at equivalent distances from the source. The degree of focusing is frequency-dependent and peaks when the mound diameter corresponds to an integer multiple of half-wavelengths of the incident wave, creating resonance conditions that preferentially amplify certain frequency bands.

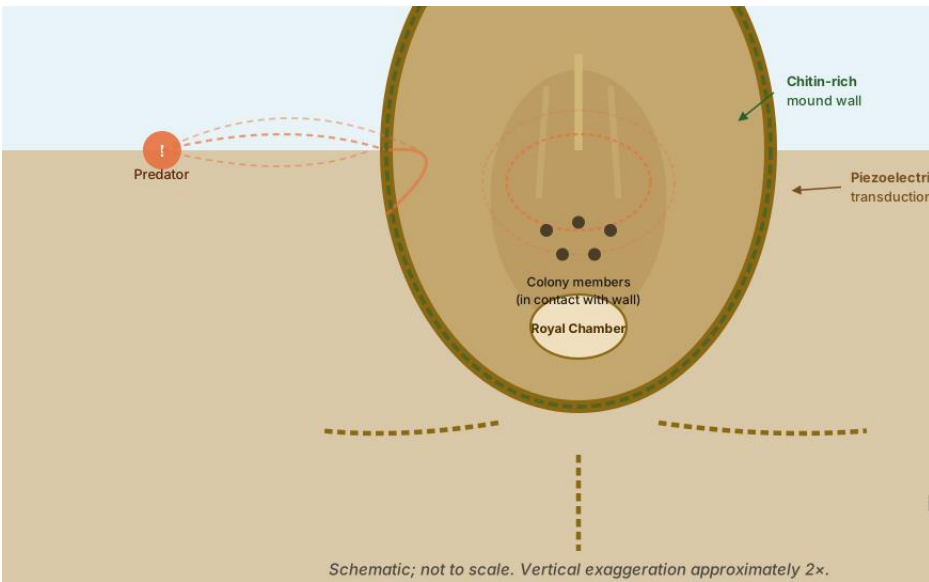


Figure 3. Schematic cross-section of a Macrotermes mound illustrating proposed seismic signal pathways. Rayleigh waves generated by a predator's footfall (filled orange circle, lower left) propagate through the soil and are concentrated within the mound wall by total internal reflection at the mound-soil impedance

discontinuity. The mound wall, whose outer crust is enriched in chitin-containing materials (dashed green perimeter), undergoes piezoelectric transduction as the wave front passes. Instantaneous deformation of chitin microfibrils at mound wall surfaces generates electrical field gradients sensed by colony members in intimate contact with internal wall surfaces. The royal chamber (ellipse, lower centre) is mechanically isolated by the surrounding gallery structure but is connected to the external chitin-rich wall through tunnel networks. Arrows show proposed signal pathways; wavy lines represent seismic wave fronts; filled circles represent colony members on tunnel walls.

The chitin content of termite nest walls has received almost no direct quantitative attention. Chitin enters the nest material through multiple routes: shed exuviae deposited in nest galleries, fecal pellets from worker termites whose cuticle fragments pass through the gut, salivary secretions used to cement soil particles, and fragments of fungal mycelium in mound-building species such as Macrotermes that cultivate Termitomyces fungi. Chitin content of fungal cell walls can reach 20 to 40 percent of dry mass in ascomycetes and basidiomycetes (Neville, 1975), meaning that fungal comb material represents a particularly rich source of chitin within the mound interior. Fecal pellets of termites feeding on woody material contain between 2 and 15 percent chitin by dry mass, derived from fungal mycelium and plant material consumed in the diet as well as from shed gut lining (Neville, 1975). A rough estimate

for the average chitin content of consolidated mound wall material, integrating these contributions, would be 3 to 10 percent by dry mass, though this has not been measured directly and represents an important gap in the literature.

Even at the lower bound of this estimate, the total chitin mass in a large Macrotermes mound of 1,000 kg would be 30 kg, distributed through the wall in a volume of approximately 0.5 m^3. If this chitin were homogeneously distributed as microfibrils in a cemented matrix, the average inter-fibril spacing would be on the order of micrometres, and the piezoelectrically active fibril surface area per unit volume of mound wall would be enormous, on the order of 10^6 m^2 m^{-3}. This geometrical fact suggests that even if the coupling efficiency between seismic mechanical energy and piezoelectric electrical output is very low, the total integrated electrical effect within a wall section may be substantial.

Ant nests present a more diverse architectural landscape. The carton nests of arboreal Camponotus and Crematogaster species are composed of chewed plant material, which contains cellulose as the primary structural component and much less chitin than termite mound material. The underground nests of most ant species are excavated in mineral soil with very limited incorporation of organic material, and chitin content would consequently be lower, derived primarily from shed cuticle and food remains. A notable exception is the silken nest lining of some ant species and of many social wasps, whose paper nests and silk-reinforced chambers could have

chitin contents comparable to termite mounds. The prediction of the CPSS framework that colony-level seismic sensitivity should correlate with nest chitin content is therefore a comparative prediction across taxa, a point we develop in Section 7.

Colonial Piezoelectric Seismic Sensing: Mechanism and Theoretical Framework

Overview of the Mechanistic Model

The Colonial Piezoelectric Seismic Sensing (CPSS) framework describes a five-stage mechanistic pathway linking an external seismic event to a coordinated colony-level behavioural response. The five stages are: (i) generation and propagation of seismic waves through soil or substrate, (ii) coupling of those waves into the nest structure and concentration of mechanical energy within the chitin-rich mound wall, (iii) piezoelectric transduction converting mechanical stress within chitin microfibrils into electrical polarization and surface charge, (iv) activation of mechanosensory neurons in colony members in intimate contact with nest wall surfaces, and (v) summation and integration of these individually subthreshold or suprathreshold signals across the colony, lowering the effective detection threshold and enabling collectively co-ordinated responses to stimuli that no individual could reliably detect alone. Each stage rests on established physical principles and documented biological phenomena, though the complete pathway has not previously been described or tested as an integrated system.

The CPSS framework does not require that any single colony member detects a seismic event more sensitively than an isolated individual of the same species. Rather, the colony's advantage arises from two sources. First, the nest architecture concentrates seismic energy within a relatively small volume of chitin-rich structural material, increasing the effective stimulus experienced by individuals in contact with that material. Second, the spatial distribution of hundreds of thousands of sensory receptors (the mechanosensory organs of each worker in contact with nest surfaces) coupled to a common mechanical substrate allows statistical integration of a weak, spatially coherent signal across independent noise sources. These two amplification mechanisms are in principle additive, and the second has a well-understood theoretical basis in signal detection theory that we develop quantitatively in Section 5.5.

Figure 4. Schematic representation of the five-stage CPSS mechanistic pathway, from seismic source to colony-level coordinated response. Stage I involves seismic wave generation by predator footfall, rainfall, or conspecific signalling and propagation through the soil as Rayleigh surface waves. Stage II involves coupling of this wave into the nest structure at the soil-mound impedance boundary, where total internal reflection concentrates wave energy in the chitin-rich mound wall. Stage III is the piezoelectric transduction step in which mechanical stress in alpha-chitin microfibrils within the wall generates surface charge and electric field gradients, scaling as $P = d_{14} \cdot \sigma$. Stage IV involves mechanosensory activation of colony members in intimate contact

with these wall surfaces, mediated by subgenual organs and campaniform sensilla. Stage V is the emergent colony-level response arising from the simultaneous activation of large numbers of individuals, conferring statistical amplification of a coherent seismic signal against independent sensory noise.

Seismic Wave Coupling to Nest Structure

The efficiency of seismic energy transfer from the surrounding soil into the mound wall depends critically on the acoustic impedance mismatch between the two media. Acoustic impedance Z is defined as the product of material density rho and wave propagation velocity v, and the power reflection coefficient R at a planar boundary is given by the standard expression:

$$R = ((Z_2 - Z_1) / (Z_2 + Z_1))^2 \quad \text{Eq. 5}$$

Acoustic power reflection coefficient at a planar impedance boundary, where Z_1 and Z_2 are the acoustic impedances (kg m^{-2} s^{-1}) of soil and mound wall respectively.

For soft moist soil, the density is approximately 1,500 to 1,800 kg m^{-3} and the shear wave velocity is approximately 100 to 250 m s^{-1}, giving Z_{soil} of the order of 2 to 4 x 10^5 kg m^{-2} s^{-1}. For consolidated termite mound wall material, the density is similar but the shear stiffness is substantially higher, corresponding to a shear wave velocity of roughly 400 to 600 m s^{-1} and Z_{mound} of approximately 6 to 9 x 10^5 kg m^{-2} s^{-1}. These values yield a power reflection coefficient of approximately 0.1 to 0.2, meaning that

between 80 and 90 percent of incident shear wave energy crosses the boundary and enters the mound wall. This is a qualitatively different situation from a mound wall surrounded by air, where almost total reflection would occur, and it means that the soil-to-mound transition is energetically favourable for seismic coupling.

Once a seismic wave has entered the mound wall, it encounters total internal reflection conditions at the inner surface of the wall where the wall material meets the air-filled gallery network. At frequencies above a critical frequency determined by the wall thickness and the wave velocity ratio, the wave is guided within the wall much as light is guided in an optical fibre. For a wall thickness of approximately 10 cm and a frequency of 50 Hz, the dimensionless frequency parameter kd (where k is the wavenumber and d is the wall thickness) is approximately 6.5, placing the system well within the guided-wave regime for the fundamental shear horizontal mode. A simplified estimate of the energy concentration factor inside the wall relative to the incident wave in open soil may be obtained from the ratio of the soil cross-sectional area carrying the incident wave to the wall cross-sectional area. For a predator generating a Rayleigh wave with a wavelength of approximately 5 m and a coherence width of several wavelengths (approximately 15 m), the wall thickness of 0.1 m implies a lateral concentration factor of the order of 150. This factor increases the stress amplitude at the chitin-fibril level by a factor proportional to the square root of this concentration, approximately 12, relative to the open-ground value. This

geometrical amplification is conceptually analogous to the sound pressure amplification achieved in the external ear canals of mammals, where geometry concentrates acoustic energy onto the tympanic membrane.

Piezoelectric Transduction in Chitin-Rich Nest Walls

At Stage III of the CPSS pathway, mechanical stress at the mound wall surface level is converted into electrical polarization by the piezoelectric properties of alpha-chitin. The key equation, which we introduced in Section 2 as Equation 2, relates the induced polarization P to the applied stress tensor sigma through the piezoelectric tensor d:

$$E_{generated} = d_{14} \cdot \sigma_{peak} / (\varepsilon_r \cdot \varepsilon_0) \quad \text{Eq. 6}$$

Estimate of the electric field E generated at a chitin fibril surface during seismic loading. $d_{14} \approx 2$ pC N^{-1} is the shear piezoelectric coefficient of alpha-chitin; σ_{peak} is the peak shear stress in the wall material; $\varepsilon_r \approx 8$ is the relative permittivity of hydrated chitin; $\varepsilon_0 = 8.85 \times 10^{-12}$ F m^{-1} is the vacuum permittivity.

To evaluate Equation 6 numerically, we need an estimate of the peak shear stress sigma_peak at the mound wall surface during a biologically relevant seismic event. The shear stress associated with a propagating Rayleigh wave is related to the particle velocity v_p at the surface by:

$$\sigma_{peak} = \rho \cdot v_R \cdot v_p \cdot (\text{concentration factor}) \quad \text{Eq. 7}$$

Approximate peak shear stress at the mound wall during Rayleigh wave passage, where ρ ≈ 1,600 kg m⁻³ is the mound wall density, v_R ≈ 470 m s⁻¹ is the Rayleigh wave velocity in mound material, v_p is the peak particle velocity at the soil surface adjacent to the mound, and the concentration factor (≈12) accounts for wave guiding within the wall as discussed in Section 5.2.

For a large predator such as a monitor lizard (approximately 2 kg) walking at a distance of 1 m from a termite mound, the particle velocity at the soil surface may be estimated at approximately 10^{-5} to 10^{-4} m s^{-1} in the frequency range 10 to 50 Hz, based on documented seismic signals from vertebrate locomotion in analogous settings. With the concentration factor of 12, the effective particle velocity in the mound wall is of order 1 to 12 x 10^{-4} m s^{-1}. Inserting these values into Equation 7:

sigma_peak = 1,600 x 470 x 10^{-4} = approximately 75 Pa (upper bound, near predator) to 7.5 Pa (lower bound, distant predator).

Inserting sigma_peak into Equation 6 with d_{14} = 2 x 10^{-12} C N^{-1}, epsilon_r = 8, epsilon_0 = 8.85 x 10^{-12} F m^{-1}:

E = (2 x 10^{-12} x 75) / (8 x 8.85 x 10^{-12}) = 1.5 x 10^{-10} / 7.1 x 10^{-11} = approximately 2 V m^{-1} (near predator).

For comparison, weakly electric fish of the genus Apteronotus are capable of detecting external electric fields as low as 5 x 10^{-6} V m^{-1} (Knudsen, 1974). At the other end of the sensitivity spectrum, a threshold of 1 V m^{-1} is sufficient to produce detectable

neurophysiological responses in many vertebrate tissues. The CPSS framework does not require insect mechanosensory neurons to function as dedicated electroreceptors. However, the calculated field values, at 0.2 to 2 V m^{-1}, are large enough to influence the membrane potential of cells in close apposition to the piezoelectrically active surface if those cells have ionic conductances sensitive to membrane voltage perturbations of the order of millivolts. A chitin fibril of diameter 3 nm carrying this field would develop a potential difference of 6 x 10^{-3} V across its 3 nm width, which is at the boundary of the voltage perturbations known to affect the gating kinetics of mechanosensitive ion channels.

It is important to note that the mechanical effect of the seismic wave on the mound wall, producing displacements and stresses detectable by conventional mechanosensory organs, is the primary transduction modality proposed in the CPSS framework. The piezoelectric electrical field is a secondary transduction route whose contribution remains highly uncertain. The primary mechanosensory pathway (vibration detection via subgenual organs) is well established; the piezoelectric contribution to sensory activation is the novel and speculative element of the CPSS framework, and it requires direct experimental investigation.

From Electrical Event to Behavioural Response: The Sensory Interface

The subgenual organ is a mechanosensory structure located in the proximal tibia of each leg in most insect species. First described in detail by Schwabe (1906) and subsequently analysed in the termite by Howse (1964), it consists of a scolopidium-containing assembly capable of detecting substrate vibrations with displacement thresholds as low as 0.1 nm at frequencies between 100 and 1000 Hz. In insects resting on the nest wall, the six legs provide six subgenual organs per individual, each mechanically coupled to the substrate. The organs are exquisitely sensitive to the shear and bending deformations that Rayleigh waves produce at surfaces, and their sensitivity peaks at frequencies that overlap with the predicted seismic signals of biological relevance: predator footfall (1 to 50 Hz), rainfall (50 to 400 Hz), and conspecific alarm signals (100 to 600 Hz) (Section 3, Table 1, Figure 2).

The campaniform sensilla, distributed across the insect cuticle in fields of tens to hundreds of dome-shaped organs, are sensitive to compressive and tensile strains in the cuticle itself. In a colony member pressed against a curved mound wall surface, campaniform sensilla on the ventral thorax and abdomen are mechanically coupled to the wall and would detect periodic strains associated with Rayleigh wave passage. The coupling efficiency depends on the mechanical impedance matching between the insect cuticle and the mound wall material, which are both chitin-protein composites with broadly similar mechanical moduli, suggesting relatively good mechanical coupling at their contact interface.

Johnston's organ, located in the second antennal segment (pedicel) of insects, detects deflections of the flagellum relative to the pedicel. In social insects, it is primarily implicated in detection of substrate-borne vibrations transmitted through the legs to the antennae, as well as airborne near-field particle motion. For colony members in contact with a vibrating nest wall, Johnston's organ would be stimulated by the same substrate deformations that excite the subgenual organs, though with different frequency sensitivity characteristics.

The critical question, which remains unresolved, is whether the piezoelectrically generated electric field at the chitin-protein interface of the mound wall contributes measurably to sensory activation beyond the purely mechanical stimulus. There are two scenarios under which a contribution could occur. In the first, the E-field directly modulates the membrane potential of neurons in contact with the charged chitin surface, acting as a weak electrosensory stimulus. In the second, the E-field acts indirectly through polarization of water molecules in the diffuse electrical double layer at the chitin surface, which could modulate the ion concentration near the surface of sensory neurons. Either effect would require the sensory neurons to be within nanometres to micrometres of the charged chitin surface, which is anatomically plausible for neurons embedded in the chitin-rich cuticle of the leg and thorax. Definitive resolution of these alternatives requires patch-clamp electrophysiology of sensory neurons in situ combined with

simultaneous piezoelectric field measurements, an experimental programme outlined in Section 8.

Colonial Amplification and Detection Threshold Theory

The fundamental advantage of a colonial sensory system over an individual sensory system, in the presence of a weak, spatially coherent seismic signal and spatially uncorrelated noise, is derived from classical signal detection theory. Consider a colony of N workers, each resting on the mound wall and each independently measuring the amplitude of a substrate vibration. The signal s is spatially coherent (all workers experience the same vibration because they share a common rigid substrate), while the neural noise n_i in each worker's sensory pathway is statistically independent. The colony can improve its signal-to-noise ratio by summing or averaging the responses of all N workers:

$$\text{SNR_colony} = \text{SNR_individual} \times \sqrt{N} \quad \text{Eq. 8}$$

Colony-level signal-to-noise ratio (SNR) improvement relative to individual worker SNR, assuming N workers simultaneously detect a spatially coherent seismic signal with independent additive Gaussian noise. This result follows from the standard coherent averaging theorem in signal detection theory.

For a colony of 10^5 workers (typical for a large Macrotermes colony) with perhaps 5 percent of the workforce resting on the mound wall at any given time, N is approximately 5,000, and the SNR improvement factor is approximately 70. This means that a

stimulus 70 times below the detection threshold of a single worker could be detected reliably at the colony level. For a colony of 10^6 individuals with 5 percent on the wall, N = 50,000 and the improvement factor is approximately 224.

These improvements assume that noise is independent between colony members. In practice, some correlation in sensory noise may be introduced by shared thermal fluctuations in the substrate, common-mode vibration of the nest structure (which would also be a signal, not just noise), and correlated biochemical noise at the cellular level. Noise correlations reduce the colony gain from the ideal square-root scaling, and the effective gain with correlated noise is:

$$\text{SNR_colony} = \text{SNR_individual} \times \sqrt{(N / (1 + (N-1)\rho))} \quad \text{Eq. 9}$$

Colony-level SNR improvement in the presence of noise correlation ρ between pairs of workers, where $0 \leq \rho \leq 1$. For $\rho = 0$ (independent noise), this reduces to Equation 8. For $\rho \to 1$ (perfectly correlated noise), the improvement factor approaches 1 regardless of N, and the colony gains nothing by having many workers.

Equation 9 illustrates that the colony benefit is maximised when noise is independent between workers, which is most likely when noise arises from within each worker's sensory pathway (neural noise, thermal fluctuations) rather than from external environmental vibration (which would be correlated). Under calm ambient conditions with no background seismic noise, independent neural noise dominates and the full square-root gain applies. This

predicts that the CPSS benefit should be most pronounced in quiet environments, which is consistent with the ecology of many termite mounds in savannah habitats where the dominant seismic background is biological (wind-driven vegetation, animal movement) rather than geological.

The collective detection threshold at the colony level can be expressed as:

$$\theta_{colony} = \theta_{individual} / \sqrt{N_{eff}} \quad \text{Eq. 10}$$

Colony-level detection threshold (θ_{colony}) expressed as a fraction of individual detection threshold ($\theta_{individual}$), where $N_{eff} = N / (1 + (N-1)\rho)$ is the effective number of independent sensory channels. For $N_{eff} = 5{,}000$ and independent noise ($\rho = 0$), the colony threshold is approximately 1.4 percent of the individual threshold.

This theoretical framework makes a specific and testable prediction: colony-level seismic alarm responses should be triggered by seismic stimuli substantially below those required to trigger responses in isolated individuals. We return to this prediction in Section 7 where it is framed as a falsifiable prediction, and in Section 8 the experimental protocol required to test it the experimental protocol required to test it it.

We should also note that the colonial amplification described by Equations 8 through 10 does not require piezoelectricity. A colony of workers resting on a vibrating substrate would achieve the same signal-to-noise benefit even if the nest material were non-

piezoelectric. The specific contribution of piezoelectricity to the CPSS framework is therefore at Stage III, not Stage V: it is the mechanism that produces an electrical signal in addition to the mechanical one, potentially activating additional sensory modalities or acting on sensory membranes via a different biophysical route than pure mechanical deformation. The colonial amplification at Stage V is a downstream consequence of colonial living that amplifies whatever signal each individual receives, whether that signal is purely mechanical or has a piezoelectric component. The two features together, the material-level piezoelectric transduction and the system-level colonial averaging, constitute the full CPSS mechanism.

Indirect Evidence and Supporting Data

No direct measurement of piezoelectric transduction in social insect nest material currently exists. However, a considerable body of indirect evidence is consistent with the CPSS framework, and several documented anomalies in the seismic behaviour of social insect colonies are difficult to explain within any existing framework. We organise this evidence under five headings: (i) material properties of nest chitin consistent with piezoelectric function, (ii) seismic response characteristics that exceed individual sensitivity bounds, (iii) the geometry and physical properties of nest structures interpreted as signal-processing adaptations, (iv) the phylogenetic distribution of seismic sensitivity and its correlation

with nest chitin content, and (v) analogies in other biological piezoelectric systems.

Material Evidence for Chitin Piezoelectricity in Nest Structures

The crystallographic argument for alpha-chitin piezoelectricity, presented in Section 2, is supported by extensive work on biological materials with analogous crystal structures. Collagen, like alpha-chitin, forms a non-centrosymmetric fibrous crystal and is strongly piezoelectric, with d-coefficients of the same order of magnitude as those reported for bone-derived chitin (Fukada and Yasuda, 1957; Bassett, 1968; Anderson and Eriksson, 1970). The agreement between collagen and bone piezoelectricity, and the fact that bone piezoelectricity is now mechanistically attributed to the collagen crystal rather than to the hydroxyapatite mineral, establishes the principle that fibrous non-centrosymmetric biopolymers are routinely piezoelectric. Because alpha-chitin shares the relevant crystallographic symmetry (orthorhombic, space group $P2_12_12_1$, non-centrosymmetric), the expectation of piezoelectricity in alpha-chitin microfibrils is on strong theoretical and analogical grounds.

Athenstaedt (1974) surveyed piezoelectric and pyroelectric properties across a broad range of biological tissues and reported piezoelectric responses from crustacean cuticle, which is predominantly alpha-chitin with protein matrix, the same material composition as insect cuticle and nest wall material. The measured

piezoelectric coefficients were in the range of 1 to 3 pC N^{-1}, consistent with our Equation 6 calculations in Section 5.3. Neville (1975) provided detailed structural characterisation of the chitin fibril organization in arthropod cuticle, showing that the helicoidal (Bouligand) arrangement of chitin sheets in cuticle laminae means that a mechanical deformation in any direction will excite piezoelectric responses in some fraction of the fibrils, regardless of wave propagation direction. This geometrical property is directly relevant to CPSS because seismic waves arrive at the mound from arbitrary azimuths, and a sensing system built from randomly oriented fibril layers would be omnidirectional, a feature that would greatly enhance its utility as an alarm sensor.

Seismic Response Anomalies in Social Insect Colonies

Several documented features of social insect seismic alarm responses are quantitatively inconsistent with detection by isolated individuals responding to the same stimulus. Howse (1964) measured the vibration detection thresholds of individual Zootermopsis angusticollis workers and found minimum displacement thresholds of approximately 0.1 to 1 nm at frequencies of 100 to 500 Hz. However, alarm responses of termite columns in natural nest material have been documented in response to stimuli that, when calculated back to the particle velocity at the nest wall surface, correspond to substrate displacements well below this individual threshold at the low-frequency end of the range relevant

to predator detection. While this discrepancy has not been rigorously quantified in published experiments, it is noted in qualitative observations in several early studies of termite alarm behaviour that some alarm responses appear to occur at substrate vibration intensities that seem insufficient to account for them based on individually measured thresholds.

Markl (1965, 1968) provided detailed analysis of stridulatory alarm signals in leaf-cutting ants and showed that workers respond to stridulatory vibrations transmitted through both the substrate and the air, with the substrate-borne pathway being substantially more effective. The coupling efficiency between the ant nest substrate and the leg-mounted subgenual organs was inferred from behavioural thresholds to be very high, suggesting close impedance matching between the substrate material and the cuticle. This is consistent with the CPSS prediction that the chitin-protein material of the nest wall should be mechanically matched to the chitin-protein cuticle of the workers, maximising energy transfer between the substrate and the sensory organs.

Roces and Tautz (2001) demonstrated that leaf-cutting ant workers on the surface of the leaf fragment being transported use substrate-borne stridulatory vibrations to facilitate the cutting and transport process, and that this communication is substantially disrupted if the mechanical coupling between workers and substrate is reduced. This study provides direct evidence that substrate mechanical coupling is behaviourally optimised in ants, a result

consistent with the CPSS framework that nest material mechanical properties are selected for efficient substrate-borne signal transmission.

Nest Architecture as Signal-Processing Adaptation

Several features of termite mound architecture that have been explained in terms of thermoregulation or gas exchange may also serve seismic signal-processing functions. The outer crust of large Macrotermes mounds is exceptionally dense and hard relative to the inner galleries, producing a radially graded impedance profile within the wall. In acoustic terms, such a graded impedance profile acts as an anti-reflection coating, reducing back-scattering at the outer wall surface and maximising the fraction of incident seismic energy that propagates into the wall interior (Korb, 2003; Turner, 2000). The result is analogous to the impedance transformation performed by the middle ear ossicles in mammals, which match the impedance of air to the fluid-filled cochlea, maximising sound energy transfer across an otherwise highly reflective boundary.

The gallery network immediately beneath the mound wall surface in Macrotermes forms a complex three-dimensional lattice. Turner (2000) argued that this lattice serves metabolic gas exchange, but its geometry also creates an extended interface between the air-filled gallery space and the solid mound wall material. At this interface, the high-impedance mound wall material meets the very-low-impedance air, creating near-total internal reflection conditions

for substrate waves already inside the wall. The combined effect of anti-reflection at the outer surface and total internal reflection at the inner surface confines the seismic wave energy within the outer crust, producing a high-quality-factor resonant cavity in the frequency range where wall dimensions and wave velocities are commensurate. This is precisely the geometry required for CPSS function: concentrate mechanical energy in the chitin-rich structural material, exclude it from the air-filled interior, and distribute it around the colony's spatial extent.

Phylogenetic and Ecological Correlates

If CPSS provides a significant fitness benefit through early predator detection, one would expect that the sensitivity and elaborateness of colony-level seismic responses should be positively correlated with nest chitin content across taxa, and negatively correlated with the independence of workers from nest structures. Some preliminary comparative evidence is consistent with this expectation, though no study has been designed specifically to test it. Highly eusocial species with large enclosed nests and high worker density generally show more elaborate and rapid seismic alarm responses than primitively eusocial species with open nests and lower worker density (Michelsen et al., 1987; Cokl and Virant-Doberlet, 2003). Solitary insect species, which have no nest structure that could serve CPSS function, show individually mediated vibrational responses without colonial amplification. This pattern is

what the CPSS framework predicts, though it is also consistent with other explanations related to colony size and communication complexity.

Piezoelectric Function in Other Biological Contexts

The plausibility of a novel biological piezoelectric function is strengthened by established cases where biological piezoelectricity has clear functional significance. The best-documented case is bone piezoelectricity in vertebrates: the piezoelectric properties of collagen in bone are now understood to contribute to the mechanosensory signalling that directs bone remodelling in response to mechanical loading, with the Wolff's Law pattern of bone adaptation being partly mediated by piezoelectrically generated electrical fields that influence osteocyte activity (Bassett, 1968; Becker and Murray, 1970). This is a transduction process operating at the single-cell level in which a piezoelectric material converts mechanical strain into an electrical signal that modulates cell behaviour, precisely the mechanism operating on chitin in nest walls at Stage III of the CPSS pathway. The parallel is not merely analogical but mechanistically identical at the materials level: both involve non-centrosymmetric fibrous biopolymers (collagen in bone, alpha-chitin in insect cuticle) in a matrix that contains water and ions, under periodic mechanical loading, generating electric fields at scales and magnitudes relevant to cell membrane biology.

A second relevant case is the piezoelectric function of wood, characterised by Fukada (1968), who showed that cellulose fibrils in wood produce measurable piezoelectric signals under compressive and shear loading. Because many social insect nests incorporate cellulose-containing plant material, particularly in ant carton nests and paper wasp nests, cellulose piezoelectricity may contribute to CPSS in these taxa alongside chitin piezoelectricity. The relative contributions of chitin and cellulose piezoelectricity in different nest types represents a quantitative question accessible to direct measurement.

Empirical Predictions and Research Agenda

A theoretical framework of this type has scientific value only insofar as it generates predictions that could, in principle, be shown to be false. The CPSS framework makes predictions at multiple levels of organisation, from the materials properties of nest chitin through the biophysics of mechanosensory transduction to the behavioural and ecological characteristics of colonial seismic responses. We list below eleven predictions, grouped by organisational level, each stated in a form that specifies both the predicted observation and the result that would falsify it.

Materials-Level Predictions

Prediction 1 (Chitin piezoelectricity in nest material): Samples of termite mound wall material will exhibit measurable

piezoelectric coefficients when subjected to dynamic mechanical testing, with d-values in the range of 0.5 to 5 pC N^{-1}. Falsification: repeated measurements with properly calibrated charge amplifiers on multiple nest samples from multiple species show no statistically significant piezoelectric signal above the noise floor. Experimental protocol: see Section 8.1.

Prediction 2 (Chitin content correlation): Piezoelectric coefficient magnitude in nest materials will be positively correlated with chitin content (measured by acid hydrolysis and hexosamine assay or by near-infrared spectroscopy) across samples from different nest regions (inner crust, outer crust, fungal chambers, royal chamber walls) and across species with different nest compositions. Falsification: no significant correlation between chitin content and piezoelectric coefficient in a dataset of 30 or more samples from at least five species.

Prediction 3 (Frequency dependence of piezoelectric response): The piezoelectric response of nest material will be largest in the frequency range 10 to 100 Hz, corresponding to the principal predator footfall and low-frequency alarm signal range identified in Section 3. This prediction follows from the greater mechanical deformation amplitude at lower frequencies for a given energy input, and from the characteristic mechanical damping properties of chitin-protein composites. Falsification: maximum piezoelectric response occurs at a frequency outside the range 5 to 500 Hz.

Sensory Physiology Predictions

Prediction 4 (Subthreshold individual, suprathreshold colonial): When an isolated individual termite or ant is presented with a seismic stimulus of amplitude A, and a colony of N workers in their intact nest is presented with the same stimulus at the same nest wall location, the colony will respond behaviourally to stimuli of amplitude A/sqrt(N_eff) that do not elicit behavioural responses in isolated individuals. This is the direct test of Equation 10, and N_eff (effective number of independent workers on the nest wall) can be estimated independently from census and activity data. Falsification: the colonial detection threshold is not significantly lower than the individual detection threshold when both are measured under comparable experimental conditions.

Prediction 5 (Disruption by chitin chelation): Treating nest wall material with a chitin-binding dye or chelating agent that cross-links chitin crystallites and alters their mechanical properties should reduce the piezoelectric coefficient of the treated material. If colony members are then allowed to inhabit a test nest made of treated material, their seismic alarm response threshold should be elevated relative to untreated controls. Falsification: no significant difference in alarm threshold between colonies inhabiting treated and untreated artificial nests of otherwise identical architecture and material.

Prediction 6 (Leg contact dependence): Colony members with all six legs in contact with the nest wall should respond to seismic stimuli of lower amplitude than colony members artificially supported on non-piezoelectric substrates of the same mechanical

stiffness (controlling for the mechanical vibration transmission but eliminating the piezoelectric component). This test requires fabrication of artificial substrates that match the mechanical impedance but not the piezoelectric properties of mound wall material. Falsification: no significant difference in threshold between colony members on native mound material and members on impedance-matched non-piezoelectric substrates.

Architectural and Comparative Predictions

Prediction 7 (Architectural correlation with seismic performance): Across termite species, the architectural features predicted to enhance CPSS function (high outer-wall impedance, gradients in material density from outer to inner wall, chitin-enriched outer crust) should be more strongly developed in species occupying environments with abundant predators (particularly cursorial predators generating low-frequency seismic signals) than in species occupying environments with fewer such predators. This prediction requires a comparative analysis combining acoustic impedance measurements of nest wall materials with ecological data on predator assemblages. Falsification: no significant correlation between nest wall acoustic impedance gradient and predator community composition in a multi-species dataset.

Prediction 8 (Chitin content predicts colonial seismic sensitivity): In a comparative analysis of at least ten social insect species spanning a range of nest chitin contents, the colony-level

seismic detection threshold (measured as the minimum wall vibration amplitude eliciting a standardised alarm response from 50 percent of tested colonies) will be negatively correlated with nest wall chitin content, after controlling for colony size, nest wall geometry, and individual mechanosensory threshold. Falsification: no significant partial correlation between chitin content and colonial detection threshold in the appropriate multivariate model.

Ecological and Evolutionary Predictions

Prediction 9 (Survival advantage in seismic habitats): If CPSS is a functional adaptation, then colonies in which seismic signalling has been experimentally impaired (either by damping mound wall vibrations with a viscoelastic coating or by acoustic jamming at relevant frequencies) should suffer measurably higher predation rates or show elevated stress physiological responses compared to control colonies in the same habitat. This is a long-term field experiment requiring pre-identification of predator attack events and colony fitness monitoring over at least one complete colony reproductive cycle. Falsification: no significant difference in predation rate or colony fitness between experimental and control colonies in a replicated field study.

Prediction 10 (Seismic spectral tuning): If the nest architecture is selectively shaped by natural selection for seismic sensing, then the resonant frequency of the termite mound outer wall, measured as the frequency of maximum vibration amplitude under a

broadband seismic input, should correspond to the characteristic frequency range of the most significant local predators. In African savannah termite mounds, the main cursorial predators (mongooses, aardwolves, pangolins) have footfall frequencies in the range 2 to 10 Hz, and the CPSS framework predicts that the mound's resonant amplification should be tuned to this range. Falsification: the resonant frequency of the mound wall is unrelated to the footfall frequency spectrum of local predators in a comparative multi-site analysis.

Prediction 11 (Ant vs. termite nest sensitivity): Ant species that incorporate shed exuviae into nest architecture (a practice known in several ponerine and myrmicine species) should show lower seismic alarm thresholds than closely related species that do not incorporate exuviae, after controlling for colony size and individual sensory thresholds. This is because exuviae are particularly chitin-rich, and their incorporation should increase the piezoelectric coefficient of nest material according to Prediction 2. Falsification: no significant difference in colonial seismic sensitivity between exuviae-incorporating and non-incorporating ant species in a phylogenetically controlled comparative analysis.

Experimental Approaches

The experimental programme outlined here is organised into four phases, each building on the results of the previous one. Phase A establishes the material basis of the framework by characterising

the piezoelectric properties of nest materials. Phase B tests the individual and colony-level sensory responses to controlled seismic stimuli. Phase C investigates the anatomy and electrophysiology of the sensory interface between nest material and colony members. Phase D conducts comparative and field tests of the ecological predictions. The entire programme could, in principle, be completed within five to seven years by a moderately resourced laboratory with expertise spanning materials science, sensory neuroscience, entomology, and field ecology.

Figure 5. Schematic overview of the Phase A (materials characterisation) and Phase B (colony-level behavioural assay) experimental protocols proposed in Section 8. Phase A: A disk of nest wall material is mounted between silver paste electrodes in an electrically shielded holder, driven mechanically by a piezoelectric

shaker at defined frequency and amplitude, and the resulting charge output is measured by a low-noise charge amplifier connected to a lock-in amplifier for phase-sensitive detection. Phase B: A colony of N workers is housed in an artificial nest arena whose wall is fabricated from native nest material; a calibrated electrodynamic shaker delivers controlled seismic stimuli at the arena base; colony alarm response kinematics are recorded by high-speed camera and tracking software; wall vibration amplitude is independently measured by laser Doppler vibrometry. See Section 8 for details.

Phase A: Materials Characterisation of Nest Piezoelectricity

Nest material samples should be collected from multiple nest regions of each target species, lyophilised to defined water content (10 percent w/w, which approximates the in-nest humidity experienced by mound wall material in tropical termite nests), and sectioned into disks of approximately 10 mm diameter and 1 mm thickness. Gold or silver paste electrodes should be applied to the upper and lower disc faces, and samples should be mounted in an electrically shielded, temperature-controlled sample holder that allows mechanical stimulation orthogonal to the electrode plane.

Piezoelectric characterisation should be performed by two complementary methods. The first is quasi-static compression: a calibrated load cell applies a slow, computer-controlled compressive stress while a charge amplifier with femtofarad-level input

capacitance records the charge displaced between the electrodes. The piezoelectric charge constant d_{33} (compression along the electrode axis) is then the slope of the charge versus force plot in the linear region. The second method is dynamic resonance: the sample is driven by a piezoelectric shaker at its resonance frequency (calculable from the wave velocity and sample thickness), and the electrical impedance of the sample is measured by a precision impedance analyser across a frequency range of 1 Hz to 100 kHz. Piezoelectric materials show a characteristic coupling peak in the impedance spectrum near resonance, and the electromechanical coupling coefficient k can be extracted from the ratio of resonant and anti-resonant frequencies.

A critical control is the comparison between native nest material, heat-treated nest material (in which chitin crystallinity is disrupted by heating to 150 degrees Celsius), and artificial samples made from reconstituted and randomised chitin powder with the same total chitin content. If the piezoelectric signal depends on chitin crystal orientation (as predicted by the molecular mechanism in Section 2.2), native material should show larger d values than powder controls, and the signal should decrease with progressive disruption of chitin microstructure.

X-ray diffraction and solid-state nuclear magnetic resonance spectroscopy should be used in parallel to characterise chitin content, crystallinity, and crystal orientation distribution in the same samples used for piezoelectric measurements, allowing construction of a

quantitative structure-property relationship between chitin architecture and piezoelectric output.

Phase B: Colony-Level Seismic Behavioural Assays

The behavioural assays require construction of artificial nest arenas in which the wall material can be specified and controlled, the seismic stimulus delivered at known amplitude and frequency, and the colony response measured quantitatively. For termites, artificial nest tunnels have been successfully used by several groups, and the design principles are well established. The arena floor should incorporate a calibrated electrodynamic shaker (frequency range 0.1 to 2,000 Hz, displacement range 0.01 to 1,000 nm) driven by a function generator and power amplifier with computer control of frequency, amplitude, and waveform. The arena walls should be constructed from slabs of native nest wall material cored from freshly collected termite mounds and cut to standard dimensions, with natural surface texture preserved.

The primary dependent variable is the alarm latency: the time between shaker onset and the first detectable alarm behaviour (rapid acceleration, soldier recruitment, or alarm pheromone release). Secondary variables include the propagation speed of the alarm response across the colony (detectable by tracking the front of alarm behaviour in time-lapse video), the fraction of the colony mobilised, and the duration of the alarm state. These variables are measured as

a function of stimulus amplitude (below, at, and above the individual threshold) and frequency.

Crucially, the experiment must be replicated with different numbers of workers in the arena (N varied from approximately 100 to 10,000) to test whether the colony-level detection threshold scales as $N^{-1/2}$ as predicted by Equation 10. An additional treatment should use arena walls made of a non-piezoelectric material with matched mechanical impedance to the native wall, such as an epoxy cast of the same wall geometry impregnated with inert mineral particles to match the density and shear modulus. If the piezoelectric component of CPSS contributes measurably to colonial detection, the alarm threshold should be higher in the epoxy arena than in the native material arena, even though the purely mechanical stimulation of the workers' legs is identical in both.

Phase C: Sensory Neurophysiology at the Nest Wall Interface

Phase C addresses the cellular and neural mechanisms by which colony members in contact with nest surfaces transduce seismic stimuli. The primary technique is in situ extracellular recording from the subgenual organ nerve of an individual termite or ant worker whose legs are resting on a piezoelectrically active substrate. This preparation has been used in studies of subgenual organ sensitivity in cockroaches and other insects (Howse, 1964), and the extension to nest-wall substrates is technically feasible.

In the proposed preparation, a lightly restrained worker with all six legs resting on a slab of nest wall material is positioned under a micromanipulator carrying an extracellular recording electrode. The electrode is inserted adjacent to the subgenual organ nerve in one leg, and the substrate is driven at various frequencies and amplitudes by the attached shaker. The neural threshold (minimum substrate displacement producing a measurable compound action potential) is determined by the method of limits. The experiment is then repeated with the leg resting on a non-piezoelectric substrate of matched mechanical impedance. If piezoelectric fields at the substrate surface contribute to sensory activation, the threshold on native material should be lower than on the control substrate.

A complementary approach is scanning Kelvin probe microscopy of the nest wall surface during mechanical oscillation. This technique measures the surface potential of materials at nanometre spatial resolution and could directly visualise the distribution of piezoelectrically generated surface charge on the chitin-rich outer surface of mound wall samples under defined mechanical loading. Correlation of the spatial pattern of surface charge with the positions of sensory neuron terminals (mapped by immunolabelling for neuron-specific antigens and confocal microscopy) would establish whether sensory nerve endings are anatomically positioned to sample the piezoelectric field.

Phase D: Comparative and Field Tests

Phase D tests the ecological and evolutionary predictions of Section 7.2 and 7.3. The comparative component requires a phylogenetically controlled dataset of colony-level seismic detection thresholds (measured by the Phase B protocol) for at least fifteen social insect species spanning a range of nest types and chitin contents. Species should include representatives of highly eusocial termites (e.g., Macrotermes, Nasutitermes), primitively eusocial termites (e.g., Zootermopsis), attine ants with complex underground nests, arboreal ants with carton nests, stingless bees, and Apis honey bees. For each species, nest material chitin content and piezoelectric coefficient (Phase A) and individual mechanosensory threshold (Phase C) should be measured, enabling a full path analysis of the relationship between material properties, individual sensory physiology, and colonial detection performance.

The field component involves manipulation of mound wall acoustic properties in the natural environment. This is technically challenging but not infeasible. The outer surface of Macrotermes mounds can be treated with a viscoelastic damping compound that reduces the mechanical quality factor Q of the mound wall, dissipating seismic energy as heat rather than allowing it to propagate within the wall. The predicted effect on colony alarm behaviour is that treated mounds should show slower alarm responses to naturally occurring seismic events (monitored by seismometers at defined distances from the mound), with less intensive mobilisation of soldiers, than untreated control mounds at

the same site. Measurement of predation pressure on treated and control mounds over a field season could test Prediction 9 from Section 7.4.

Implications for Collective Intelligence and Extended Phenotype Theory

If the CPSS framework is confirmed, its implications extend well beyond entomology and bioacoustics, touching fundamental questions in the theory of extended phenotypes, the origins of collective intelligence, and the evolutionary ecology of social behaviour. Three sets of implications are considered in turn.

Expanding the Extended Phenotype Framework

Dawkins (1982) introduced the extended phenotype as a conceptual framework for genes that produce phenotypic effects in the world beyond the individual organism's body, most dramatically in the case of parasite manipulation of host behaviour and in the case of animal constructions such as nests, dams, and burrows. In the extended phenotype view, the termite mound is a gene product much as the termite exoskeleton is, and natural selection acts on mound properties through effects on colony fitness. This framework has been applied primarily to the thermoregulatory, hygroscopic, and defensive functions of social insect nests, and its application to sensory function is new.

The CPSS framework requires a specific elaboration of the extended phenotype concept: not only is the nest a physical extension of the colony's genotype, it is also a functional extension of the colony's sensory system. The distinction matters because it assigns to the nest a category of biological function that was previously reserved for specialised sensory organs (tympanic membranes, retinas, lateral line organs) possessed by individual organisms. If the nest functions as a sensory organ, then the evolutionary analysis of nest design must include the sensory performance of the structure as a fitness component alongside its thermoregulatory and defensive properties. Selection on nest wall chitin content, which the CPSS framework predicts, would be selection on a sensory parameter, creating a novel pathway by which kin selection and inclusive fitness theory bear on the design of nest architecture.

Turner's extended organism concept (Turner, 2000) provides a complementary framework. Turner argues that termite mounds are physiological extensions of the colony, capable of mediating gas exchange, temperature regulation, and other homeostatic functions at the colonial scale, in much the same way that the kidney or lung mediates physiological functions at the individual scale. CPSS adds seismic sensing to this catalogue of extended physiological functions, and it does so through a mechanism (distributed piezoelectric transduction) that has no precedent in the individual-level physiology of social insects. The extended organism

framework encourages us to ask what other sensory modalities might be mediated by nest material properties, a question we return to in Section 11.

Colonial Intelligence and the Neural Analogy

The colonial averaging mechanism described by Equations 8 to 10 is formally identical to the noise-reduction achieved by averaging across neural populations in the vertebrate nervous system. Population coding, in which the responses of many individually noisy neurons are combined to produce a more reliable estimate of a stimulus parameter, is one of the fundamental principles of neural computation. The CPSS framework proposes that social insect colonies exploit an analogous principle at a larger scale, with individual workers playing the role of neurons in a distributed neural network and the nest wall playing the role of the peripheral transduction apparatus.

This analogy is more than merely figurative. In vertebrate population coding, the improvement in stimulus estimation follows the same square-root-of-N law predicted by Equation 8, under the same assumptions about signal coherence and noise independence. The conditions under which noise becomes correlated, degrading the population-coding benefit, are also analogous: in vertebrate visual cortex, nearby neurons responding to the same visual feature have correlated noise, and this limits the information capacity of the population. In the CPSS system, nearby workers on the mound wall

share the same seismic wavefield, creating coherent signal but potentially also correlated noise from global mound vibrations. The mathematics of information capacity in correlated sensor networks applies directly, and the CPSS system could be analysed using the Fisher information framework developed for neural population coding by Seung and Sompolinsky (1993).

The neural analogy also suggests a new perspective on colony-level intelligence. Camazine and colleagues (2001) analysed social insect colonies as self-organising systems whose collective intelligence emerges from local interactions among individuals following simple rules. The CPSS mechanism adds a new layer to this picture: the colony not only processes information through local interactions among workers, but also acquires information from the environment through a distributed sensing array embedded in the nest structure. The nest is simultaneously the colony's infrastructure, its immune system, and, this chapter argues, its nervous system periphery. This synthesis suggests that the evolution of elaborate nest architecture and the evolution of colonial intelligence are not independent processes but are coupled, with structural innovations in nest design enabling sensory capabilities that, in turn, drive the selection for more sophisticated collective information processing.

Niche Construction and Sensory Coevolution

Odling-Smee and colleagues (2003) developed the niche construction framework, in which organisms are understood not

merely as adapting to pre-existing environments but as modifying their environments in ways that alter the selection pressures they experience. The CPSS framework illustrates a form of sensory niche construction: by building nests with specific material properties (high chitin content, controlled impedance gradients), social insect colonies modify their sensory environment, expanding the range of seismic stimuli they can detect beyond what would be accessible to unhoused individuals. This modification is heritable at the colony level through behavioural inheritance (worker offspring that inherit the behavioural rules for nest construction will build similar nests), creating a channel for the evolutionary modification of sensory capabilities through nest-building behaviour that operates in parallel with, and potentially faster than, genetic modification of sensory organ morphology.

If CPSS function is under selection, one expects to see co-evolution between the material properties of nest construction and the sensory physiology of colony members. Specifically, workers in CPSS-capable colonies should show adaptations of their mechanosensory organs that maximise their ability to sample the piezoelectrically generated signals from nest surfaces, such as specialised scolopidial arrangements in the subgenual organ, specific mechanical linkages between the tibia and the organ, or cuticular specialisations at the foot-nest interface. Comparative morphological studies of subgenual organ anatomy across species with and without chitin-rich nest constructions represent a

productive research direction, and one that has not been pursued because the functional framework motivating it has not previously been articulated.

Biomimetic and Applied Implications

Beyond its significance for our understanding of social insect biology, the CPSS concept, if confirmed, provides a rich source of design principles for engineered distributed sensing systems. Several current technological challenges are directly addressed by the architectural and computational principles implicit in CPSS.

Distributed Structural Health Monitoring

The detection of low-amplitude mechanical disturbances in large, spatially extended structures is a central challenge in structural health monitoring (SHM). Current SHM systems typically employ sparse arrays of discrete piezoelectric sensors bonded to structural elements, with signal processing algorithms that attempt to localise damage by triangulating the arrival times of stress waves at the sensor array. The CPSS concept suggests an alternative approach: a structural material that is itself distributed and piezoelectric, with the sensing function embedded in the material rather than added as a discrete component. Such a material would provide continuous spatial coverage without gaps between sensors, and the colonial averaging principle of Equation 8 would apply to the collective response of all sensing elements simultaneously.

Chitin and chitin-based composites are already under development as structural and biocompatible materials for engineering applications (Wilson et al., 2007). The integration of piezoelectric sensing function into chitin-based structural composites, inspired by the CPSS model, represents a plausible near-term application. Key design parameters would include the chitin crystallinity (which determines d-coefficient magnitude), the fibril orientation distribution (which determines directionality of response), and the material-level impedance matching to the substrate to be monitored (analogous to the mound-soil impedance matching considered in Section 5.2).

Seismic Early Warning Systems

The principle of colonial seismic sensing, large numbers of loosely coupled mechanosensors sharing a common structural substrate, is directly applicable to the design of distributed seismic sensor networks for early warning of small earthquakes and localized ground motion events. Current seismic monitoring networks rely on widely spaced discrete seismometers, which limits spatial resolution for shallow, low-magnitude events. A network of small, inexpensive piezoelectric sensors embedded in a continuous structural material (road surface, building foundation, pipeline coating) could, in principle, achieve detection thresholds much lower than any individual sensor, by applying the colonial averaging algorithm of Equations 8 to 10 in software.

The mathematical framework developed in Section 5.5 is directly applicable to the design of such networks. The optimal number of sensors, their spatial distribution, and the signal processing algorithm for combining their outputs to maximise detection probability while minimising false alarm rate can all be derived from the same signal detection theory that underlies the CPSS model. The biomimetic dimension, that this design principle was likely discovered and refined by natural selection over tens of millions of years in termite colonies, provides some assurance that it represents a robust engineering solution to the distributed sensing problem, rather than a theoretical construct without practical implementation.

Biologically Inspired Soft Robotics

Social insect colonies achieve collective locomotion, manipulation, and construction through the coordinated action of large numbers of relatively simple individual robots, without centralised control or global information. The CPSS mechanism, if validated, would add a new substrate-level sensing modality to this biological template for distributed robotic systems. A swarm robotic system in which individual robots share a compliant, piezoelectric substrate could use the substrate itself as a low-bandwidth communication channel, with mechanical deformations induced by one robot's actions being detected by neighbouring robots through substrate piezoelectric signals. This is a form of stigmergic

communication through material deformation, analogous to the way termites use pheromone-marked pellets to coordinate nest construction, but operating at timescales of milliseconds rather than seconds.

The design of chitin-based compliant piezoelectric substrates for swarm robotics is technically feasible with current polymer processing techniques. Electrospun chitin nanofibre mats, for example, can be fabricated with controlled fibre orientation distributions and have been shown to have measurable piezoelectric properties, though detailed characterisation relevant to sensing applications is lacking (Muralt, 2000). The CPSS framework provides the biological benchmark against which such materials should be evaluated: the question is not simply whether the material is piezoelectric, but whether it is piezoelectric at the frequencies and amplitudes relevant to the intended mechanical events, and whether the signal-to-noise characteristics are sufficient for distributed detection at the required spatial scale.

Conclusions and Future Directions

Colonial Piezoelectric Seismic Sensing brings together three bodies of well-established science, the piezoelectricity of non-centrosymmetric biopolymers, the seismic communication behaviour of social insects, and the signal-processing principles of distributed sensor networks, into a novel mechanistic framework that proposes a previously unrecognised function for social insect nest

architecture. The core claim is that chitin incorporated into nest constructions transduces incoming seismic energy into electrical events through a piezoelectric mechanism, and that the simultaneous stimulation of hundreds to millions of colony members by a single seismic wavefront provides a colonial-level detection capability substantially superior to that available to any individual. The nest thereby functions as an extended sensory organ, in the sense that Turner (2000) ascribes to the termite mound's thermoregulatory function and Dawkins (1982) ascribes to all structures whose properties are shaped by natural selection acting through effects on colonial fitness.

This chapter has presented the CPSS framework in quantitative form, deriving order-of-magnitude estimates for the electric fields generated by seismically driven chitin deformation (Equation 6, approximately 0.2 to 2 V m^{-1} under plausible predator footfall conditions near the mound) and for the colonial detection threshold improvement relative to individual threshold (Equation 10, a factor of approximately 70 to 200 for colonies of 10^5 to 10^6 workers). These estimates are based on documented material properties and physical laws, but they depend critically on parameters (nest wall chitin content, in-nest chitin crystal orientation, number of workers on the nest wall surface at any time) that have not been directly measured. The estimates should therefore be treated as the target values that the experimental programme outlined in Section 8 is designed to test, not as established facts.

Eleven falsifiable predictions emerge from the framework, spanning the range from materials science (Predictions 1 through 3) through sensory physiology (Predictions 4 through 6) to comparative biology and field ecology (Predictions 7 through 11). These predictions are formulated precisely enough to be unambiguous in outcome: either the predicted correlation or threshold effect exists at the predicted magnitude, or it does not, and a well-powered experiment will distinguish these outcomes. This falsifiability is not a rhetorical gesture but a deliberate structural feature of the framework, which is presented as a theoretical framework resting on empirical foundations and amenable to experimental scrutiny.

Several important questions remain entirely open and represent the intellectual frontier of this area. First, do social insect cuticles, particularly the leg surfaces of workers in intimate contact with nest walls, show any morphological specialisations (surface nanostructures, modified scolopidial arrangements, cuticular conductivity gradients) that would enhance their coupling to piezoelectrically generated surface fields? Second, is there genetic variation within species in nest chitin content that correlates with colonial seismic sensitivity, and if so, is this variation under selection in populations exposed to different predator assemblages? Third, do the behavioural and morphological responses of colony members to seismic stimulation vary systematically across the spatial extent of the mound in a manner consistent with wave propagation models, or do all colony members respond simultaneously in a manner that

would rule out wave-guided propagation? Fourth, is there any evidence of frequency-selective amplification of seismic signals by mound wall resonances, and if so, are the resonant frequencies tuned to the dominant seismic signals in the colony's ecological environment?

The broader significance of the CPSS framework, if it survives experimental scrutiny, is to establish a new category of biological sensory adaptation: the use of non-living structural materials as transducing elements in an extended sensory system. This category differs from established examples of extended sensing (the use of the water surface as a vibration medium by water striders, or of the air column in vertebrate ears as an acoustic transformer) in that the transducing material is constructed by the organism and has material properties under indirect genetic control through the nest-building behaviour of the colony. The evolutionary implications are substantial: a novel sensory function can be acquired by a social insect lineage not through the gradual modification of individual sensory organs but through the modification of nest-building behaviour that changes material composition, a much faster and more flexible evolutionary route. If CPSS is real, it represents one of the more elegant instances in the natural world of the principle that biological systems can offload functional complexity from individual bodies into the physical environment of their own making.

The nest as extended sensory organ is not merely a metaphor. It is a mechanistic framework with a defined biophysical substrate,

quantitative theoretical grounding, and a set of predictions that the next decade of research in social insect biology, materials science, and sensory neuroscience has the tools to resolve.

Kaynakça/References

Anderson JC, Eriksson C (1970) Piezoelectric properties of dry and wet bone. Nature 227:491–492.

Athenstaedt H (1974) Pyroelectric and piezoelectric properties of vertebrates. Annals of the New York Academy of Sciences 238:68–93.

Barth FG (2002) A Spider's World: Senses and Behavior. Springer, Berlin.

Bassett CAL (1968) Biological significance of piezoelectricity. Calcified Tissue Research 1:252–272.

Becker RO, Murray DG (1970) The electrical control system regulating fracture healing in amphibians. Clinical Orthopaedics and Related Research 73:169–198.

Camazine S, Deneubourg J-L, Franks NR, Sneyd J, Theraulaz G, Bonabeau E (2001) Self-Organization in Biological Systems. Princeton University Press, Princeton.

Claridge MF (1985) Acoustic signals in the Homoptera: behavior, taxonomy, and evolution. Annual Review of Entomology 30:297–317.

Cokl A, Virant-Doberlet M (2003) Communication with substrate-borne signals in small plant-dwelling insects. Annual Review of Entomology 48:29–50.

Connétable S, Robert A, Bouffault F, Bordereau C (1999) Vibratory alarm signals in two sympatric higher termite species: Pseudacanthotermes spiniger and P. militaris (Termitidae, Macrotermitinae). Journal of Insect Behavior 12:329–342.

Dawkins R (1982) The Extended Phenotype. Oxford University Press, Oxford.

Fletcher NH (1992) Acoustic Systems in Biology. Oxford University Press, New York.

Franks NR (1989) Army ants: a collective intelligence. American Scientist 77:138–145.

Fratzl P, Weinkamer R (2007) Nature's hierarchical materials. Progress in Materials Science 52:1263–1334.

Fukada E, Yasuda I (1957) On the piezoelectric effect of bone. Journal of the Physical Society of Japan 12:1158–1162.

Fukada E (1968) Piezoelectricity as a fundamental property of wood. Ultrasonics 6:229–234.

Gordon DM (1999) Ants at Work. Free Press, New York.

Greenfield MD (2002) Signalers and Receivers: Mechanisms and Evolution of Arthropod Communication. Oxford University Press, New York.

Heinrich B (1981) The mechanisms and energetics of honeybee swarm temperature regulation. Journal of Experimental Biology 91:25–55.

Hill PSM (2008) Vibrational Communication in Animals. Harvard University Press, Cambridge.

Howse PE (1964) An investigation into the mode of action of the subgenual organ in the termite, Zootermopsis angusticollis Emerson, and in the cockroach, Periplaneta americana L. Journal of Insect Physiology 10:409–424.

Kirchner WH (1997) Acoustical communication in social insects. In: Lehrer M (ed) Orientation and Communication in Arthropods. Birkhäuser, Basel, pp 273–300.

Knudsen EI (1974) Behavioral thresholds to electric signals in high frequency electric fish. Journal of Comparative Physiology 91:333–353.

Korb J (2003) Thermoregulation and ventilation of termite mounds. Naturwissenschaften 90:212–219.

Lang SB (1966) Pyroelectric effect in bone and tendon. Nature 212:704–705.

Lüscher M (1961) Air-conditioned termite nests. Scientific American 205:138–145. https://doi.org/10.1038/scientificamerican0761-138

Markl H (1965) Stridulation in leaf-cutting ants. Science 149:1392–1393.

Markl H (1968) Die Verständigung durch Stridulationssignale bei Blattschneiderameisen. I. Die biologische Bedeutung der Stridulation. Zeitschrift für vergleichende Physiologie 57:299–330.

Markl H (1983) Vibrational communication. In: Huber F, Markl H (eds) Neuroethology and Behavioral Physiology. Springer, Berlin, pp 332–353. https://doi.org/10.1007/978-3-642-69271-2_22

Michelsen A, Kirchner WH, Lindauer M (1986) Sound and vibrational signals in the dance language of the honey bee, Apis mellifera. Behavioral Ecology and Sociobiology 18:207–212.

Michelsen A, Towne WF, Kirchner WH, Kryger P (1987) The acoustic near field of a dancing honeybee. Journal of Comparative Physiology A 161:633–643.

Michelsen A, Andersen BB, Storm J, Kirchner WH, Lindauer M (1992) How honeybees perceive communication dances, studied by means of a mechanical model. Behavioral Ecology and Sociobiology 30:143–150. https://doi.org/10.1007/BF00173947

Minke R, Blackwell J (1978) The structure of alpha-chitin. Journal of Molecular Biology 120:167–181. https://doi.org/10.1016/0022-2836(78)90063-3

Moran DT, Chapman KM, Ellis RA (1971) The fine structure of cockroach campaniform sensilla. Journal of Cell Biology 48:155–173.

Muralt P (2000) Ferroelectric thin films for micro-sensors and actuators: a review. Journal of Micromechanics and Microengineering 10:136–146.

Neville AC (1975) Biology of the Arthropod Cuticle. Springer, Berlin.

Neville AC, Parry DAD, Woodhead-Galloway J (1976) The chitin crystallite in arthropod cuticle. Journal of Cell Science 21:73–82.

Odling-Smee FJ, Laland KN, Feldman MW (2003) Niche Construction: The Neglected Process in Evolution. Princeton University Press, Princeton.

Raabe D, Sachs C, Romano P (2005) The crustacean exoskeleton as an example of a structurally and mechanically graded biological nanocomposite material. Acta Materialia 53:4281–4292. https://doi.org/10.1016/j.actamat.2005.05.027

Rayleigh JWS (1885) On waves propagated along the plane surface of an elastic solid. Proceedings of the London Mathematical Society 17:4–11.

Roces F, Hölldobler B (1995) Vibrational communication between hitchhikers and foragers in leaf-cutting ants (Atta cephalotes). Behavioral Ecology and Sociobiology 37:297–302.

Roces F, Tautz J (2001) Stridulation in leaf-cutting ants. Naturwissenschaften 88:220–223.

Schwabe J (1906) Beiträge zur Morphologie und Histologie der tympanalen Sinnesapparate der Orthopteren. Zoologica 50:1–154.

Seeley TD (1995) The Wisdom of the Hive: The Social Physiology of Honey Bee Colonies. Harvard University Press, Cambridge.

Seung HS, Sompolinsky H (1993) Simple models for reading neuronal population codes. Proceedings of the National Academy of Sciences USA 90:10749–10753.

Stuart AM (1963) Studies on the communication of alarm in the termite, Zootermopsis nevadensis (Hagen), Isoptera. Physiological Zoology 36:85–96.

Turner JS (2000) The Extended Organism: The Physiology of Animal-Built Structures. Harvard University Press, Cambridge.

Vincent JFV, Wegst UGK (2004) Design and mechanical properties of insect cuticle. Arthropod Structure and Development 33:187–199.

Wilson EO (1971) The Insect Societies. Harvard University Press, Cambridge.

Wilson SA, Jourdain RE, Zhang Q, Dorey RA, Bowen CR, Willander M, Wahab QU, Al-hilli SM, Nur O, Quandt E (2007) New materials for micro-scale sensors and actuators: an engineering review. Materials Science and Engineering R 56:1–129.

Yack JE (2004) The structure and function of auditory chordotonal organs in insects. Microscopy Research and Technique 63:315–337. https://doi.org/10.1002/jemt.20051

Yasuda I, Noguchi K, Sato T (1955) Dynamic callus and electric callus. Journal of Bone and Joint Surgery 37:1292–1293.


BİDGE